

**The role of the Fur protein for maintenance of iron homeostasis in
the strictly anaerobic bacterium *Clostridium acetobutylicum***

Dissertation

zur

Erlangung des akademischen Grades
doctor rerum naturalium(Dr. rer. nat.)
der Mathematisch-Naturwissenschaftlichen Fakultät
der Universität Rostock

vorgelegt von

Delyana Peteva Vasileva

geb. am 14.05.1986 in Gabrovo, Bulgarien

Rostock, Januar 2014

urn:nbn:de:gbv:28-diss2014-0067-0

Datum der Einreichung: 15.01.2014

Wissenschaftliches Kolloquium: 14.03.2014

Gutachter:

Prof. Dr. Hubert Bahl

Universität Rostock,

Mathematisch-Naturwissenschaftliche Fakultät,

Institut für Biowissenschaften, Mikrobiologie

Prof. Dr. Martin Hagemann

Universität Rostock

Mathematisch-Naturwissenschaftliche Fakultät,

Institut für Biowissenschaften, Pflanzenphysiologie

Contents

Contents	I
Abbreviations	VI
1 Introduction	1
2 Materials and Methods	7
2.1 Bacterial strains and plasmids	7
2.2 Oligonucleotides	7
2.3 Media and growth conditions	7
2.3.1 Growth media for <i>E. coli</i>	7
2.3.2 Growth media for <i>B. subtilis</i>	8
2.3.3 Growth media for <i>C. acetobutylicum</i>	9
2.3.4 Antibiotics and additives	11
2.3.5 Titan-(III)-NTA solution	11
2.3.6 Growth conditions	11
2.4 Storage of strains and control of purity	11
2.5 Analytical procedures	12
2.5.1 Optical density	12
2.5.2 Determination of growth rates	12
2.5.3 pH measurement	12
2.5.4 Light microscopy	12
2.5.5 Glucose consumption	12
2.5.6 Lactate production	13
2.5.7 Gas chromatography	13
2.5.8 Quantification of gaseous fermentation products	13
2.5.9 Riboflavin identification and quantification	13
2.5.9.1 Visible and fluorescence spectra	13
2.5.9.2 Analytical TLC (Thin Layer Chromatography)	13
2.5.9.3 Quantification of riboflavin	14
2.5.10 Detection and quantification of siderophores	14
2.5.10.1 Arnow assay	14

2.5.10.2	Ferric perchlorate assay	15
2.5.10.3	CAS liquid assay	15
2.5.11	Intracellular iron content	15
2.6	Extraction of nucleic acids	16
2.6.1	Isolation of plasmid DNA from <i>E. coli</i>	16
2.6.2	Isolation of chromosomal DNA from <i>C. acetobutylicum</i>	16
2.6.3	Isolation of total cellular RNA from <i>C. acetobutylicum</i>	17
2.7	Standard molecular biology techniques	17
2.7.1	Purification of DNA	17
2.7.1.1	Extraction of DNA from agarose gels	17
2.7.2	Agarose gel electrophoresis	18
2.7.2.1	Standard agarose gel electrophoresis	18
2.7.2.2	Denaturing agarose gel electrophoresis	18
2.8	Manipulation of nucleic acids	19
2.8.1	PCR primer design	19
2.8.2	PCR methods	19
2.8.2.1	Standard PCR procedures	19
2.8.2.2	'High Fidelity' PCR	20
2.8.2.3	'Splicing of overlap extension' (SOE) PCR	20
2.8.3	Enzymatic modifications of DNA	21
2.8.3.1	Digestion with restriction endonucleases	21
2.8.3.2	Dephosphorylation of plasmid DNA	21
2.8.3.3	Ligation	21
2.9	Construction of recombinant strains	22
2.9.1	DNA transfer into <i>E. coli</i>	22
2.9.1.1	Preparation of <i>E. coli</i> competent cells by CaCl ₂ treatment	22
2.9.1.2	Transformation into CaCl ₂ -competent <i>E. coli</i> cells	22
2.9.1.3	Preparation of <i>E. coli</i> electrocompetent cells	22
2.9.1.4	Electroporation into <i>E. coli</i>	22
2.9.2	DNA transfer into <i>B. subtilis</i>	22
2.9.2.1	Preparation of <i>B. subtilis</i> competent cells	22
2.9.2.2	Transformation into <i>E. coli</i> RR1	23
2.9.2.3	Transformation into <i>B. subtilis</i>	23

2.9.3	Transformation into <i>C. acetobutylicum</i> by electroporation	24
2.10	Insertional mutagenesis via the Clostron [®] system	25
2.10.1	Intron re-targeting and assembly of recombinant pMTL007C-E2 plasmids	25
2.10.2	Transformation into <i>C. acetobutylicum</i>	25
2.10.3	Verification of Clostron [®] insertional mutants	26
2.11	DNA and RNA blotting techniques	26
2.11.1	Probe labeling	26
2.11.2	Transfer of DNA onto a membrane (Southern blot)	26
2.11.2.1	Southern hybridization	27
2.11.2.2	Immunological detection (Southern blot)	28
2.11.3	Transfer of RNA onto a membrane (Northern blot)	29
2.11.3.1	Northern hybridization	29
2.11.3.2	Immunological detection (Northern blot)	29
2.12	Microarray analysis	31
2.13	sqRT-PCR	31
2.14	5' RACE	31
2.15	Protein techniques	32
2.15.1	Preparation of crude extracts	32
2.15.2	Determination of protein concentration	32
2.15.3	SDS-PAGE	32
2.15.4	2D-PAGE	32
2.15.4.1	Sample preparation	32
2.15.4.2	Isoelectric focusing (IEF)	33
2.15.4.3	2D SDS-PAGE	34
2.15.4.4	Staining with colloidal Coomassie	34
2.15.4.5	Documentation of 2D-PAGE gels	34
2.15.4.6	Mass spectrometric detection of proteins	34
2.15.5	Enzyme assays	36
2.15.5.1	β -galactosidase assay	36
2.15.6	Overproduction and purification of recombinant proteins	36
2.15.6.1	Overproduction and purification of <i>Strep</i> -tag II fusion proteins	36
2.15.6.2	Overproduction and purification of His-tag fusion proteins	37

2.15.7 Western blotting (transfer and detection of proteins on a nitrocellulose membrane)	38
2.15.7.1 Detection of <i>Strep</i> -tag II fusion proteins	38
2.15.8 Cross-linking experiments	39
2.16 Stress experiments	40
2.16.1 O ₂ and H ₂ O ₂ stress experiments	40
2.17 Chemicals and materials	40
3 Results	41
3.1 Identification of CAC1682 from <i>C. acetobutylicum</i> as an iron-sensing repressor	41
3.1.1 Generation of homology models	41
3.1.2 Biochemical characterization	45
3.1.2.1 Heterologous expression of CAC1682 and CAC0951 proteins	45
3.1.2.2 Determination of protein oligomeric state	46
3.1.2.3 Metal content quantification	47
3.1.3 Functional <i>in vivo</i> characterization of CAC1682	48
3.1.3.1 Construction of pTCatP recombinant plasmids	48
3.1.3.2 Complementation of the <i>fur</i> defective <i>E. coli</i> H1780 strain	49
3.1.3.2.1 Quantification of β -galactosidase reporter activities	50
3.1.3.2.2 Detection of enterobactin production	51
3.1.3.3 Complementation of the Fur ⁻ <i>B. subtilis</i> H6543	52
3.2 Generation and verification of a <i>fur</i> mutant in <i>C. acetobutylicum</i>	53
3.3 Functional <i>in trans</i> complementation of the <i>fur</i> defective strain	55
3.4 Physiological characterization of the <i>C. acetobutylicum fur</i> mutant	56
3.4.1 Growth characterization, morphology and product formation	56
3.4.2 Growth in the presence of an iron chelator	60
3.4.3 Quantification of intracellular iron content	61
3.4.4 Sensitivity to oxidative stress	61
3.5 An intersection between response to <i>fur</i> mutation and iron limitation	62
3.5.1 Assessment of potential siderophore production	62
3.5.2 Riboflavin biosynthesis	63
3.6 Global expression analyses and 2D-PAGE	66
3.6.1 Fur modulon	68
3.6.1.1 Validation of the microarray data through sqRT-PCR	71
3.6.1.2 Bioinformatic prediction of potential Fur binding sites	71

3.6.1.3	Determination of transcriptional start sites by 5' RACE	73
3.6.1.4	Relationship between flavodoxin (CAC0587) expression and riboflavin biosynthesis in <i>C. acetobutylicum</i>	75
3.6.2	Additional transcriptional reshaping in response to iron limitation and <i>fur</i> gene mutation	75
4	Discussion	77
4.1	Identification and characterization of a functional Fur regulator in <i>C. acetobutylicum</i>	78
4.1.1	Power of the trans-complementation studies for establishing the role of CAC1682 as an iron-responsive regulator (Fur)	78
4.1.2	Comparative <i>in silico</i> and biochemical analysis	79
4.2	Physiological importance of Fur in <i>C. acetobutylicum</i>	84
4.2.1	Growth profiling and product formation	84
4.2.2	Relationship between the intracellular iron levels and sensitivity to oxidative stress	86
4.3	Overview of the transcriptional response to iron limitation and <i>fur</i> inactivation	87
4.3.1	Regulatory potential of CacFur	88
4.3.2	Fur-Fe ²⁺ regulon	90
4.3.2.1	Genes involved in iron acquisition	92
4.3.2.2	Genes involved in energy metabolism	93
4.3.3	Role of the riboflavin biosynthesis	96
4.3.4	Additional transcriptional changes in response to iron limitation and <i>fur</i> gene inactivation	97
4.4	Other genes with predicted role in iron transport and metabolism in <i>C. acetobutylicum</i>	98
5	Summary	100
6	References	101
7	Appendix	118
	Acknowledgements	137
	Selbstständigkeitserklärung	139

Abbreviations

2D-PAGE	two-dimensional polyacrylamide gel electrophoresis
A	adenine, Ampere
Amp	ampicillin
AP	alkaline phosphatase
Asp	aspartic acid
ATCC	American Type Culture Collection
ATP	adenosine 5'-triphosphate
<i>B.</i>	<i>Bacillus</i>
bp	base pair
BSA	bovine serum albumin
°C	degree Celsius
C	cytosine, carbon
<i>C.</i>	<i>Clostridium</i>
C-	carboxy-
Cam	chloramphenicol
CAS	Chrome Azurol-S
cfu	colony forming units
CGM	Clostridial Growth Medium
CHAPS	3-[(3-cholamidopropyl) dimethylammonio]-1-propanesulfonate
COG	Cluster of Orthologous Groups
Cys	cysteine
Da	Dalton
dH ₂ O	distilled water
DIG	digoxigenin
DNA	deoxyribonucleic acid
DNase	deoxyribonuclease
dNTP	2'-deoxynucleoside 5'-triphosphate
DOPE	Discrete Optimized Protein Energy
DP	2,2'-dipyridyl
DTT	dithiothreitol
<i>E.</i>	<i>Escherichia</i>
EDTA	ethylene diamine tetraacetate
EGTA	ethylene glycol tetraacetic acid
Erm	erythromycin
<i>et al.</i>	and others
Fd	ferredoxin

Fig.	Figure
FPLC	Fast protein Liquid Chromatography
fw	forward
g	gram
G	guanine
GTP	guanosine 5'-triphosphate
h	hour
<i>H.</i>	<i>Helicobacter</i>
HDTMA	Hexadecyltrimethyl ammonium bromide
His	histidine
ICP-AES	inductively-coupled plasma atomic emission spectroscopy
IEF	isoelectric focusing
IPTG	isopropyl-β-D-thiogalactoside
k	kilo
Kan	kanamycin
kb	kilobase
l	liter
LB	Luria-Bertani medium
μ	micro (10 ⁻⁶)
m	meter, milli (10 ⁻³), 'messenger'
M	molar
MALDI-TOF	matrix-assisted laser desorption ionization time-of-flight
MES	2-(N-morpholino)ethanesulfonic acid
min	minute
mod.	modified
mol	mole
MOPS	3-(N-morpholino)propanesulfonic acid
n	nano (10 ⁻⁹)
N-	amino-
NAD	nicotinamide adenine dinucleotide
NADH	reduced nicotinamide adenine dinucleotide
NBT/BCIP	nitro blue tetrazolium/5-bromo-4-chloro-3-indolyl-phosphate
NTA	Nitrilotriactic acid
o	ortho
OD	optical density
ORF	Open Reading Frame
ox	oxidized
PAGE	Polyacrilamide Gel Electrophoresis
PCR	Polymerase Chain Reaction
pH	negative logarithm of the hydrogen ion concentration

pI	isoelectric point
RACE	rapid amplification of cDNA ends
RAM	'Retrotransposition Activated selectable Marker'
RCA	Reinforced Clostridial Agar
red	reduced
RT-PCR	reverse transcription; real-time PCR
rev	reverse
RNA	ribonucleic acid
RNase	ribonuclease
ROS	reactive oxygen species
rpm	rounds per minute
rRNA	ribosomal RNA
RT	room temperature
s	second
<i>S.</i>	<i>Streptomyces</i>
SDS	sodium dodecyl sulfate
SOE	'Splicing by overlap extension'
sq	semi-quantitative
T	thiamine
Tc	tetracycline
T _m	melting temperature
Tm	thiamphenicol
Tris	Tris-aminomethane
TSS	transcriptional start site
U	Unit
UV	ultraviolet
wHTH	winged helix-turn-helix
WT	wild-type
w/v	weight per volume
V	volt
Vol.	volume
vs.	<i>versus</i>
v/v	volume per volume
X-gal	5-bromo-4-chloro-3-indolyl-b- β -galactopyranoside

1 Introduction

During the first billion years of life on Earth the environment was anaerobic and ferrous iron (Fe^{2+}) was abundantly available (Imlay, 2006). Because of its unique physicochemical properties, iron has been incorporated into numerous proteins serving as a catalyst or electron carrier (Andrews *et al.*, 2003). This choice in the early steps of evolution rendered the biological systems strongly dependent on iron. Today iron is an indispensable micronutrient for virtually all bacterial species. It plays a paramount role in many biological processes, such as DNA biosynthesis, respiration, H_2 production and consumption among others (Andrews *et al.*, 2003). However, the transition from the anaerobic to the aerobic era about 2 billion years ago significantly altered the predominant chemistry of iron (Frausto da Silva and Williams, 2001; Andrews *et al.*, 2003). The oxidation of ferrous (Fe^{2+}) to ferric (Fe^{3+}) iron has led to formation of highly insoluble $\text{Fe}(\text{OH})_3$ complexes (Crichton, 2001). Thus, although plentiful in most ecological niches, this transition metal is not readily available for the biological systems (Fig. 1.1). On the other hand, excess of intracellular unincorporated iron could promote via the Haber-Weiss-Fenton reaction formation of reactive oxygen species (ROS) (Fig. 1.2), which might compromise key cellular structures (Imlay *et al.*, 1988; 2003). In order to address these issues, aerobic and facultative bacteria have developed a number of strategies.

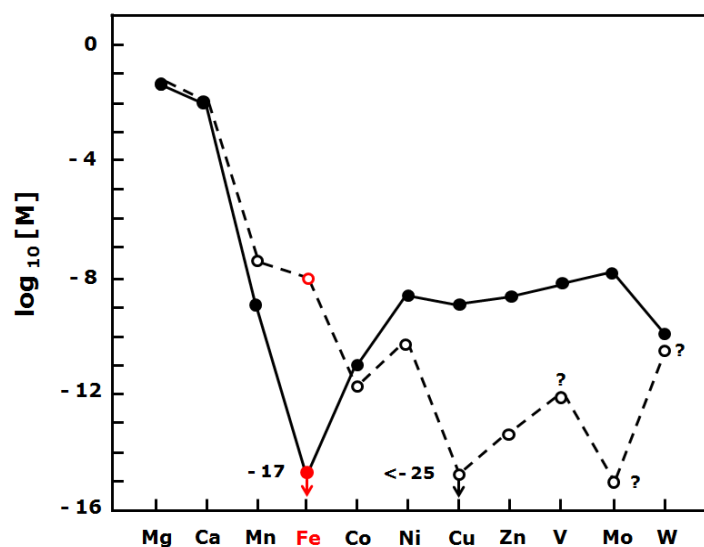


Fig. 1.1 Dramatic reduction in the bioavailability of iron upon transition from the anaerobic to the aerobic era (adapted from Frausto da Silva and Williams, 2001). Concentration of selected metals [M] in the primitive sulphide sea (open symbols) and the aerobic sea (closed symbols), which reflects the relative availability of these elements for the biological systems.

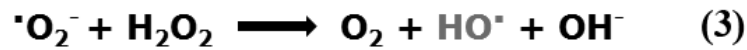
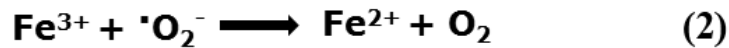


Fig. 1.2 Mechanism of iron-induced toxicity in the biological systems (adapted from Crichton, 2001). Increased intracellular free iron levels could lead to formation via the Fenton reaction (1) of HO \cdot , a highly reactive oxidant. Superoxide (O $_2^\cdot$) can reduce Fe $^{3+}$ to Fe $^{2+}$ and molecular O $_2$ (2). The sum of reaction (2) and the Fenton reaction (1) is the so-called Haber-Weiss reaction (3).

To capture limiting iron from the environment almost all aerobic microorganisms synthesize and export low-molecular-weight high-affinity chelators termed siderophores ("sideros phoros", iron carriers) (Neilands, 1995; Wandersman and Delepelaire, 2004; Miethke and Marahiel, 2007). The resultant Fe(III)-siderophore complexes are subsequently transported back into the cell via dedicated uptake systems, followed by release of iron into the intracellular milieu (Köster, 2001). Alternatively, Fe $^{3+}$ is solubilised through reduction by cell-surface associated or extracellular assimilatory ferric iron reductases (Schröder *et al.*, 2003). On the other hand, to combat the deleterious effect of ROS, bacteria employ sophisticated adaptive detoxification and repair systems, which include catalase (Kat), superoxide dismutase (SOD) and alkyl hydroperoxide reductase (AhpCF) (Imlay, 2003; 2008). But most importantly microorganisms had to establish molecular mechanisms for effective monitoring and dynamic control of the intracellular iron content so that it meets the metabolic requirements of the cell.

The paradigm of the bacterial iron-dependent response is the ferric uptake regulator (Fur) protein as originally described more than 30 years ago in *Escherichia coli* (Hantke, 1981; Bagg and Neilands, 1987). Since then Fur orthologs have been identified and characterized in numerous Gram-negative as well as Gram-positive bacteria (Lee and Helmann, 2007). Many of these homologues were able to complement Fur deficiency in *E. coli fur* mutants, suggesting that the molecular mechanisms of Fur-dependent regulation are conserved among bacteria (Escobar *et al.*, 1999). Alternatively, in *Corynebacterium* spp. and *Mycobacterium* spp. responsible for maintenance of an adequate iron status are the functionally analogous DtxR and IdeR proteins (Brune *et al.*, 2006; Ranjan *et al.*, 2006; Rodriguez, 2006; Wennerhold and Bott, 2006).

Fur is an iron-sensing homodimeric metalloprotein, which serves as a transcriptional repressor of genes implicated in iron acquisition and storage (Hantke, 2001; Andrews *et al.*, 2003). The Fur monomer (17-19 kDa) is characterized by a bipartite structural organization composed of an N-terminal DNA-binding domain (DBD), which adopts a canonical winged helix-turn-helix fold (wHTH), and C-terminal dimerization domain (DD) (Coy and Neilands, 1991; Stojiljkovic and

Hantke, 1995; Lee and Helmann, 2007). In addition to the regulatory Fe(II)-binding site, structural and biochemical studies have established Zn(II) as a structural element of several characterized Fur regulators (Jacquamet *et al.*, 1998; Althaus *et al.*, 1999; Dian *et al.*, 2011; Butcher *et al.*, 2012). Fig. 1.3 depicts the classical model of Fur-mediated regulation in response to changing levels of iron in the environment. Under iron-sufficient conditions, Fur interacts with a conserved motif, known as a Fur box, in the promoter region of genes involved in iron uptake, thereby preventing access of the RNA polymerase (Escolar *et al.*, 1999; Andrews *et al.*, 2003). Conversely, when iron is scarce the Fur protein is no longer associated with its co-repressor Fe^{2+} , leading to derepression of the corresponding genes.

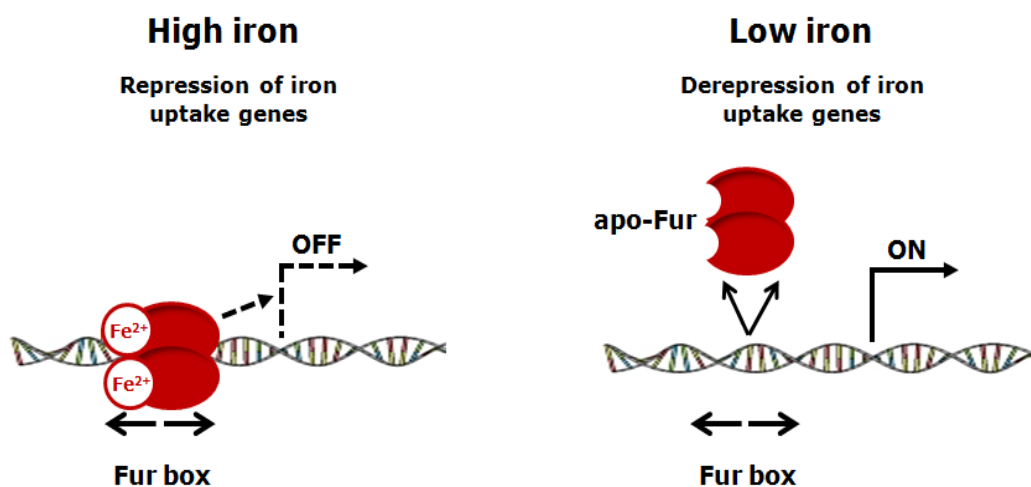


Fig. 1.3 Classical model of iron-dependent Fur regulation in bacteria (adapted from Andrews *et al.*, 2003).

More recent discoveries have highlighted a functional diversity within the Fur family of proteins defining several subclasses (Fig. 1.4). Members of the Fur protein family have been demonstrated to exert control on zinc (Zur, zinc uptake regulator), manganese (Mur, manganese uptake regulator) and nickel (Nur, nickel uptake regulator) homeostasis in bacteria (Patzner and Hantke, 1998; Gaballa and Helmann, 1998; Diaz-Mirelez *et al.*, 2004; Ahn *et al.*, 2006). Fur-like proteins sense also signals other than metal ions (Lee and Helmann, 2007). For instance, PerR (peroxide regulon repressor), originally discovered in *Bacillus subtilis*, is a metalloprotein, which controls a hydrogen peroxide-inducible repertoire of genes involved in oxidative stress defence (Chen *et al.*, 1995; Bsat *et al.*, 1998; Lee and Helmann, 2006a).

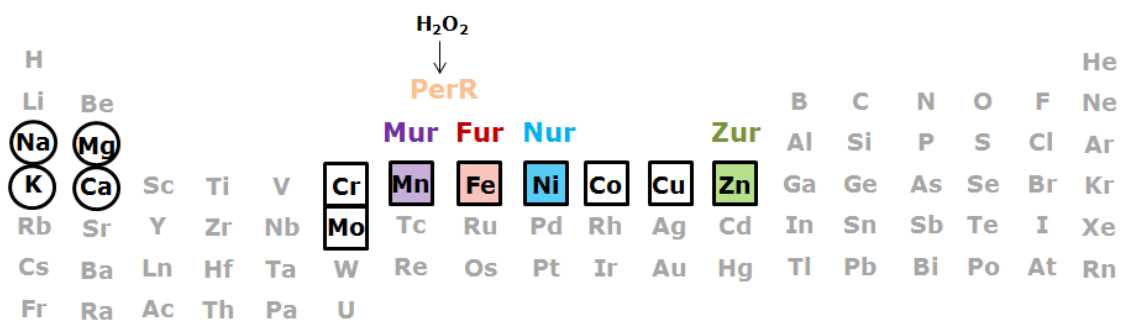


Fig. 1.4 Role of the Fur family of regulators in maintenance of homeostasis of biologically significant metal ions and response to oxidative stress in bacteria (adapted from Frausto da Silva and Williams, 2001 and Giedroc and Arunkumar, 2007). Bulk biological metals are indicated in circles and important trace metals in squares. PerR binds Fe²⁺ or Mn²⁺ to a metalloreulatory site, senses intracellular H₂O₂ levels by metal-catalysed histidine oxidation and regulates accordingly the transcription of genes involved in oxidative stress defence (Lee and Helmann, 2006a).

In addition to redox conditions, bioavailability of iron in the environments is also influenced by competitive pressure from other organisms, as well as by some common variables like pH, temperature and ionic strength (Crichton, 2001; Fabiano *et al.*, 1994; Liu and Millero, 2002). For pathogenic microorganisms the access to this essential micronutrient is further affected by the host defence mechanisms, which employ iron-sequestration proteins such as albumin, transferrin and lactoferrin (Braun and Killmann, 1999). Thus, iron could be considered as a cue for adaptation to a particular microenvironment. Consistently, the role of the iron-responsive regulators is not solely confined to direct control of iron supply, but also involves a broad array of processes including redox- and acid-stress resistance, virulence, motility, quorum sensing, energy and carbon metabolism, among others (Boyd *et al.*, 1990; Foster and Hall, 1992; Ratledge and Dover, 2000; Hantke, 2001; Bijlsma *et al.*, 2002; McHugh *et al.*, 2003; Oglesby *et al.*, 2008; da Silva Neto *et al.*, 2009). Therefore, Fur as well as the functionally equivalent DtxR and IdeR, are now appreciated as global, pleiotropic regulators.

The role of the iron-responsive regulators has been extensively studied in aerobic and facultative microorganisms. However, the mechanisms for maintenance of iron homeostasis in strictly anaerobic bacteria have received less attention. This arises from the fact that in the anoxic environments, bioavailable form of iron is expected to be sufficiently accessible. Moreover the lack of oxygen in these habitats prevents formation of detrimental ROS. Therefore, the need for a sophisticated system coordinating an iron-dependent response in free-living strict anaerobes is not apparent. The Gram-positive, endospore-forming bacterium *Clostridium acetobutylicum* is a classical representative of this group. *C. acetobutylicum* is characterized by a biphasic fermentation pattern and complex cell cycle (Jones *et al.*, 1982; Jones and Woods, 1986). It ferments sugars to the organic acids acetate and butyrate with concomitant release of H₂ and

CO₂ during the exponential growth phase (acidogenesis) and switches to formation of the solvents ethanol, acetone and butanol upon entry into the stationary phase (solventogenesis) (Fig. 1.5) (Jones and Woods, 1986). The latter has attracted much interest as an attractive biofuel (Dürre, 2007; Lee *et al.*, 2008; Ni and Sun, 2009). Therefore, *C. acetobutylicum* has been a subject of an

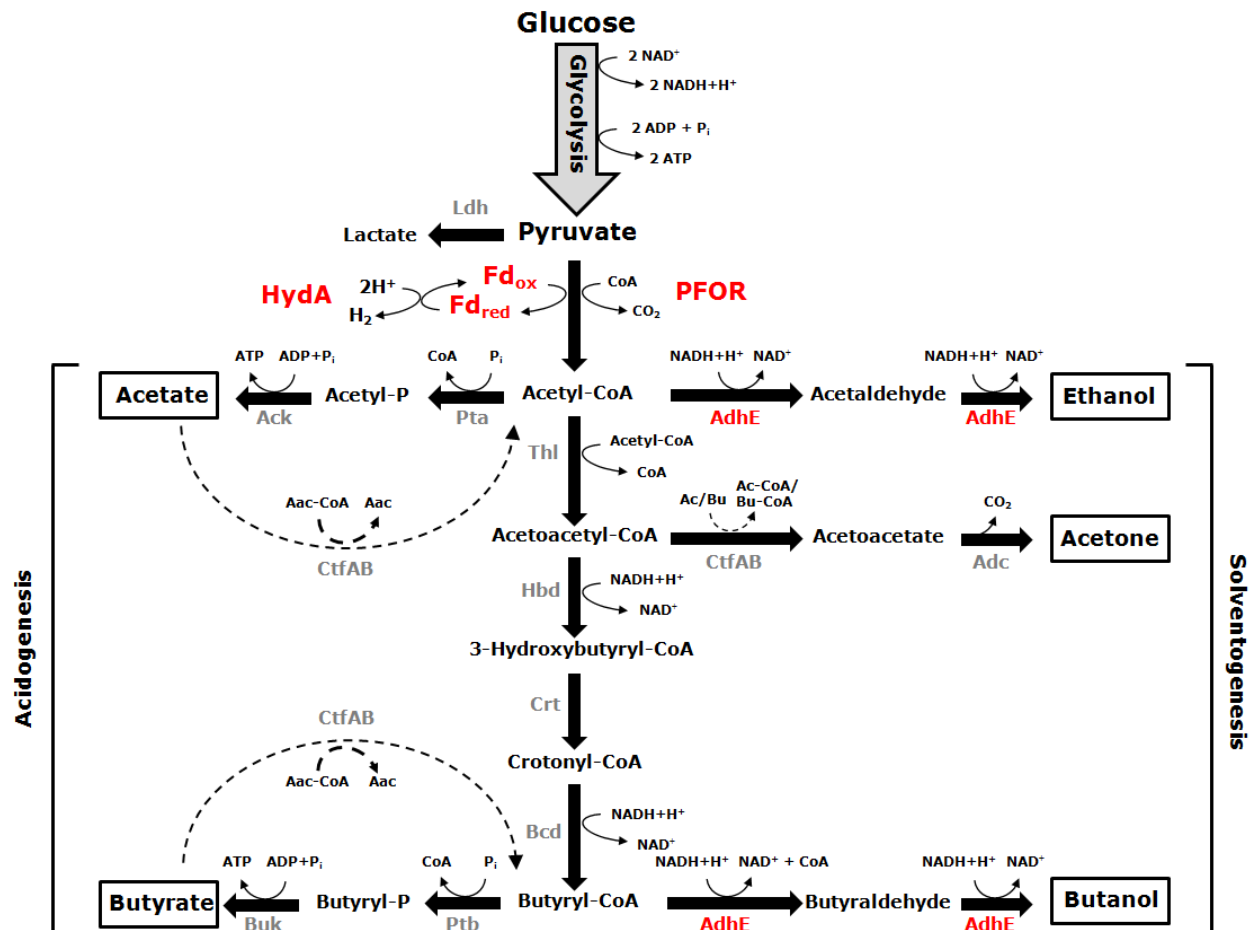


Fig. 1.5 Significance of iron for the central metabolic pathways in *C. acetobutylicum* (adapted from Lütke-Eversloh and Bahl, 2011). Experimentally determined and predicted iron-containing proteins are indicated in red (Jones and Woods, 1986; Meinecke *et al.*, 1989; Fischer *et al.*, 1993; Demuez *et al.*, 2007). Ldh, lactate dehydrogenase; HydA, hydrogenase; PFOR, pyruvate:ferredoxin oxidoreductase; Fd, ferredoxin; Pta, phosphotransacetylase; Ack, acetate kinase; AdhE, aldehyde/alcohol dehydrogenase; CtfAB, acetoacetyl-CoA:acyl-CoA transferase; Adc, acetoacetate decarboxylase; Thl, thiolase; Hbd, 3-hydroxybutyryl-CoA dehydrogenase; Crt, crotonase; Bcd, butyryl-CoA dehydrogenase; PtB, phosphotransbutyrylase; Buk, butyrate kinase; AAc, acetoacetate; AAc-CoA, acetoacetyl-CoA; Ac/Bu, acetate/butyrate; Ac-CoA/Bu-CoA, acetyl-CoA/ butyryl-CoA; ox, oxidized; red, reduced.

active investigation in the recent years, in order to better understand its complex multi-branched central metabolism with the ultimate goal to optimize productivity (Lehmann and Lütke-Eversloh, 2011; Lehmann *et al.*, 2012a, b; Cooksley *et al.*, 2012). The primary metabolic pathways in this microorganism are strongly dependent on iron due to participation of key iron-containing proteins, including the H₂-evolving hydrogenase (HydA), pyruvate:ferredoxin oxidoreductase

(PFOR) and the electron carrier ferredoxin (Fig. 1.5). Previous studies have demonstrated a pronounced effect of iron availability on the physiology of *C. acetobutylicum* and suggested a more complex iron-dependent regulation (Bahl *et al.*, 1986; Junelles *et al.*, 1988; Peguin and Soucaille, 1995). Sequencing of the genome of *C. acetobutylicum* allows now the interpretation of these results in light of the coding sequence (Nölling *et al.*, 2001).

The genome of *C. acetobutylicum* has revealed a plethora of putative metalloregulatory proteins, including three Fur homologs (CAC0951, CAC1682 and CAC2634) (Nölling *et al.*, 2001). Previous studies have established the role of CAC2634 as a PerR regulator, which controls an assortment of genes involved in oxidative stress defence (Hillmann *et al.*, 2008; 2009b). In fact, *C. acetobutylicum* has been demonstrated to be far from defenceless and able to tolerate limited exposure to ambient air (O'Brien and Morris, 1971; Kawasaki *et al.*, 2004). Based on these results, it could be implied that this microorganism might experience periodically aeration in its natural microenvironments. This necessitates a sophisticated system for iron-dependent regulation that would sense and respond to the special requirements of a strictly fermentative anaerobe (Vasileva *et al.*, 2012). This work represents an initial study on the molecular mechanisms for maintenance of iron homeostasis in *C. acetobutylicum*. A comparative modelling and experimental analysis of CAC0951 and CAC1682 allowed the identification of a functional ferric uptake regulator (Fur) protein. The role of Fur in the lifestyle of *C. acetobutylicum* was investigated by employing a combined physiological, transcriptomic and proteomic approach. Collectively, the results obtained in the presented study demonstrate that maintenance of a proper intracellular iron status is an important facet for this microorganism and emphasize the central role of Fur in this process.

2 Materials and Methods

2.1 Bacterial strains and plasmids

The bacterial strains, vectors and recombinant plasmids, employed in this study are listed in Table 7.1, Table 7.2 and Table 7.3 (Appendix), respectively.

2.2 Oligonucleotides

All oligonucleotides used in this study are listed in Table 7.4 (Appendix).

2.3 Media and growth conditions

All media and thermostable supplements were autoclaved for 20 min at 121 °C. Thermolabile additives were sterilized by filtration (0.2 µm pore size, Sarstedt).

2.3.1 Growth media for *E. coli*

LB medium (Sambrook and Russell, 2001)

Trypton	10	g
Yeast extract	5	g
NaCl	10	g
dH ₂ O up to	1000	ml

* For preparation of agar plates the medium was supplemented with 1.5 % [w/v] agar.

** In order to meet the performance specifications for the β-galactosidase assay (see 2.15.5.1), liquid LB medium was supplemented with 100 µM FeSO₄, where indicated.

MacConkey-lactose agar medium

Enzymatic digest of gelatine	17	g
Enzymatic digest of caseine	1.5	g
Enzymatic digest of animal tissue	1.5	g
Lactose	10	g
Bile salts	5	g
NaCl	5	g
Agar	12	g
Neutral red	0.05	g
dH ₂ O up to	1000	ml

* The medium was supplemented with FeSO₄ as indicated.

CAS agar medium (Schwyn and Neilands, 1987)

PIPES	30.24	g
10x MM9	100	ml
NaOH	6	g
Agar	15	g
dH ₂ O	750	ml
Casamino acids (10% [w/v]) *	30	ml
Glucose (20 % [w/v]) *	10	ml
MgCl ₂ (1 M) *	1	ml
CaCl ₂ (100 mM) *	1	ml
Thiamine.HCl (0.2 % [w/v]) *	1	ml
L-Tryptophan (1 % [w/v]) *	3	ml
CAS-HDTMA solution *	100	ml

* These components were added to the medium from sterile stock solutions after autoclavation and cooling to 50 °C.

10x MM9

KH ₂ PO ₄	3	g
NaCl	5	g
NH ₄ Cl	10	g
dH ₂ O up to	1000	ml

CAS solution

CAS	60.5	mg
dH ₂ O	50	ml
1 mM FeCl ₃ (dissolved in 10 mM HCl)	10	ml

HDTMA solution

HDTMA	72.9	mg
dH ₂ O	40	ml

The CAS and HDTMA solutions were mixed slowly under stirring and the resulting solution was autoclaved.

2.3.2 Growth media for *B. subtilis***TBAB agar medium**

Trypton	10	g
Beef extract	3	g
NaCl	15	g
Agar	15	g
dH ₂ O up to	1000	ml

Minimal medium with low-phosphate content (Chen *et al.*, 1993)

MOPS (adjusted to pH 7.4 with 2 M KOH)	40	mM
Potassium phosphate (pH 7.0)	2	mM
Glucose *	20	g/l
(NH ₄) ₂ SO ₄	2	g/l
MgSO ₄ ·7 H ₂ O	0.2	g/l
Na ₃ -Citrate·2 H ₂ O	1	g/l
Potassium glutamate	1	g/l
Tryptophan *	8	mg/l
FeCl ₃ **	5	μM
(NH ₄) ₆ Mo ₇ O ₂₄	3	nM
H ₃ BO ₄	400	nM
CoCl ₂	30	nM
CuSO ₄	10	nM
ZnSO ₄	10	nM
MnCl ₂	80	nM

* These components were added from sterile stock solutions to the medium after autoclavation.

** Iron-limiting conditions were achieved by omitting FeCl₃ from the medium.

2.3.3 Growth media for *C. acetobutylicum*

Preparation of anaerobic media for *C. acetobutylicum* was performed as described by Breznak and Costilow (1994). Liquid media were boiled in a microwave oven in order to eliminate oxygen and subsequently cooled down to RT while gasing with N₂. Anaerobic Ti-III-NTA solution (2.3.5) was used to reduce trace amounts of oxygen immediately prior to inoculation if necessary.

RCA (Reinforced Clostridial Agar) (Oxoid GmbH, Wesel)

Glucose	5	g
Yeast extract	3	g
Trypton	10	g
NaCl	5	g
Beef extract	10	g
Sodium acetate	3	g
L-cystein-HCl	0.5	g
Starch	1	g
Agar	15	g
dH ₂ O up to	1000	ml

* To mimic iron-limiting conditions the iron chelator 2,2'-dipyridyl (Sigma Aldrich) was added in concentrations of 50, 100 and 150 μM to the RCA agar medium.

CGM (clostridial growth medium) (Wiesenborn *et al.*, 1988, mod.)

Glucose (50 % [w/v]) *	100	ml
Yeast extract	5	g

K ₂ HPO ₄ x 3 H ₂ O	0.75	g
KH ₂ PO ₄	0.75	g
MgSO ₄ x 7 H ₂ O	0.71	g
MnSO ₄ x H ₂ O	10	mg
FeSO ₄ x 7 H ₂ O	10	mg
NaCl	1	g
Asparagine	2	g
(NH ₄) ₂ SO ₄	2	g
Resazurin (0.1 % [w/v])	1	ml
dH ₂ O up to	1000	ml

* Glucose was added from a sterile anaerobic stock solution after autoclavation.

MS-MES (medium synthétique) (Monot *et al.*, 1982, mod.)

Glucose	60	g
K ₂ HPO ₄	0.55	g
KH ₂ PO ₄	0.55	g
MgSO ₄ x 7 H ₂ O	0.22	g
FeSO ₄ x 7 H ₂ O	11	mg
Acetic acid	2.3	ml
PABA (8 mg/l) **	10	ml
Biotin (0.08 mg/l) **	1	ml
MES	21.23	g
Resazurin (0.1 %, [w/v])	1	ml
dH ₂ O up to	1000	ml

* The pH value of the medium was adjusted to 6.6 with NH₄OH before addition of MES.

** These components were added from sterile-filtered stock solutions after adjustment of the pH value.

MS-CaCO₃ agar medium

Glucose	24	g
K ₂ HPO ₄	0.22	g
KH ₂ PO ₄	0.22	g
MgSO ₄ x 7 H ₂ O	0.088	g
FeSO ₄ x 7 H ₂ O	4.4	mg
Acetic acid	0.92	ml
PABA (8 mg/l) **	2	ml
Biotin (0.08 mg/l) **	0.4	ml
CaCO ₃	0.8	g
Agarose	6	g
dH ₂ O up to	400	ml

* The pH value of the medium was adjusted to 6.6 with NH₄OH before the addition of CaCO₃.

** These components were added from sterile-filtered stock solutions after adjustment of the pH value.

2.3.4 Antibiotics and additives

For the purpose of selection and screening, media contained antibiotics or additives listed in Table 2.1. Stock solutions were prepared according to Sambrook and Russell (2001), sterilized by filtration (0.2 µm pore size, Sarstedt), aliquotted and stored at - 20 °C.

Table 2.1 Antibiotics and additives

Antibiotics or additives	Stock solution/ Solvent	Final concentration		
		<i>E. coli</i>	<i>B. subtilis</i>	<i>C. acetobutylicum</i>
Ampicillin (Amp)	50 mg/ml/ sterile dH ₂ O	100 µg/ml	-	-
Chloramphenicol (Cam)	34 mg/ml/ 96 % ethanol [v/v]	25 µg/ml	5 µg/ml	-
Kanamycin (Kan)	50 mg/ml/ sterile dH ₂ O	30 µg/ml	-	-
Tetracycline (Tc)	10 mg/ml/ 50 % ethanol [v/v]	5 µg/ml	-	-
Erythromycin (Erm)	50 mg/ml/ 96 % ethanol [v/v]	-	-	30 µg/ml
Thiamphenicol (Tm)	15 mg/ml/ 96 % ethanol [v/v]	-	-	15 µg/ml
X-Gal	20 mg/ml/ Dimethylformamide	50 µg/ml	-	-

2.3.5 Titan-(III)-NTA solution

Titan-(III)-NTA solution was prepared as described previously (Mann, 2012).

2.3.6 Growth conditions

Strains of *E. coli* and *B. subtilis* have been propagated under aerobic conditions in Erlenmeyer flasks or on agar medium. Liquid cultures were grown on a rotary shaker (180 rpm) at 37 °C. Cultures of *C. acetobutylicum* have been grown under anaerobic conditions in Hungates or Müller & Krempel serum bottles or on solid medium as described in detail by Lehmann (2012).

2.4 Storage of strains and control of purity

Frequently used *E. coli* and *B. subtilis* strains were stored on agar plates for up to two months at 4 °C. For long-term storage, glycerol stock cultures were prepared by adding 1 ml of an exponentially grown culture to 500 µl LB-glycerol solution (60 % [v/v] glycerol and 40 % [v/v] LB medium) in sterile flasks. The flasks were appropriately labeled and stored at - 70°C. Strains

of *C. acetobutylicum* were stored as spore suspension at - 20 °C in MS-MES medium (2.3.3). For control of purity, cells from the stock cultures have been routinely restreaked on agar medium supplemented with appropriate antibiotics for selection (Table 7.1 and Table 2.1)

2.5 Analytical procedures

2.5.1 Optical density

Bacterial growth has been evaluated by measuring the optical density (OD) of cell suspensions at 600 nm wavelength in 1 cm single-use plastic cuvettes using a spectrophotometer (Ultraspec® 3000, Amersham, Braunschweig). Water or medium served as blank.

2.5.2 Determination of growth rates

Specific growth rates (μ) of batch cultures were determined using the following equation:

$$\mu \text{ (h}^{-1}\text{)} = \frac{\log x_2 - x_1}{\log e \cdot (t_2 - t_1)}$$

Equation 1 Calculation of specific growth rates (μ). t_1/t_2 , two distinct experimental time points; x_2/x_1 , OD_{600} , measured at two time points from the exponential growth.

2.5.3 pH measurement

Determination of pH values in cell-free supernatants from cultures of *C. acetobutylicum* was performed using a pH meter (pH Meter pH526, WTW GmbH).

2.5.4 Light microscopy

Cell morphology has been documented using a bright-field microscope (Olympus BX41TF-microscope, Olympus Deutschland GmbH, Hamburg) at a magnification of 400X (Objective: A40LP).

2.5.5 Glucose consumption

Glucose concentration in cell-free supernatants from cultures of *C. acetobutylicum* was determined spectrophotometrically using an enzymatic assay as described by Wietzke (2013).

2.5.6 Lactate production

Quantification of D- and L-lactic acid in cell-free culture supernatants from *C. acetobutylicum* was performed using the "D-lactic acid and L-lactic acid" commercial kit (Megazym, Wicklow, Ireland) essentially as described by the manufacturer.

2.5.7 Gas chromatography

Quantification of the accumulated fermentation products (acetate, butyrate, acetone, ethanol and butanol) in cell-free culture supernatants from *C. acetobutylicum* was performed using gas chromatography as described in detail by Lehmann (2012).

2.5.8 Quantification of gaseous fermentation products

Total gas volumes and H₂:CO₂ ratios were measured in the headspace of 50-ml MS-MES (2.3.3) cultures from *C. acetobutylicum* as described by Wietzke (2013).

2.5.9 Riboflavin identification and quantification

2.5.9.1 Visible and fluorescence spectra

Cell-free culture supernatants from *C. acetobutylicum* were tested for presence of flavins spectrophotometrically and fluorimetrically. An aqueous solution of riboflavin (≥ 99 %, Sigma Aldrich) served as a flavin standard. Visible spectra were obtained at a range between 310 and 550 nm wavelength using Spectramax ME2 Multi-Mode Microplate Reader (Molecular Devices). Fluorescence emission spectra were determined using the same device with an excitation beam of 450 nm. Scanning was performed between 480 and 650 nm wavelength.

2.5.9.2 Analytical TLC (Thin Layer Chromatography)

For the purpose of analytical TLC, *C. acetobutylicum* strains of interest were grown in 200 ml MS-MES medium (2.3.3). Cell-free supernatants were then aliquotted, lyophilized (Vacuum Concentrator NVZ150, Zirbus Apparate- und Maschinenbau GmbH, Bad Grund) and stored in the dark at RT until further use. Standards of flavin mononucleotide (FMN) (≥ 70 %, Sigma Aldrich), flavin adenine dinucleotide (FAD) (≥ 95 %, Sigma Aldrich) and riboflavin (≥ 95 %, Sigma Aldrich), as well as the lyophilized supernatants, were dissolved in 96 % pure ethanol. Five µg of each were loaded on a silica gel plate (TLC Silica gel 60 F₂₅₄, Merck). The plate was

afterwards developed in the dark with *n*-butanol: acetic acid: water at a ratio of 4: 1: 5 and the spots were visualized using 302 nm UV light.

2.5.9.3 Quantification of riboflavin

Riboflavin concentration in culture supernatants was quantified spectrophotometrically at 444 nm wavelength with use of a standard curve.

$$\text{riboflavin concentration} \left(\frac{\text{mg}}{\text{ml}} \right) = \frac{\text{Absorbance}_{444} - 0.0720}{12.5640}$$

Equation 2 Quantification of riboflavin in cell-free supernatants from cultures of *C. acetobutylicum*. The equation is based on a standard curve, prepared with aqueous riboflavin solutions of known concentration.

2.5.10 Detection and quantification of siderophores

2.5.10.1 Arnou assay (Arnou, 1937)

The colorimetric Arnou assay was performed to detect and quantify catechol siderophores in culture supernatants. The following reagents were added to 1 ml of cell-free culture supernatant in the exact order given, mixing well after each: 1 ml 0.5 M HCl; 1 ml nitrite-molybdate reagent (catechol siderophores produce a yellow colour) and 1 ml 1M NaOH (the colour changes to red). Absorbance was measured at 510 nm and values were normalized to the optical density (OD₆₀₀) of the corresponding cultures.

Nitrite-molybdate reagent

NaNO ₂	10	g
Na ₂ MoO ₄	10	g
dH ₂ O up to	100	ml

2.5.10.2 Ferric perchlorate assay (Atkin *et al.*, 1970)

The ferric perchlorate assay was employed for detection of hydroxamate siderophores in culture supernatants. This assay is specific for hydroxamates since iron is usually dissociated from catechols at low pH (Payne, 1994). To 0.5 ml of cell-free culture supernatant, 2.5 ml of ferric perchlorate reagent were added and mixed well. Hydroxamate siderophores, if present, produce orange to purple colored complexes (Payne, 1994).

Ferric perchlorate reagent

Fe(ClO ₄) ₃	5	mM
------------------------------------	---	----

HClO₄ 0.1 M

2.5.10.3 CAS liquid assay (Schwyn and Neilands, 1987)

The Chrome Azurol-S (CAS) assay is a universal test used for detection of siderophores irrespective of their structure. It uses an iron-dye complex, which changes its colour from blue to yellow upon loss of iron withdrawn from compounds with higher affinity. The iron-dye complex could be used in a liquid assay or integrated into agar medium (2.3.1) for *in vivo* detection of siderophores. The strains of interest were grown overnight in low-phosphate medium (2.3). 500 µl of cell-free culture supernatant was mixed with 500 µl CAS assay solution and 10 µl shuttle solution. The mixture was incubated for a few minutes at RT and absorbance was recorded at 630 nm wavelength.

CAS assay solution

CAS (2 mM)	7.5	ml
1 mM FeCl ₃ (dissolved in 10 mM HCl)	1.5	ml
HDTMA	50	ml
Piperazine buffer	36.75	ml
dH ₂ O up to	100	ml

HDTMA solution

HDTMA	0.0219	g
dH ₂ O up to	50	ml

Piperazine buffer (pH 5.6)

Piperazine	4.307	g
dH ₂ O up to	30	ml
HCl	6.75	ml

Shuttle solution

Sulfosalicylic acid	0.2	M
---------------------	-----	---

2.5.11 Intracellular iron content

Total iron content in cells of *C. acetobutylicum* was determined using the colorimetric ferrozine assay and a standard curve prepared with FeSO₄ solutions of known concentration (Riemer *et al.*, 2004). Ferrozine forms a complex with ferrous iron, which has an absorption maximum at 550 nm wavelength (Riemer *et al.*, 2004). Cells of *C. acetobutylicum* grown in 50 ml CGM medium (2.3.3) were harvested by centrifugation (10.000 x g, 15 min, 4 °C). In order to remove any

adventitiously associated metal ions, the pellets were washed twice with 10 ml EDTA-containing buffer (50 mM Tris-HCl (pH 8.0), 1 mM EDTA) and once with 10 ml dH₂O. After cell disruption by sonication (2.15.1), crude cell extracts were appropriately diluted with ddH₂O. Aliquots (300 µl) were placed in 2-ml tubes and mixed with 300 µl of 10 mM HCl and 300 µl of freshly prepared iron-releasing solution (150 µl 1.4 M HCl and 150 µl 4.5 % [w/v] KMnO₄) followed by incubation for 2 h at 60 °C. Pre-treatment with the KMnO₄ acidic solution has been reported to be sufficient for release of iron even from iron storage proteins like ferritin (May *et al.*, 1978; Riemer *et al.*, 2004). After the samples had cooled down to RT, iron-detection reagent was added to each vial, followed by incubation for 30 min. The absorbance at 550 nm was afterwards recorded and iron content was calculated according to Equation 3. The obtained quantities were normalized to the protein content in the samples.

$$\text{iron concentration} \left(\frac{\text{nmol}}{\text{mg}} \right) = \frac{\text{Absorbance}_{550} - 0.022}{0.028}$$

Equation 3 Determination of intracellular iron content using the ferrozine assay. The equation is based on a standard curve, prepared with FeSO₄ solutions of known concentration.

Iron-detection reagent

Ferrozine	6.5	mM
Neocuproine	6.5	mM
NH ₄ Acetate	2.5	M
Ascorbic acid	1	M

2.6 Extraction of nucleic acids

2.6.1 Isolation of plasmid DNA from *E. coli*

Analytical and preparative plasmid isolation from cells of *E. coli* was performed according to Birnboim and Doly (1979). Cells grown overnight in 5 ml LB medium (2.3.1) were pelleted by centrifugation (5.000 x g, 10 min, 4 °C) and further treated according to a standard laboratory protocol described by Lehmann (2012).

2.6.2 Isolation of chromosomal DNA from *C. acetobutylicum*

For isolation of chromosomal DNA from *C. acetobutylicum*, 50-ml CGM cultures were grown at 37 °C to an OD₆₀₀ of 1. Cells were then harvested by centrifugation (6.000 x g, 5 min, 4 °C) and stored at - 20 °C until further use. Extraction of chromosomal DNA was conducted according to a

standard laboratory procedure described by Lehmann (2012). The quality of the isolated DNA was monitored on a 1 % agarose gel (2.7.2.1)

2.6.3 Isolation of total cellular RNA from *C. acetobutylicum*

The method used for isolation of total RNA from cells of *C. acetobutylicum* is based on the procedure described by Oelmüller *et al.*, 1990. Cells (30-40 ml) grown to mid-log phase (OD₆₀₀, 1) were harvested by centrifugation (10.000 x g, 1 min, 4 °C). The pellets were resuspended in 1 ml sterile TE buffer, transferred to a 2-ml Eppendorf tube, spun down (13.000 x g, 1 min, 4 °C) and immediately frozen in liquid nitrogen. The samples were stored at - 70 °C until further use. Total cellular RNA was extracted using a standard laboratory SDS-hot phenol protocol, described by Janssen (2010). For the purpose of microarray analysis and sqRT-PCR, the extracted RNA was treated with RNase-free recombinant DNase I (10 U/μl) (Roche Applied Science) according to Janssen (2010).

TE buffer

Tris-HCl (pH 8.0) 10 mM	800 μl from a 1 M stock solution
EDTA 1 mM	160 μl from a 0.5 M stock solution

The pH value of the buffer was adjusted to 8.0 by addition of HCl.

2.7 Standard molecular biology techniques

2.7.1 Purification of DNA

2.7.1.1 Extraction of DNA from agarose gels

'PeqGOLD Gel Extraction Kit' (Peqlab Biotechnologie GmbH) has been routinely used for isolation of electrophoretically separated DNA fragments in the course of this work. After sufficient separation on an agarose gel of suitable concentration and staining with ethidium bromide (2.7.2.1), the fragments of interest were cut with a sharp sterile scalpel under UV light and placed in clean Eppendorf tubes. The DNA fragments were afterwards subjected to purification as recommended by the manufacturer.

2.7.2 Agarose gel electrophoresis

2.7.2.1 Standard agarose gel electrophoresis (Sambrook and Russell, 2001)

Analytical and preparative agarose gel electrophoresis of DNA fragments was carried out in horizontal electrophoresis tanks (Power Pack P 25, Biometra, Göttingen) according to a standard laboratory procedure described by Wietzke (2013).

2.7.2.2 Denaturing agarose gel electrophoresis (Sambrook and Russell, 2001)

For the purpose of Northern hybridization analysis (2.11.3), total cellular RNA was separated on a denaturing agarose gel containing formaldehyde, which prevents formation of secondary structures. 0.5-30 µg of RNA were mixed with 0.2 Vol. loading buffer. The samples were denatured for 10 min at 65 °C, shortly chilled on ice, spinned down and loaded on a 1.5 % [w/v] denaturing agarose gel. The electrophoresis was performed at 60 V in 1x formaldehyde containing running buffer.

Denaturing agarose gel (1.5 % [w/v])

Agarose	0.45	g
dH ₂ O	26.6	ml
Formaldehyde (37 % [w/v])	0.54	g
10x Running buffer	3	ml

The formaldehyde and the 10 x Running buffer were added after autoclavation and cooling of the agarose solution to 50 °C.

Loading buffer

Bromophenol Blue	20	mg
1x Running buffer	25	ml
Glycerine (86 % [v/v])	25	ml
EDTA (0.5 M; pH 8.0)	10	µl

Immediately before use 200 µl of the autoclaved loading buffer were mixed with 24 µl formaldehyde (37 % [v/v]) and 109 µl formamide.

10x Running buffer

MOPS	41.8	g
Na ₂ Acetate x 3H ₂ O	6.8	g
EDTA	3.7	g
dH ₂ O up to	1000	ml

The pH value of the buffer was adjusted to 7.0 with NaOH before autoclavation.

1x Running buffer

10 x Running buffer	100	ml
dH ₂ O	880	ml
Formaldehyde (37 % [v/v])	8.2	ml

Formaldehyde was added after autoclavation of the buffer.

2.8 Manipulation of nucleic acids**2.8.1 PCR primer design**

Primer design for analytical and preparative PCR assays was performed using the Primer3Plus online-based platform (<http://www.bioinformatics.nl/cgi-bin/primer3plus/primer3plus.cgi/>) and T_m values were calculated employing the OligoCalc software (<http://www.basic.northwestern.edu/biotools/oligocalc.html>).

2.8.2 PCR methods**2.8.2.1 Standard PCR procedures**

PeqGOLD *Pwo*-Polymerase (Peqlab, Erlangen) has been routinely used for standard analytical and preparative PCR assays in the course of this study. PCR reactions contained the following components:

Template DNA	10-200	ng
Primer fw (10 μ M)	0.4	μ M
Primer rev (10 μ M)	0.4	μ M
dNTP mix (10 mM)	0.2	mM
<i>Pwo</i> -Polymerase (1 U/ μ l)	1	μ l
10x <i>Pwo</i> complete buffer	5	μ l
MgSO ₄ (25 mM)	2	μ l
dH ₂ O up to	50	μ l

Amplification was performed according to the following PCR program:

Denaturation	94 °C	3	min	}	1x
Denaturation	94 °C	30	s		
Annealing	T_m (Primer) - 3 °C	30	s		29x
Elongation	72 °C	1	min/kb		
Final extension	72 °C	10	min		1x
Storage	4 °C	∞			

2.8.2.2 'High Fidelity' PCR

PCR using 'High Fidelity Enzyme Mix' (Thermo Scientific, Braunschweig) has been performed for amplification of long DNA fragments (> 2 kb). PCR reactions contained the following components:

Template DNA	10-200	ng
Primer fw (10 μ M)	1	μ M
Primer rev (10 μ M)	1	μ M
dNTP mix (10 mM)	0.2	mM
High Fidelity Enzyme Mix (5 U/ μ l)	0.5	μ l
10x High Fidelity PCR Buffer + MgCl ₂ (15 mM)	5	μ l
MgCl ₂ (25 mM)	2	μ l
dH ₂ O up to	50	μ l

Amplification was performed according to the following PCR program:

Denaturation	94 °C	5	min	}	1x
Denaturation	94 °C	30	s		
Annealing	T _m (Primer) - 3 °C	30	s	}	11x
Elongation	68 °C	1	min/kb		
Denaturation	94 °C	30	s	}	21x
Annealing	T _m (Primer) - 3 °C	30	s		
Elongation	68 °C	1	min/kb		
Final extension	68 °C	10	min		1x
Storage	4 °C	∞			

2.8.2.3 'Splicing by overlap extension' (SOE) PCR (Ho *et al.*, 1989)

The Clostron[®] mutagenesis system (2.10) employs a group II intron mobile element for directed insertional disruption of genes in *C. acetobutylicum*. The target specificity of the intron is determined by base-pairing between the target DNA sequence and the intron RNA (Heap *et al.*, 2010). In order to introduce the necessary nucleotide changes within the group II intron 350-bp re-targeting region for disruption of the gene of interest, SOE PCR was performed. The PCR was assembled using a primer mix containing IBS, EBS1d, EBS2 and EBS Universal and the intron-encoding pMTL007 vector as template. For details see (2.10).

IBS Primer (100 μ M)	2	μ l
EBS1d Primer (100 μ M)	2	μ l
EBS2 Primer (20 μ M)	2	μ l
EBS Universal (20 μ M)	2	μ l
dH ₂ O up to	20	μ l

2.8.3 Enzymatic modifications of DNA

2.8.3.1 Digestion with restriction endonucleases

All restriction endonucleases used in this study are listed in Table 2.2.

Table 2.2 Restriction endonucleases

Restriction endonuclease	Target sequence	Buffer system (Thermo Scientific)
<i>Bam</i> HI	5'-G [^] G A T C C-3' 3'-C C T A G [^] G-5'	1x BamHI buffer, 2x Tango TM
<i>Cfr</i> 9I (<i>Xma</i> I)	5'-C [^] C C G G G-3' 3'-G G G C C [^] C-5'	2x Tango TM
<i>Bsp</i> 1407I (<i>Bsr</i> GI)	5'-T [^] G T A C A-3' 3'-A C A T G [^] T-5'	1x Tango TM
<i>Hind</i> III	5'-A [^] A G C C T-3' 3'-T T C G G [^] A-5'	1x Tango TM
<i>Eco</i> 32I (<i>Eco</i> RV)	5'-G A T [^] A T C-3' 3'-C T A [^] T A G-5'	1x Buffer R
<i>Nco</i> I	5'-C [^] C A T G G-3' 3'-G G T A C [^] C-5'	1x Tango TM
<i>Fnu</i> 4HI (<i>Sat</i> I)	5'-G C [^] N G C-3' 3'-C G N [^] C G-5'	1x Buffer G

[^] Restriction site

2.8.3.2 Dephosphorylation of plasmid DNA

Recircularization of plasmid DNA was minimized by treatment with alkaline phosphatase (FastAP, Thermo Scientific). The closed circular plasmid DNA was digested with appropriate restriction enzymes (2.8.3.1). When the digestion was complete, the samples were incubated with 2.5 U FastAP (1 U/ μ l) for 5-30 min at 37 °C in 1x FastAP reaction buffer, followed by heat inactivation for 5 min at 75 °C and purification with 'GeneJET Plasmid Miniprep Kit' (Thermo Scientific) according to the manufacturer's instructions.

2.8.3.3 Ligation

Ligation has been performed employing T4-DNA-Ligase (Thermo Scientific). A molar ratio of vector to insert of 3:1 was used. Ligation mixtures were prepared as follows:

vector DNA	0.1-0.2	μ g
insert	0.3-1	μ g
10x T4-DNA ligase buffer	2	μ l
T4-DNA-ligase	2	μ l
H ₂ O up to	20	μ l

2.9 Construction of recombinant strains

2.9.1 DNA transfer into *E. coli*

2.9.1.1 Preparation of *E. coli* competent cells by CaCl₂ treatment (Hanahan, 1983 mod.)

Preparation of *E. coli* CaCl₂ competent cells was performed according to a standard laboratory procedure described by Fiedler (2006).

2.9.1.2 Transformation into CaCl₂-competent *E. coli* cells

Transformation of CaCl₂-competent cells of *E. coli* was performed according to a standard laboratory protocol described by Lehmann (2012).

2.9.1.3 Preparation of *E. coli* electrocompetent cells (Dower *et al.*, 1988)

For electroporation of *E. coli* strains (ER2275), cells were made electrocompetent following the procedure described below. Cells from a stock culture of the desired *E. coli* strain were streaked on LB agar medium, supplemented with the appropriate antibiotics (Table 7.1 and table 2.1), if necessary, and incubated at 37 °C overnight. A single colony was used to inoculate 5 ml of LB medium and the culture was grown at 37 °C and 180 rpm overnight. On the next day, the 5-ml preculture was used to inoculate 250 ml LB medium and cells were propagated at 37 °C and 180 rpm until an OD₆₀₀ of 0.5-1.0 was reached. The culture was then chilled on ice and pelleted by centrifugation (5.000 x g, 10 min, 4 °C). Cells were washed twice with ice-cold sterile distilled water and once with 30 ml glycerine solution (10 % [v/v]). Finally, the pellets were resuspended in 0.5-0.75 ml of the 10 % [v/v] glycerine solution, aliquotted (40 µl) in sterile 1.5-ml tubes and stored at - 70 °C.

2.9.1.4 Electroporation into *E. coli* cells

Transformation of *E. coli* electrocompetent cells was performed according to a standard laboratory protocol described by Wietzke (2013).

2.9.2 DNA transfer into *B. subtilis*

2.9.2.1 Preparation of *B. subtilis* competent cells (Cutting and Youngman, 1994)

B. subtilis strains to be made competent were streaked on TBAB agar plates (2.3.2) containing the appropriate antibiotics for selection (Table 7.1 and Table 2.1) and incubated at 37 °C overnight. On the next day the cells were used to inoculate 20 ml of freshly prepared SpC medium (OD₆₀₀ 0.5) and the culture was grown at 37 °C with periodic monitoring of the OD₆₀₀ (2.5.1). When stationary phase had been reached, the 20-ml culture was used to inoculate 200 ml fresh pre-warmed SpII medium. After 90 min of incubation at 37 °C, cells were pelleted by centrifugation (5.000 x g, 5 min, RT) and the supernatant was decanted in a sterile container. The cell pellet was gently resuspended in 17 ml of the saved supernatant and 2 ml 70 % [v/v] sterile glycerol solution was added. The competent cells were dispensed into aliquotes of 500 µl in 1.5-ml sterile tubes and stored at - 70 °C until further use.

T-base

(NH ₄)SO ₄	2	g
K ₂ HPO ₄	14	g
KHPO ₄	6	g
Na ₃ -Citrate.2 H ₂ O	1	g
dH ₂ O up to	1000	ml

SpC medium

T-base	20	ml
Glucose (50 % [w/v])	0.2	ml
MgSO ₄ x 7 H ₂ O (1.2 % [w/v])	0.3	ml
Yeast extract (10 % [w/v])	0.4	ml
Casamino acids (1 % [w/v])	0.5	ml

SpII medium

T-base	200	ml
Glucose (50 % [w/v])	2	ml
MgSO ₄ x 7 H ₂ O (1.2 % [w/v])	14	ml
Yeast extract (10 % [w/v])	2	ml
Casamino acids (1 % [w/v])	2	ml
CaCl ₂ (0.1 M)	1	ml

2.9.2.2 Transformation into *E. coli* RR1

E. coli RR1 has been used for plasmid amplification prior to transformation into *B. subtilis* (Raleigh *et al.*, 1988). Plasmid DNA is mainly presented in oligomeric state in this strain, which facilitates the subsequent transfer into *B. subtilis* (2.9.2.3).

2.9.2.3 Transformation into *B. subtilis* competent cells (Cutting and Youngman, 1994)

For transformation of *B. subtilis* strains, competent cells were rapidly thawed at 37 °C and immediately mixed with 1 Vol. SpII medium + EGTA. Plasmid DNA (2.6.1) was added to the cell suspension, followed by incubation at 37 °C for 30-60 min without shaking. Finally, the transformed cells were plated onto selective TBAB agar medium (2.3.2).

SpII medium + EGTA

SpII medium without CaCl ₂	100	ml
EGTA (0.1 M, pH 8.0)	4	ml

2.9.3 Transformation into *C. acetobutylicum* by electroporation

Transformation of *C. acetobutylicum* was performed according to Mermelstein *et al.* (1992). Electrocompetent cells were always prepared freshly. An overnight preculture was used to inoculate a 50-ml CGM culture (OD₆₀₀ ~ 0.3). The cells were grown to an OD₆₀₀ of 1 and further handled according to the following protocol:

1. Incubation for 30 min on ice.
2. Centrifugation: 5 min, 5.000 x g, 4 °C (3K30; Rotor 12150).
3. Resuspension of the pellet in 10 ml electroporation buffer.
4. Centrifugation: 5 min, 5.000 x g, °C (3K30; Rotor 12150).
5. Resuspension of the pellet in 2 ml electroporation buffer.
6. Addition of 400 µl cell suspension and 500 ng plasmid-DNA in a pre-cooled electroporation cuvette (0.4 cm).
7. Incubation for 5 min on ice.
8. Electroporation: 50 µF, 600 Ω, 1.8 kV (time constant 14.8-29.4 ms).
9. Incubation for 4-5 h in 1 ml CGM medium.
10. 250 µl of the transformed cells were plated on RCA medium (2.3.3), supplemented with the appropriate antibiotics for selection (Table 7.1 and Table 2.1).
11. Incubation at 37 °C for 48 h.

Sodium phosphate buffer (pH 7.4)

NaH ₂ PO ₄ (200 mM)	22.6	ml
Na ₂ HPO ₄ (200 mM)	77.4	ml

Electroporation buffer

Sucrose (270 mM)	10	ml
Sodium phosphate buffer	150	μl

2.10 Insertional mutagenesis via the Clostron[®] system

(Heap *et al.*, 2007, 2010)

2.10.1 Intron re-targeting and assembly of recombinant pMTL007C-E2 plasmids

The Clostron[®] system is based on the mobile group II intron element from the *ltrB* gene of *Lactococcus lactis* (Ll.ltrB) (Heap *et al.*, 2007). In order to re-target the group II intron for insertion into the coding sequence of the desired gene, a splicing by overlap extension (SOE) PCR (2.8.2.3) was performed using a set of primers (IBS, EBS1d, IBS2) designed via a computer algorithm (Perutka *et al.*, 2004), the EBS universal primer and the pMTL007 plasmid as an intron template. The amplified 350-bp gene-specific intron fragment was digested with *Hind*III and *Bsp*1407I (an isoshizomer of *Bsr*GI) and cloned into the intron-encoding pMTL007C-E2 vector (Fig. 7.1, Appendix). The resultant recombinant plasmid was then introduced into *E. coli* DH5α for *in vivo* amplification (2.9.1.1 and 2.9.1.2). Transformants were plated on LB medium supplemented with chloramphenicol (25 μg/ml). Positive clones were identified via blue-white screening, followed by test restriction. From these, two representative clones were selected, and the plasmids were subjected to sequencing using the corresponding IBS and EBS1d primers (LGC Genomics, Berlin), in order to exclude any point mutations in the re-targeting regions.

2.10.2 Transformation in *C. acetobutylicum*

Presence of the *Cac*824I restriction endonuclease in *C. acetobutylicum* prevents successful transformation of the recombinant pMTL007C-E2 plasmids into this strain, since it recognizes sequences frequently carried on shuttle vectors used in *E. coli*. To overcome this problem, the purified recombinant pMTL007C-E2 plasmids were first electroporated into *E. coli* ER2275 for *in vivo* methylation (2.9.1.3 and 2.9.1.4). ER2275 harbors a pAN-II plasmid encoding a methyltransferase (ϕ3tI) from the *B. subtilis* ϕ3tI phage, which protects the transformed DNA from degradation in *C. acetobutylicum* (Mermelstein and Papoutsakis, 1993). The pAN-II plasmid

confers resistance to Tc. After electroporation, positive *E. coli* ER2275 clones were selected on LB agar medium supplemented with Cam (25 µg/ml) and Tc (10 µg/ml). Next, the methylated plasmids were isolated, subjected to a test restriction with *Fnu*4HI, and electrotransformed into *C. acetobutylicum* (2.9.3). To select for transformants, cells were plated on RCA agar containing Tm (15 µg/ml) and incubated for two days at 37 °C. Single colonies were used to induce insertion of the re-targeted intron by growing them in 500 µl liquid CGM medium supplemented with 7.5 µg/ml Tm. After 4 h, aliquots were plated on RCA agar plates containing 30 µg/ml erythromycin and cells were incubated for 48 h at 37 °C.

2.10.3 Verification of Clostron[®] insertional mutants

The erythromycin resistant clones were initially screened for presence of the desired insertion by colony PCR (2.8.2.1) at the gene-intron junction using the intron-specific EBS Universal primer and either forward or reverse gene-specific primer, depending on whether the intron is integrated into the sense or the antisense DNA strand. Furthermore, whole gene PCR amplification (2.8.2.2) and Southern hybridization analysis (2.11.2) were performed to confirm the correct insertion of the intron sequence and to rule out multiple incorporations into the genome.

2.11 DNA and RNA blotting techniques

2.11.1 Probe labeling

Digoxigenin (DIG)-labeled DNA hybridization probes have been generated using a 'DIG Labeling DNA Kit' (Roche Applied Science) as described by the manufacturer.

2.11.2 Transfer of DNA onto a membrane (Southern blot)

Transfer of DNA onto a nylon membrane (Roti[®]-Nylon plus, Carl Roth GmbH) was performed by capillary blotting. Genomic DNA from the *C. acetobutylicum* strains of interest was extracted (2.6.2), digested with the appropriate restriction enzymes (Table 2.6) and separated on a 0.8 % agarose gel (2.7.1). Prior to blotting, the gel was incubated with 0.25 M HCl for 10 min at RT. The acid treatment facilitates transfer onto the membrane, by partial depurination of the DNA fragments, which in turn leads to strand cleavage. The gel was afterwards subjected to denaturation, followed by neutralization for 30 min at RT. During that time, a sheet of nylon membrane and five pieces of Whatman blotting paper (Schleicher und Schüll BioScience, Dassel) were cut to the dimensions of the gel. The membrane and the gel were then equilibrated for 5 min in 2x SSC buffer and the blot was assembled. To achieve the latter, 5 layers of Whatman paper,

presoked in 2x SSC buffer, were positioned on a 5-10 cm stack of paper towels. Next, the nylon membrane was laid down on the Whatman papers and the agarose gel was placed on top avoiding formation of bubbles between the layers. Finally, a glass plate was put on the gel and a weight of about 500 g was applied to the blotting sandwich. The 'semi dry' blot transfer was completed in 16-24 h and the membrane was subjected to UV cross-linking (120 kJ, 245 nm) in a UV Illuminator (Technique). The membrane was afterwards stored at 4 °C or immediately hybridized to a DIG-labeled probe (2.11.2.1).

20x SSC Buffer

NaCl	75	g
Na ₃ -Citrate.2 H ₂ O	88.2	g
dH ₂ O up to	1000	ml

The pH value of the buffer was adjusted to 7.0 with HCl.

Denaturation buffer

NaCl	35.06	g
NaOH	16	g
dH ₂ O up to	1000	ml

Neutralisation buffer

NaCl	87.76	g
Tris	60.55	g
dH ₂ O up to	1000	ml

The pH value of the buffer was adjusted before autoclavation to 7.5 with HCl.

2.11.2.1 Southern hybridization

The cross-linked nylon membrane was placed in a hybridization tube with 20 ml of pre-hybridization buffer and incubated for 1 h at 42 °C in order to avoid non-specific binding. The DIG-labeled DNA probe (2.11.1) was then denatured at 100 °C for 10 min and mixed immediately with 5 ml of hybridization solution. Incubation with the DNA probe was performed for 16-24 h at 42 °C in a hybridization oven under constant rotation (Biometra, Göttingen). The membrane was afterwards washed twice with 2x SSC, 0.1 % [w/v] SDS solution for 5 min at RT. The membrane was directly subjected to detection (2.11.2.2).

Hybridization solution

20 x SSC buffer	25	ml
Formamide (deionized)	50	ml
SDS (10 % [w/v])	200	µl
L-Lauroylsarcosine(20 % [w/v])	200	µl

Blocking reagent	2	g
dH ₂ O up to	100	ml

2.11.2.2 Immunological detection (Southern blot)

Chromogenic detection of the DIG-labeled probes was performed employing an Anti-Digoxigenin-AP conjugate (Roche Applied Science) and the AP substrates NBT (Nitro-Blue-Tetrazolium chloride) and BCIP (5-Bromo-4-Chloro-3'-Indolyphosphate) (Roche Applied Science). After hybridization and stringency washes with 2x SSC, 0.1 % SDS solution (2.11.2.1), the cross-linked nylon membrane was rinsed shortly in Buffer 1 (washing buffer) and incubated for 1-2 h in Buffer 2 (blocking buffer). After a second 5-min washing step, the membrane was incubated for 30 min with Antibody solution and washed twice for 15 min. Finally, the membrane was equilibrated for 2 min with Buffer 3 (detection buffer) and developed with 3-4 ml Staining solution. After sufficient staining had developed, the reaction was stopped with distilled water.

Buffer 1

Tris-HCl (1 M; pH 8.0)	100	g
NaCl	8.76	g
dH ₂ O up to	1000	ml

The pH value of the buffer was adjusted to 7.5 with HCl.

Buffer 2

Blocking reagent (Roche Applied Science)	1	g
Buffer 1	100	ml

Buffer 3

Tris-HCl (1 M; pH 8.0)	100	g
NaCl	5.84	g
MgCl ₂	4.76	g
dH ₂ O up to	1000	ml

The pH of the buffer was adjusted to 9.5 with NaOH.

Antibody solution (1:5000)

Anti-Digoxigenin-AP (Roche Applied Science)	4	μl
Buffer 1	20	ml

Staining solution

CDP-Star [®] (Roche Applied Science)	50	μl
Buffer 3	5	ml

2.11.3 Transfer of RNA onto a membrane (Northern blot)

Transfer of RNA onto a nylon membrane (Roti[®]-Nylon plus, Carl Roth GmbH) was performed by capillary blotting. Total RNA from cells of *C. acetobutylicum* was extracted (2.6.3) and separated on a 1 % denaturing agarose gel (2.7.2.2). Prior to blotting, the gel was incubated with 50 mM NaOH for 5 min at RT followed by neutralisation with 0.1 M Tris-HCl (pH 7.4) for 5 min. During that time, a sheet of nylon membrane and five pieces of Whatman blotting paper (Schleicher und Schüll BioScience, Dassel) were cut to the dimensions of the gel. The membrane and the gel were then equilibrated in 10x SSC buffer and the blot was assembled as described in (2.11.2). The 'semi dry' blot transfer was completed in 16-24 h and the membrane was subjected to UV cross-linking (120 kJ, 245 nm) in a UV Illuminator (Techne). The membrane was afterwards stored at 4 °C or immediately hybridized to a DIG labeled probe (2.11.3.1).

2.11.3.1 Northern hybridization

The cross-linked nylon membrane was placed in a hybridization tube with 20 ml of pre-hybridization buffer and incubated for 1-2 h at 42 °C in order to avoid non-specific binding. The DIG-labeled DNA probe (2.11.1) was then denatured at 100 °C for 10 min and mixed immediately with 5 ml of hybridization solution. Incubation with the DNA probe was performed for 16-24 h at 42 °C in a hybridization oven under constant rotation (Biometra, Göttingen). The membrane was afterwards washed twice with 2x SSC, 0.1 % SDS solution for 5 min at RT and twice with 0.1x SSC, 0.1 % [w/v] SDS solution for 15 min at 68 °C. The membrane was directly subjected to detection (2.11.3.2).

Hybridization solution

20x SSC buffer	12.5	ml
Na-Phosphate buffer (0.5 M; pH 7.2)	5	ml
Formamide (deionized)	25	ml
SDS (10 % [w/v])	3.5	g
L-Lauroylsarcosine (20 % [w/v])	50	µl
Blocking reagent	1	g
dH ₂ O	100	ml

2.11.3.2 Immunological detection (Northern blot)

The detection of DIG-labeled probes was performed employing an Anti-Digoxigenin-AP conjugate (Roche Applied Science) and the chemiluminescent AP substrate CDP. Dephosphorylation of CDP by AP is accompanied by release of visible light at 466 nm wavelength. Light emission has been recorded using the imaging system STELLA 2000 (Raytest

Isotopenmessgeräte GmbH, Straubenhardt). After hybridization and stringency washing, the cross-linked nylon membrane was washed for 1 min with Washing buffer (Buffer 1 + 0.3 % Tween-20), followed by incubation for 30 min in 40 ml Buffer 2 (blocking buffer). Next, the membrane was incubated with 20 ml Antibody solution for 30 min, washed twice for 15 min and equilibrated for 2 min in Detection solution. Finally, the membrane was developed with 3-4 ml CDP-*Star*[®] solution (Roche Applied Science) for 5 min, packed in nylon foil and subjected to detection. Images have been processed and documented using the AIDA software (Raytest Isotopenmessgeräte GmbH, Straubenhardt).

Buffer 1

Maleic acid (1 M; pH 8.0)	11.6	g
NaCl	8.76	g
dH ₂ O up to	1000	ml

The pH value of the buffer was adjusted to 7.5 with HCl.

Washing buffer

Tween-20	300	µl
Buffer 1	100	ml

Buffer 2

Blocking reagent (Roche Applied Science)	1	g
Buffer 1	100	ml

Buffer 3

Tris-HCl (1 M; pH 8.0)	100	g
NaCl	5.84	g
MgCl ₂	4.76	g
dH ₂ O up to	1000	ml

The pH of the buffer was adjusted to 9.5 with HCl.

Antibody solution (1:5000)

Anti-Digoxigenin-AP (Roche Applied Science)	4	µl
Buffer 1	20	ml

Staining solution

NBT/BCIP (Roche Applied Science)	50	µl
Buffer 3	5	ml

2.12 Microarray analysis

Microarray experiments were performed in triplicate (n=3) on array slides that contain 3840 oligonucleotides, which represent 99.8 % of all annotated protein-coding genes in *C. acetobutylicum*, as reported by Grimmer *et al.* (2011). To this end, RNA was extracted from the strains of interest and treated with RNase-free DNase I (Roche Applied Science) (2.6.3). Verification of quality of the isolated RNA by agarose gel electrophoresis and quantification of its concentration was performed as described by Janssen (2010). RNA was afterwards reverse-transcribed into cDNA, labeled with Cy3 and Cy5 (GE Healthcare, Munich) and purified as previously described (Janssen, 2010). The protocol for microarray analysis is reported by Hillmann *et al.*, 2009b. In order to rule out any dye-specific effects, dye-swap experiments were performed in this study. Thus, twelve transcriptional scores were attained for each gene. A gene was considered to be differentially transcribed when the average expression ratio (ratio of medians) from all twelve datasets was ≥ 3 or ≤ 0.33 .

2.13 sqRT-PCR

The reliability of the microarray data (2.12) was confirmed by conventional sqRT-PCR analysis. Total cellular RNA was extracted from the *C. acetobutylicum* strains of interest, treated with RNase-free DNase I (Roche Applied Science) (2.6.3) and reverse transcribed into cDNA (see 2.12). cDNA was then appropriately diluted and used as template for the PCR analysis (2.8.2.1). All primers used for the sqRT-PCR assays are listed in Table 7.4. The number of the applied amplification cycles is indicated where appropriate. The obtained DNA fragments were tested on 1 % agarose gels (2.7.2.1).

2.14 5' RACE

Determination of TSS (transcriptional start sites) of the genes of interest was performed using the 2nd Generation Roche 5'/3' RACE Kit as recommended by the manufacturer. Total RNA was extracted from cells of *C. acetobutylicum* and further treated with RNase-free DNase I (Roche Applied Science) (2.6.3). All primers used are listed in Table 7.4. The amplified 5' UTR were tested on 1 % agarose gels (2.7.2.1) and subjected to sequencing (LGC Genomics, Berlin).

2.15 Protein techniques

2.15.1 Preparation of crude extracts

Preparation of crude cell extracts for analytical SDS-PAGE analysis (2.15.3), recombinant protein purification (2.15.6) and 2D-PAGE (2.15.4) has been performed as previously described (Riebe, 2009; Janssen, 2010).

2.15.2 Determination of protein concentration (Bradford, 1976)

Protein concentrations in cell crude extracts (2.15.1) and protein isolates (2.15.6) were quantified by the method of Bradford (Bradford, 1976). Appropriate dilutions (1:2 to 1:200) were prepared with dH₂O and 50 µl from each dilution were mixed with 1 ml of Bradford reagent in a 1-ml plastic single-use cuvette. After 5 min of incubation at RT, the absorbance at 595 nm wavelength was measured (Ultrospec 3000, Amersham Biosciences, Freiburg) against a blank made up of 50 µl dH₂O and 1 ml Bradford reagent. The protein concentrations were estimated using a standard curve prepared with BSA (Albumin Fraction V, Carl Roth GmbH) in the 0 mg/ml to 0.15 mg/ml range.

Bradford reagent

Brilliant-Blue G-250	70	ml
Ethanol (96 % [v/v])	50	ml
H ₃ PO ₄ (85 % [v/v])	100	ml
dH ₂ O up to	1000	ml

The Bradford reagent was stored in the dark at RT.

2.15.3 SDS-PAGE

Electrophoretic separation of proteins (SDS-PAGE) and Coomassie staining of the resultant gels was performed according to Riebe (2009).

2.15.4 2D-PAGE (Schwarz *et al.*, 2007; Janssen *et al.*, 2010)

2.15.4.1 Sample preparation

For 2D-PAGE analysis of soluble proteins from *C. acetobutylicum*, crude cell extracts were prepared (2.15.1) and the protein concentrations quantified (2.15.2). The protein samples were treated according to the following protocol:

1. 300 µg protein aliquotes were lyophilized (Vacuum Concentrator NVZ150, Zirbus Apparate- und Maschinenbau GmbH, Bad Grund).
2. Samples were further used or stored at - 20 °C.
3. The protein pellets were solubilized in 400 µl rehydration buffer.
4. Samples were distributed evenly into separate slots of a Re-swelling tray (GE Healthcare, Munich). The solution is delivered slowly and carefully in order to avoid introduction of air bubbles.
5. IPG-Strips pI 4-7 (Biorad Laboratories, Munich) were positioned with the gel facing down on the solution in each prepared slot and incubated for 12-18 h at RT.

Rehydration buffer

Urea	2.85	g	9	M
Thiourea	0.76	g	2	M
Pharmalyte (3-10) [v/v]	25	µl	0.5	%
CHAPS [w/v]	0.2	g	4	%
DTT	15.4	mg	20	mM
Bromophenol Blue	trace amounts			
dH ₂ O up to	5	ml		

2.15.4.2 Isoelectric focusing (IEF)

Isoelectric focusing (IEF) of the IPG-Strips with the rehydrated protein samples was carried out in a Multiphor II electrophoresis device (GE Healthcare, Munich). The temperature of the cooling plate of the Multiphor II unit was set to 20 °C. About 10 ml of DryStrip Cover Fluid (GE Healthcare, Munich) were pipetted onto the cooling plate and the IPG chamber was positioned on top avoiding introduction of bubbles. The IPG chamber was covered with 10 ml of DryStrip Cover Fluid and the DryStrip Aligner (GE Healthcare, Munich) was placed without bubbles. Afterwards, the IPG-Strips were carefully removed from the slots of the Re-swelling tray, rinsed with distilled water and placed into the adjacent grooves of the DryStrip Aligner with the acidic end at the top of the tray near the anode and the gel side facing up. Two IEF electrode strips were cut to the length of 11 cm, moisturized with distilled water and placed across the cathode and anode ends of the aligned IPG-Strips. Both electrodes were aligned over the electrode strips and pressed down to make contact. Finally, the IPG-Strips were covered with 80 ml DryStrip Cover Fluid to prevent evaporation and electrophoresis was run according to the program given in Table 2.3. The focused IPG-Strips could either be stored at - 20 °C in aluminium foil cover or directly following two equilibration steps further used for 2D SDS-PAGE analysis.

Table 2.3 Isoelectric focusing program

Phase	Voltage (V)	Current (mA)	Power (W)	Vh
1	500	1	5	500
2	500	1	5	1000
3	3500	1	5	10000
4	3500	1	5	31500

2.15.4.3 2D SDS-PAGE

After completion of IEF (2.15.4.2), the focused IPG strips were subjected to SDS-PAGE electrophoresis. Polyacrylamide gels with dimensions 25 x 25 cm were prepared in a casting chamber (Millipore, Schwalbach). Upon full polymerization (after 1.5-2 h), the gels were placed in a horizontal electrophoresis tank (InvestigatorTM 2D Running System, France), filled with 10 l pre-cooled (15 °C) 1x Running buffer. Prior to SDS-polyacrylamide gel electrophoresis, the IPG strips were equilibrated for 15 min in DTT containing equilibration buffer A and then for 15 min in IAA containing equilibration buffer B. The equilibrated IPG strips, as well as filter papers (5 x 5 mm) loaded with 20 µl molecular weight marker (PageRuler Unstained Protein Ladder, Thermo Scientific), were placed on the surface of the SDS-gels. In order to ensure an efficient electrophoretic transfer, the strips and the filter papers were overlaid with an agarose solution. After solidification of the agarose, the upper reservoir of the tank was filled with 1x Running buffer. The electrophoresis run was performed at a power of 16000 mW per gel for the first 15 min and afterwards at a power of 1200-2000 mW pro gel overnight.

Equilibration buffer A

Urea	5.4	g	50	mM
Glycerine [v/v]	4.5	ml	30	%
SDS [w/v]	0.6	g	4	%
DTT	52.5	mg	3.5	mg/ml
Bromophenol blue	trace amounts			
Tris-HCl (pH 6.8)	15	ml	50	mM

Equilibration buffer B

Urea	5.4	g	50	mM
Glycerol [v/v]	4.5	ml	30	%
SDS [w/v]	0.6	g	4	%
Iodacetamide	0.675	g	45	mg/ml
Bromophenol Blue	trace amounts			
Tris-HCl (pH 6.8)	15	ml	50	mM

Agarose solution

Agarose [w/v]	1	%
SDS [w/v]	4	%
DTT	7.7	mg/ml
Tris-HCl (pH 6.8)	62.5	mM

10x Running buffer

Tris-HCl	0.25	M
Glycerol	1.9	M
SDS [w/v]	1	%

2.15.4.3 Staining with colloidal Coomassie

The two-dimensional protein gels (2.15.4.2) were visualized by staining with colloidal Coomassie brilliant blue G-250. To achieve that each gel was incubated for 12-24 h in 100 ml fixing solution followed by incubation in 250 ml staining solution for 24 h. The gels were destained in deionized water and documented using a Scanner (UMAX 2100, Biostep Jahnsdorf, Germany).

Fixing solution

Acetic acid [v/v]	10	%
Ethanol (96 % [v/v], pure)	50	%

Staining solution

Coomassie Brilliant Blue G250	0.75	g
(NH ₄)SO ₄	75	g
o-Phosphoric acid (85 % [v/v])	15	ml
Methanol	250	ml
dH ₂ O up to	1000	ml

2.15.4.4 Documentation of 2D-PAGE gels

Scanning, analysis and documentation of the 2D-PAGE gels was performed as described by Janssen (2010).

2.15.4.5 Mass spectrometric detection of proteins

MALDI-TOF mass spectrometric analysis of proteins was performed in the Proteomics laboratory of Prof. M. Hecker at the University of Greifswald as described by Janssen (2010).

2.15.5 Enzyme assays

2.15.5.1 β -galactosidase assay (Miller, 1972 mod.)

The method provides a simple quantitative estimate of *lacZ* expression by directly measuring β -galactosidase activities. Ortho-nitrophenyl- β -D-galactopyranoside (o-NPG) is the artificial chromogenic substrate used for this assay. It is colourless, while the product, ortho-nitrophenol is yellow. The β -galactosidase [EC 3.2.1.23] activity was measured by the rate of appearance of yellow color spectrophotometrically at 420 nm wavelength. The test was carried out in 2-ml Eppendorf tubes. 990 μ l of freshly prepared β -galactosidase buffer and 10 μ l crude cell extract (2.15.1) were mixed. The samples were pre-incubated for 2 min at 37 °C and the reaction was started by addition of 200 μ l 0.2 % o-NPG (Sigma Aldrich). When sufficient yellow color had developed, the reaction was stopped with 500 μ l 1M Na₂CO₃ and the exposure time was recorded. Extinction of the samples was recorded at 420 nm wavelength. A sample, in which the reaction was stopped before or immediately after addition of o-NPG, was used as a blank. If E₄₂₀ turned out to be above 1, less crude extract or shorter incubation period was applied. Based on the extinction coefficient of nitrophenol (ϵ_{420} 21.300 ml. mmol⁻¹.cm⁻¹), the activity in the samples was calculated according to equation 4.

$$\frac{E_{420}[\text{cm}^{-1}] * 1.7 [\text{ml}] * 10^6}{V_{\text{Sample}} * 21300 [\text{ml. mmol. cm}^{-1}] * \text{Time} [\text{min}]}$$

Equation 4 Determination of β -galactosidase activities in crude cell extracts.

Specific β -galactosidase activities (nmol.min⁻¹.mg⁻¹) were calculated taking into account the protein concentrations of the samples estimated by the method of Bradford (2.15.2).

β -galactosidase buffer

Na ₂ HPO ₄ (pH 7.0)	60	mM
NaH ₂ PO ₄	40	mM
KCl	10	mM
MgSO ₄	1	mM
β -Mercaptoethanol	5	mM

2.15.6 Overproduction and purification of recombinant proteins

2.15.6.1 Overproduction and purification of *Strep-tag II* fusion proteins

Overproduction and purification of *Strep-tag II* fusion proteins from cells of *E. coli* was performed using Strep-Tactin-Sepharose (IBA, Göttingen) as described by Riebe (2009). The

concentration of the isolated proteins was evaluated using the Bradford assay (2.15.2) and purity was tested by SDS-PAGE analysis (2.15.3).

2.15.6.2 Overproduction and purification of His-tag fusion proteins

For preparation of crude cell extracts from His-tag fusion protein expressing *E. coli* BL21 (DE3/pLys) strains, 250-ml cultures were grown from overnight pre-cultures of fresh transformants at 37 °C in LB medium supplemented with the appropriate antibiotics for selection (Table 7.1 and Table 2.1). At an OD₆₀₀ of 0.9-1, IPTG was added to a final concentration of 1 mM, and growth was continued for 3-4 h. Cells were then harvested by centrifugation (5.000 x g, 10 min, 4 °C) and suspended in 4 ml Lysis buffer. After cell disruption by sonication (Sonicator Desintegrator Sonopuls HD60, MedLab) and centrifugation (13.000 x g, 30 min, 4 °C), the His - tagged proteins were isolated from the soluble fraction using Ni-NTA agarose resin (Macherey-Nagel). Four ml of crude cell extract were mixed with 1 ml of 50 % Ni-NTA slurry and the mixture was stirred for 1 h at 4 °C. The lysate-Ni-NTA mixture was afterwards loaded on a column (Poly-Prep Chromatography Columns, Biorad). The flow-through was collected and the column was washed twice with 4 ml Washing buffer. The elution of the recombinant protein was performed with 4 x 0.5 ml Elution buffer. The concentration of the isolated proteins was evaluated using the Bradford assay (2.15.2) and purity was tested by SDS-PAGE analysis (2.15.3).

Lysis buffer

NaH ₂ PO ₄	7.8	g
NaCl	17.54	g
Imidazole	0.68	g

The pH of the buffer was adjusted to 8.0 with NaOH.

Washing buffer

NaH ₂ PO ₄	7.8	g
NaCl	17.54	g
Imidazole	1.34	g

The pH of the buffer was adjusted to 8.0 with NaOH.

Elution buffer

NaH ₂ PO ₄	7.8	g
NaCl	17.54	g
Imidazole	17.00	g

The pH of the buffer was adjusted to 8.0 with NaOH.

2.15.7 Western blotting (transfer and detection of proteins on a nitrocellulose membrane)

For Western blot analysis cultures of the *E. coli* strains of interest were collected and crude cell extracts were prepared (2.15.1). Following an electrophoretic separation (2.15.3), the proteins were transferred onto a nitrocellulose membrane (0.2 µm Biometra) using a semi-dry blotting system (Biometra). To set up the western blot, six pieces of Whatman filter paper (Schleicher und Schüll BioScience, Dassel) and a nitrocellulose membrane (0.2 µm Biometra) were cut to the dimensions of the SDS-gel and soaked shortly in Transfer buffer. The blotting sandwich was built up on the anode plate in the following order: three Whatman papers (Schleicher und Schüll BioScience, Dassel), a nitrocellulose membrane (0.2 µm Biometra), the SDS-PAGE gel and three Whatman papers on top. Excess of Transfer buffer and air bubbles captured between layers were removed by careful rolling with a clean reaction tube over the top of the membrane. The blotting apparatus was closed putting on the cathode lid and a constant current charge (5 mA/cm² of gel) was applied until the cell voltage dropped down to the half of its starting value. Successful transfer of proteins onto the nitrocellulose membrane was confirmed by Coomassie staining of the SDS-PAGE gel (2.15.3).

Transfer buffer

Tris	15.14	g	125	mM
Glycine	14.40	g	192	mM
Ethanol (96 % [v/v], pure)	200	ml	20	% [v/v]
dH ₂ O up to	1000	ml		

The buffer was stored at 4°C.

2.15.7.1 Detection of *Strep*-tag II fusion proteins

Chromogenic detection of *Strep*-tagged proteins on Western blots was performed using *Strep*-Tactin® AP conjugate (IBA, Göttingen). Colour was developed by a NBT/BCIP (Roche Applied Science) mixture, chromogenic substances of alkaline phosphatase. The nitrocellulose membrane was incubated in a fat-free milk solution (Blocking buffer) overnight at 4 °C or alternatively for 1 h at RT. The membrane was further treated according to the following protocol:

1. Washed three times with 1x TGST buffer.
2. Incubation in 50 ml 1x TGST + 5 µl *Strep*-Tactin® AP conjugate solution for 45 min.
3. Washing in 1x TGST solution (3 x 10 min).
4. Incubation in Staining solution. When sufficient staining had developed, the reaction was stopped with dH₂O.

Blocking buffer

1x TGST buffer	50	ml
BSA	0.5	g
Fat-free milk powder	2.5	g

* In order to avoid cross reactions between the *Strep*-Tactin and the Biotin Carboxyl Carrier Protein (BCCP, 22.5 kDa) from the *E. coli* protein extracts, a small amount of avidin was added to the blocking buffer.

10x TGST buffer

Tris	12.1	g
NaCl	85.5	g
Tween-20	5	ml
dH ₂ O up to	1000	ml

After adjustment of the pH value to 8.0 by addition of HCl, the buffer is stored at 4°C.

10x AP buffer

Tris	1.21	g
NaCl	5.7	g
MgCl ₂	0.47	g
dH ₂ O up to	100	ml

After adjustment of the pH value to 9.5 by addition of HCl, the buffer is stored at 4°C.

AP-staining solution

NBT/BCIP solution (Roche Applied Science)	20	μl
1x AP buffer	2	ml

2.15.8 Cross-linking experiments

Cross-linking experiments with ethylene glycol-bis (succinimidylsuccinate) (Sigma Aldrich) were used in this study to evaluate the ability of proteins to form higher order structures in solution. Protein isolates were incubated with different concentrations of EGS in 20 μl reaction buffer for 30 min at RT. The cross-linking reactions were afterwards quenched with Tris-Glycine solution (100 mM Tris, pH 7.5; 100 mM Glycine) and the samples were analysed by SDS-PAGE (2.15.3).

Reaction buffer

HEPES (pH 8.0)	25	mM
NaCl	100	mM
DTT	1	mM
EDTA	0.2	mM
Glycerol	10	% [v/v]

2.16 Stress experiments

2.16.1 O₂ and H₂O₂ stress experiments

In order to evaluate the impact of O₂ and H₂O₂ on strains of *C. acetobutylicum*, stress experiments were performed as previously described (Hillmann *et al.*, 2008).

2.17 List of chemicals and materials

Table 2.4 Chemicals and materials used in this study

Manufacturer	Chemicals and Materials
Applichem GmbH, Darmstadt	EDTA, Formaldehyde, Formamide, Erythromycin, Tween-20, X-Gal, DTT, HEPES, 30% H ₂ O ₂ solution
Biometra GmbH, Göttingen	0.2 µm Nitrocellulose membrane
Biorad Laboratories, Munich	IPG Strips, Poly-Prep Chromatography Columns
Carl Roth GmbH, Karlsruhe	Roti [®] -Nylon plus, Albumin Fraction V
Difco Laboratories, Hamburg	Agar-Agar
GE Healthcare, Munich	Cy3, Cy5, DryStrip Cover Fluid
IBA GmbH, Göttingen	<i>Strep</i> -Tactin-Sepharose, Desthiobiotin, <i>Strep</i> -Tactin [®] AP conjugate
Megazyme International Ltd., Wicklow, Irland	D-Lactic Acid (D-Lactate) and L-Lactic Acid (L-Lactate) Kit
Merck, Darmstadt	TLC Silica gel 60 F ₂₅₄
Oxoid GmbH, Wesel	RCA (Reinforced Clostridial Agar)
Macherey-Nagel & Co. KG, Düren	50% Ni-NTA slurry
Peqlab Biotechnologie GmbH, Erlangen	peqGold <i>Pwo</i> -Polymerase I, 'peqGOLD Gel Extraction Kit'
Roche GmbH, Mannheim	DIG-labeled DNA Molecular Weight Marker II, Blocking Reagent, DIG DNA Labeling Kit, NBT/BCIP Stock solution, RNase-free recombinant DNase I, Anti-Digoxigenin-AP, 5'/3' RACE Kit, CDP- <i>Star</i> [®]
Sigma-Aldrich Chemie, Taufkirchen	Ampicillin, Thiamphenicol, Oligonucleotides, Chelex 100, EGS, o-NPG, Riboflavin, FMN, FAD, 2,2'-dipyridyl, Ferrozine, Neocuproine, HDTMA, CAS, PIPES, Potassium glutamate, Piperazine, Sulfosalicylic acid
Thermo Scientific, Braunschweig	Endonucleases (Table 2.6), T4-DNA-Ligase, FastAP, dNTPs, PageRuler Unstained Protein Ladder, PageRuler Prestained Protein Ladder, 'High Fidelity Enzyme Mix', 'GeneJET Plasmid Miniprep Kit', GeneRuler 1 kb DNA Ladder

3 Results

3.1 Identification of CAC1682 from *C. acetobutylicum* as an iron-sensing repressor

The genome of *C. acetobutylicum* (Nölling *et al.*, 2001) has revealed three genes (*cac0951*, *cac1682* and *cac2634*) encoding proteins, annotated as 'Ferric uptake regulators' (Hillmann *et al.*, 2008). In previous studies CAC2634 has been defined as an H₂O₂-sensing regulator PerR (Hillmann *et al.*, 2008; 2009b). In terms of phylogeny, CAC1682 and CAC0951 have been classified as iron- and zinc-responsive regulators, respectively (Hillmann *et al.*, 2008). Functional assignment of proteins from the Fur family based on homology could be misleading (Wexler *et al.*, 2003). Therefore, comparative analyses of CAC1682 and CAC0951 were performed in the present work. *In silico* studies and biochemical examination demonstrated that CAC1682 exhibits a set of properties characteristic of the Fur family of proteins. These results coupled with *in vivo* studies delineated the identity of this protein as an authentic ferric uptake regulator (Fur).

3.1.1 Generation of homology models

To closer investigate the CAC1682 and CAC0951 protein sequences from *C. acetobutylicum*, 3D homology models were generated using structural information from *Helicobacter pylori* Fur (pdb: 2xig; Table 3.1) and *Streptomyces coelicolor* Zur (pdb: 2mwm; Table 3.2) as templates, and the Python-based software Modeller v.9.12 (script not shown) (Sali and Blundell, 1993; Dian *et al.*, 2011; Shin *et al.*, 2011). The predicted 3D structures have been visualized (Fig. 3.1 and Fig. 3.2) by the graphical interface Chimera (Pettersen *et al.*, 2004). For basic evaluation of the models, pseudo-energy calculated by the Modeller was plotted using Gnuplot (<http://www.gnuplot.info/>), a Python-based graphing utility (Fig. 7.2 and Fig. 7.3, Appendix) (script not shown). Chains A and B for both proteins were modelled separately and the dimeric structures (Fig.3.1 B and Fig. 3.2 B) were fitted using the Matchmaker extension of Chimera (Meng *et al.*, 2006).

The overall fold organization of CAC1682 and CAC0951 as judged by the generated models (Fig. 3.1 and Fig. 3.2) resembles the architecture characteristic for other members of the Fur family of proteins (Pohl *et al.*, 2003; Lucarelli *et al.*, 2007; Dian *et al.*, 2011). CAC1682 consists of an N-terminal DNA-binding domain (DBD) (residues 1-90; shaded in blue on Fig. 3.1), a C-terminal dimerization domain (DD) (residues 100-151; coloured in pink), both connected by a short hinge

region (residues 91-99; yellow). The DBD motif constitutes of $\alpha 2$ - $\alpha 4$ helices and $\beta 1$ - $\beta 2$ sheets, which collectively form a typical winged helix-turn-helix structure (wHTH) with $\alpha 4$ being considered as the DNA recognition determinant (Huffman and Brennan, 2002; Pohl *et al.*, 2003). The C-terminal DD consists of three antiparallel β sheets ($\beta 3$, $\beta 4$ and $\beta 5$) as well as two α helices ($\alpha 5$ and $\alpha 6$). Similarly to CAC1682, the CAC0951 model structure exhibited a bipartite organization, composed of a DBD (residues 1-79, coloured in green on Fig. 3.2) and a DD (residues 87-143, violet), bridged by a short loop (residues 80-86, yellow).

Table 3.1 Comparative amino acid sequence analysis of CAC1682 with HpFur* and other characterized Fur proteins.

Protein	Amino acid Identity/Similarity [%]
CAC1682 (<i>C. acetobutylicum</i>)	100/100
Fur (<i>B. subtilis</i>)	49/70
Fur (<i>E. coli</i>)	36/56
Fur (<i>H. pylori</i>) **	28/54

* HpFur, *H. pylori* Fur

**HpFur was used for construction of the predicted CAC1682 3D model.

Table 3.2 Comparative amino acid sequence analysis of CAC0951 with ScZur* and other characterized Zur proteins.

Protein	Amino acid Identity/Similarity [%]
CAC0951 (<i>C. acetobutylicum</i>)	100/100
Zur (<i>B. subtilis</i>)	28/50
Zur (<i>E. coli</i>)	26/50
Zur (<i>S. coelicolor</i>) **	26/46

* ScZur, *S. coelicolor* Zur

**ScZur was used for construction of the predicted CAC0951 3D model.

Three distinct putative metal-binding sites (S1, S2 and S3) were identified within the CAC1682 protein sequence (Fig. 3.3) based on comparative structural analysis with other Fur-like proteins (Pohl *et al.*, 2003; Lucarelli *et al.*, 2007; Dian *et al.*, 2011; Butcher *et al.*, 2012). Two binding sites (S1 and S3) are positioned within the DD and one (S2) at the junction between the DBD and DD. S1, a putative Zn(II)-binding structural site, composed of two Cys-X-X-Cys motifs (Cys104, Cys107, Cys144 and Cys147) is located in close proximity to the C-terminus (Fig. 3.3 A). S2

consists of His41, Glu89, His99 and His101 (Fig. 3.3 B) and S3 (Fig. 3.3 C), is tetrahedrally coordinated at the core of the DD by residues His97, His100, Asp119 and His136. Interestingly, only two conserved metal binding sites were identified in the protein structure model of CAC0951 (Fig. 3.4). Those were designated S1 (Cys91, Cys94, Cys130, Cys133) and S3 (His85, His87, Asp105, His122) to match the corresponding putative metal binding sites in CAC1682.

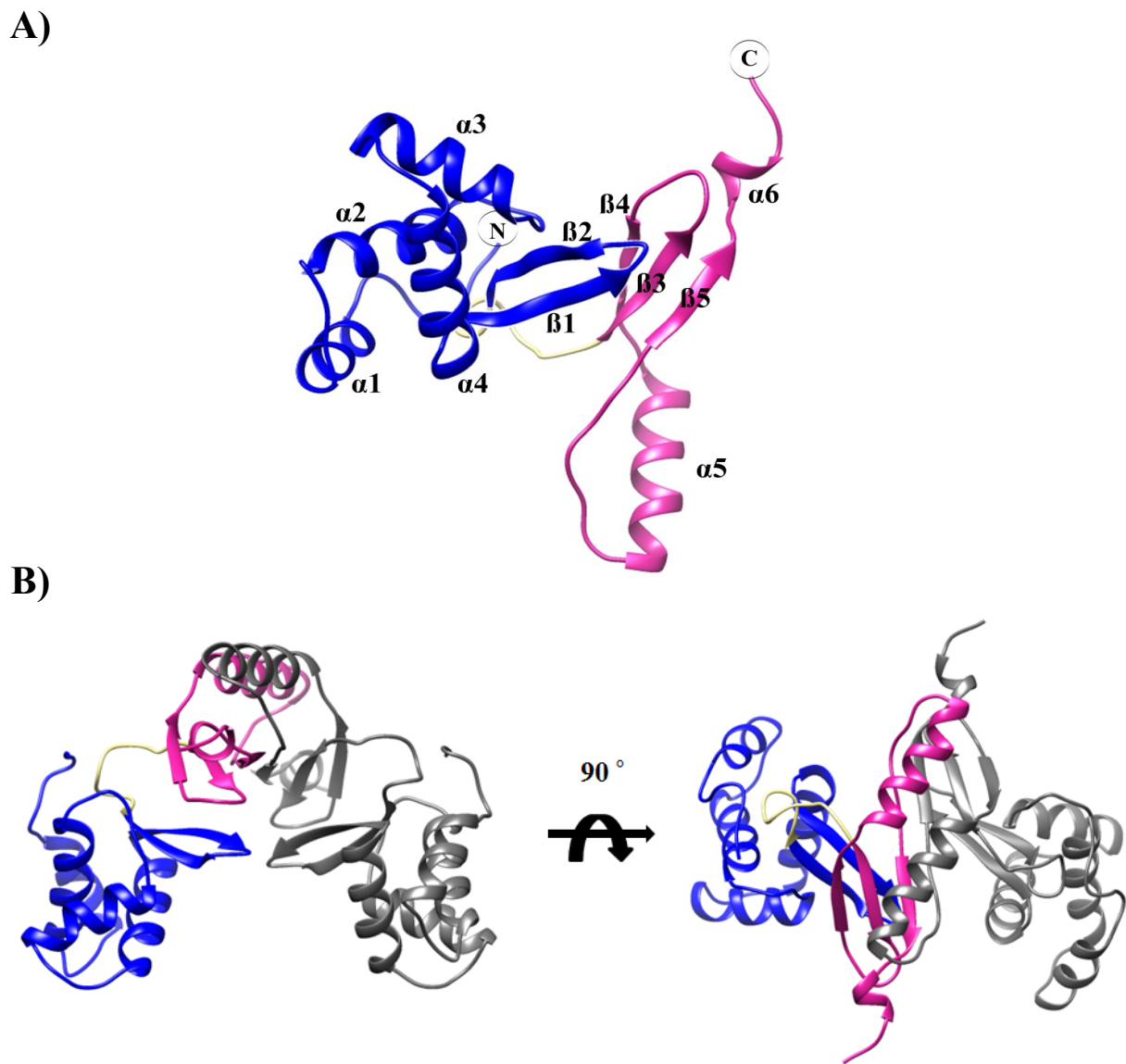


Fig. 3.1 Ribbon representation of the lowest-energy structure of CAC1682 monomer (A) and dimer (B) based on a homology model generated using HpFur (pdb: 2xig; Dian *et al.*, 2011) as reference. The 3D model structure of CAC1682 was predicted by the Modeller program (Sali and Blundell, 1993). Dimer structure was fitted using the Matchmaker. The N-terminal DBD is coloured in blue, the C-terminal DD in pink and the connecting hinge between both in yellow. The second monomer is shaded in grey.

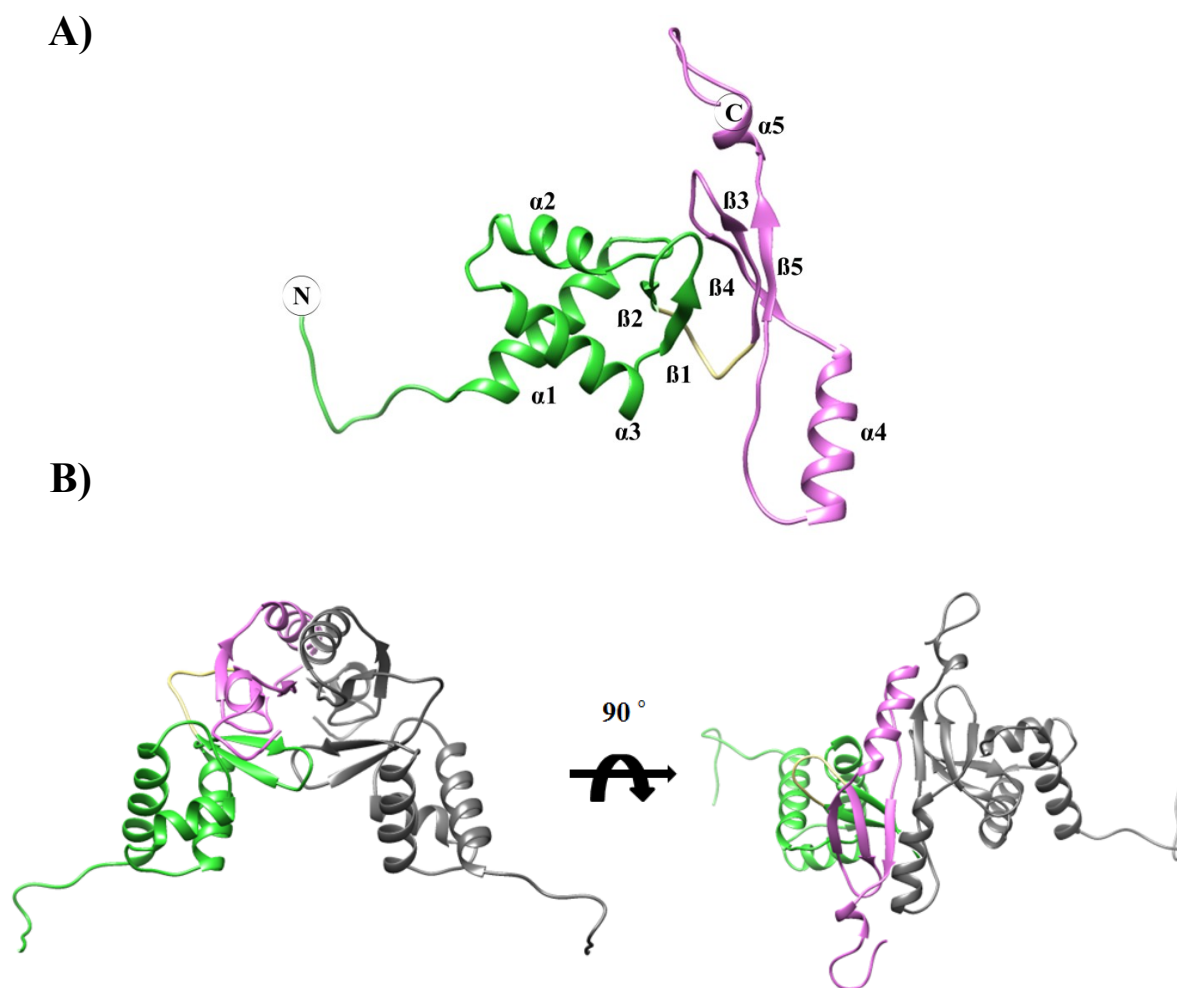


Fig. 3.2 Ribbon representation of CAC0951 monomer (A) and dimer (B) based on a homology model generated using ScFur (pdb: 2mwm; Shin *et al.*, 2011) as reference. The N-terminal DBD is coloured in green, the C-terminal DD in violet and the connecting loop between both in yellow. The second monomer is shaded in grey.

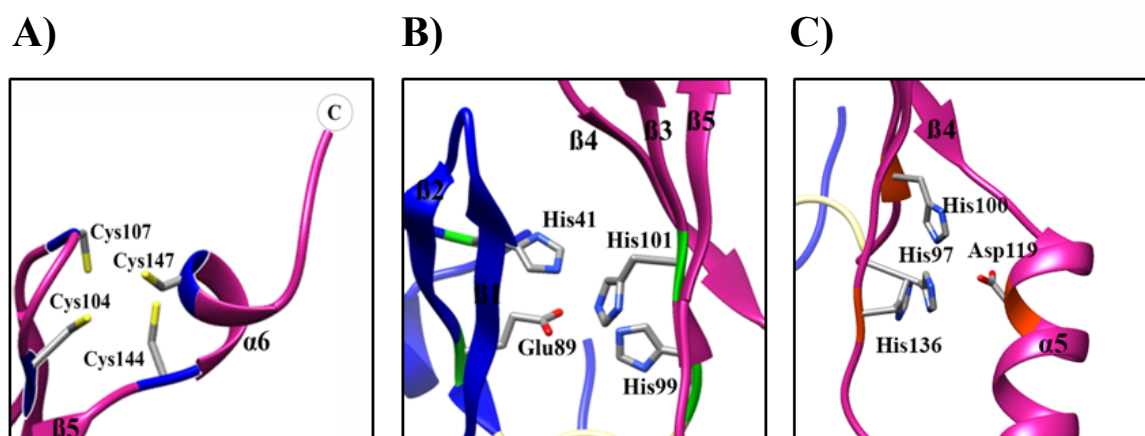


Fig. 3.3 Predicted metal binding sites in CAC1682 based on comparative structural analysis and homology model generated with the Modeller. (A) Site 1; (B) Site 2; (C) Site 3 (see text for details). The N-terminal DBD is coloured in blue, the C-terminal DD in pink and the connecting hinge between both in yellow analogically to Fig. 3.1.

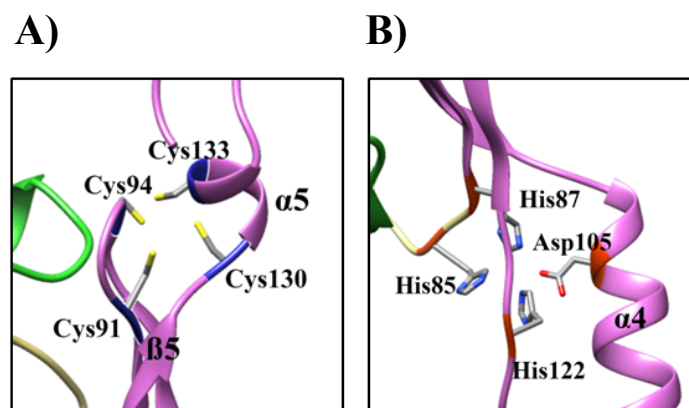


Fig. 3.4 Predicted metal binding sites in CAC0951 based on comparative structural analysis and homology model generated with the Modeller. (A) Site 1; (B) Site 3 (see text for details). The N-terminal DBD is coloured in green, the C-terminal DD in violet and the connecting loop between both in yellow analogically to Fig. 3.2.

3.1.2. Biochemical characterization

In a first set of experiments, basic biochemical properties of CAC1682 and CAC0951 like oligomeric state and metal content were examined. For that purpose, recombinant proteins were overexpressed and purified to homogeneity from cells of *E. coli*.

3.1.2.1 Heterologous expression of recombinant CAC1682 and CAC0951 proteins

Overproduction of CAC1682 in *E. coli* was performed using the pET-30a Xa/LIC inducible system (Novagen), designed for high-level expression of proteins fused with an external His[®]-tag and an internal S[®]-tagTM sequence at the N-terminus. The entire *cac1682* coding sequence was PCR amplified from *C. acetobutylicum* ATCC 824 genomic DNA (2.6.2) using the *cac1682_pET30a_fw/ cac1682_pET30a_rev* primer pair (Table 7.4), cloned into pET-30a and the resulting pET-30a::*cac1682* construct was transformed into competent *E. coli* BL21 (DE3/pLys) cells (Novagen). The His-tagged CAC1682 was extracted from the soluble cellular protein fraction with Ni-NTA agarose resin (Macherey-Nagel) essentially as described in Materials and Methods (2.15.6.2).

CAC0951 was overproduced in cells of *E. coli* BL21 using the pT system (Fig. 7.4 A, Appendix) (Girbal *et al.*, 2005). The pT vector is a shuttle plasmid, designed for expression of C-terminal *Strep*-tag II fusion proteins under control of the ribosome binding site (RBS) and clostridial thiolase promoter (P_{thlA}) (Girbal *et al.*, 2005). The coding region of the *cac0951* gene without its stop codon was PCR amplified using primers *cac0951_BamHI_fw* and *cac0951_XmaI_rev* (Table 7.4) and genomic DNA as template (2.6.2). The resulting PCR product was digested with *Bam*HI and *Cfr*9I (*Xma*I), ligated into the corresponding sites of a phosphatase treated pT vector (2.8.3.2

and 2.8.3.3) and transformed into *E. coli* BL21 competent cells (2.9.1.1 and 2.9.1.2). Recombinant CAC0951 was purified (2.15.6.2) from the soluble protein fraction by loading on a Strep-Tactin-Sepharose affinity column (IBA GmbH, Göttingen).

Purity of the recombinant CAC1682 and CAC0951 was assessed using SDS-PAGE and subsequent staining by Coomassie Blue (2.15.3) (Fig. 3.5 A and B). In addition, identity of the isolated proteins was confirmed by MALDI-TOF mass spectrometry analysis (2.15.4.6). CAC1682 migrated on SDS-PAGE gels as a doublet form with a predominant product, corresponding to the calculated molecular weight of the fusion protein monomer (~ 23 kDa). Similarly, SDS-PAGE analysis of CAC0951 revealed two isoforms with molecular weight corresponding to the theoretically estimated size of a *Strep*-tag II fusion protein (~ 18 kDa).

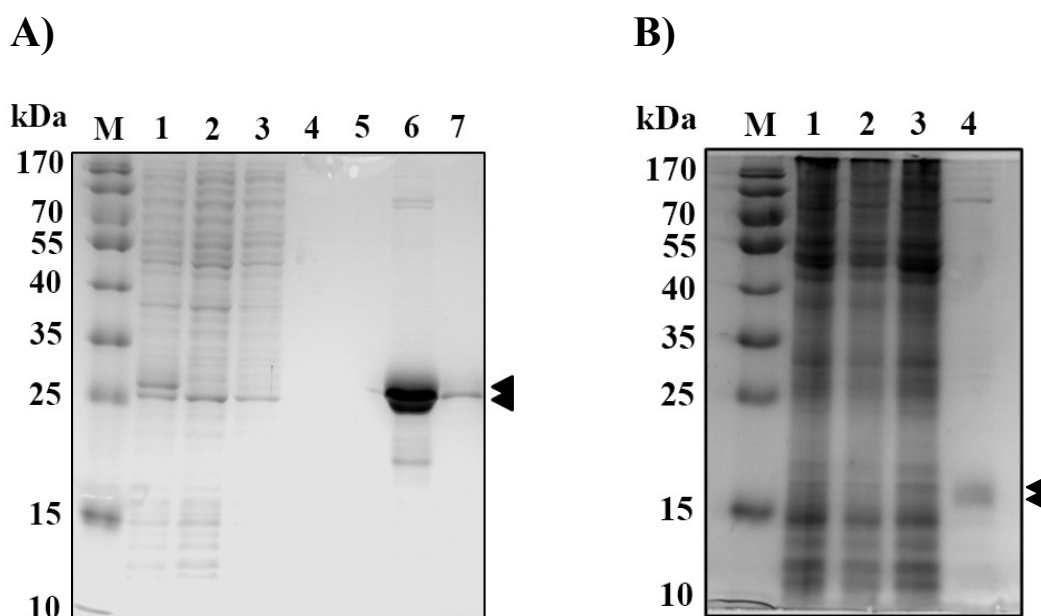


Fig. 3.5 Purification of recombinant CAC1682 (A) and CAC0951 (B) proteins from *E. coli*. SDS-PAGE analysis (12 % [w/v] gel), followed by Coomassie staining. M, PageRuler Prestained Protein Ladder (Thermo Scientific); (A) Lane 1, crude extract from IPTG induced BL21 (DE3/pLys) cells; lane 2, flow-through; lane 3-5, washing fractions; lane 6 and 7, CAC1682 containing elution fractions. (B) Lane 1, crude extract; lane 2, flow-through; lane 3, washing fraction; lane 4, CAC0951 protein containing fraction. Protein doublet forms are indicated by two arrows.

3.1.2.2 Determination of protein oligomeric state

An important aspect of Fur regulation is the ability to form oligomers (Lee and Helmann, 2007). Gel filtration experiments (FPLC) using a Superdex 200 size-exclusion column proved inefficient for oligomerization studies of the CAC1682 protein, because of its low UV absorbance and precipitation into the gel matrix. Therefore, *in vitro* chemical cross-linking assays were conducted in this study in order to evaluate the ability of CAC1682 and CAC0951 to form higher-order structures in solution. Cross-linking agents capture multimeric forms that are in a dynamic

equilibrium with the corresponding monomers and are therefore useful for determination of protein oligomerization status (Hernandez *et al.*, 2002). Recombinant CAC1682 protein was incubated with or without the cross-linking agent ethylene glycol-bis (succinimidyl succinate) (EGS) for 30 min at RT and the reactions were afterwards quenched with Tris-Glycine solution (2.15.8). As illustrated on Fig. 3.6, SDS-PAGE analysis of the cross-linked samples revealed predominant monomeric (~ 23 kDa) and dimeric (~ 46 kDa) forms of the protein (Fig. 3.6 A). Increasing concentrations of the cross-linking agent caused a shift towards formation of a protein dimer, but no overall change in the oligomerization behaviour (Fig. 3.6 B). Similarly, analysis of the recombinant CAC0951 demonstrated that this protein forms dimeric structures (~ 36 kDa) in solution (Fig. 3.6 C). Collectively, these results indicate that CAC1682, as well as CAC0951, exist as dimers, which is in agreement with the oligomeric pattern proposed for members of the Fur family of proteins studied so far (Lee and Helmann, 2007).

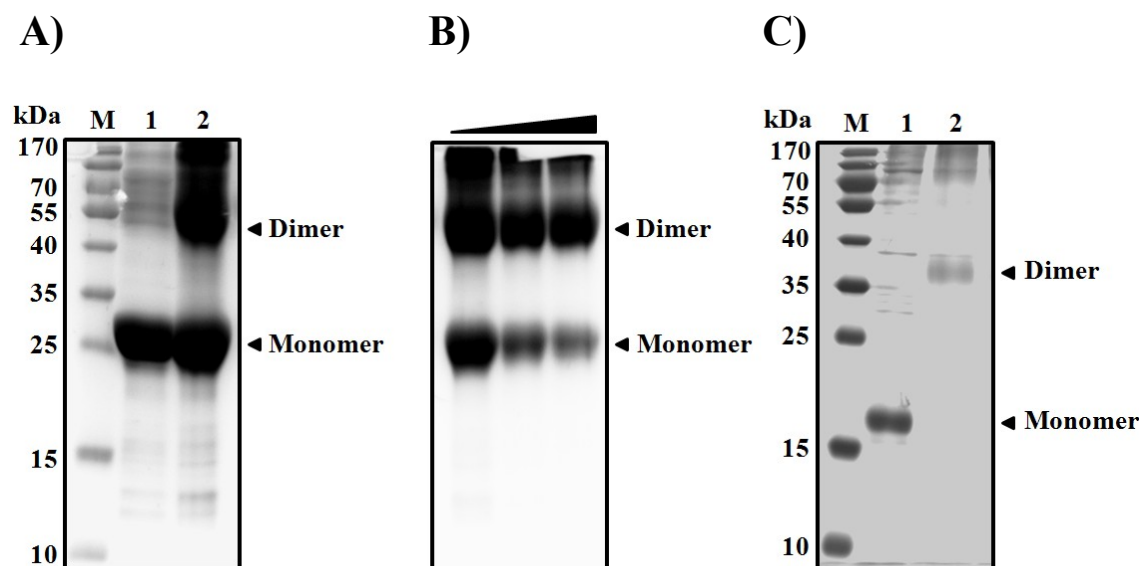


Fig. 3.6 Oligomeric state of CAC1682 (A, B) and CAC0951 (C) in solution determined by chemical cross-linking. 700 ng of recombinant CAC1682 was incubated for 30 min with 2 mM (A) and 6-10 mM (B) of the cross-linking agent EGS. (C) 300 ng of Strep-tagged CAC0951 was incubated with 2 mM EGS. Cross-linked samples were afterwards analysed on 12 % [w/v] SDS-PAGE gels. M, PageRuler Prestained Protein Ladder (Thermo Scientific); Lane 1, untreated protein; lane 2, 2 mM EGS. Arrows indicate bands corresponding to monomeric and dimeric forms of the proteins.

3.1.2.3 Metal content quantification

As the oligomeric state of CAC1682 and CAC0951 in solution was elucidated, we sought to investigate the protein metal element content. In order to remove any adventitiously associated metal ions, the purified recombinant CAC1682 and CAC0951 were extensively dialysed against 1 mM EDTA at 4 °C. Both proteins were afterwards diluted in concentrated HCl, incubated overnight and subjected to inductively coupled atomic-emission spectroscopy (ICP-AES) analysis

as previously described (Hillmann *et al.*, 2008). Elution buffer (2.15.6.1 and 2.15.6.2) treated in the same manner as the protein samples served as a control. ICP data indicated that zinc, a structural element, and iron, the cognate cofactor of the ferric uptake regulators, co-purify with CAC1682 under the conditions of the assay (Table 3.3). The other two transition metals tested (cobalt and manganese) were not detected in the samples. Surprisingly, a considerable amount of nickel has been identified in the CAC1682 protein isolates, most probably as a result of contamination during the purification protocol with Ni-NTA. Among all tested transition metals, only zinc has been identified in the CAC0951 samples, consistent with the predicted role of this protein as a zinc-responsive regulator.

Table 3.3 Metal content of recombinant CAC1682 and CAC0951 proteins.

Element	CAC1682 nmol/mg protein	CAC0951 nmol/mg protein
²⁷ Co	BDL	BDL
²⁶ Fe	0.51 ± 0.24	BDL
²⁵ Mn	BDL	BDL
²⁸ Ni	4.60 ± 0.72	BDL
³⁰ Zn	17.06 ± 1.84	41.98 ± 9.43

Quantities presented as nmol metal per mg of recombinant protein (\pm SEM) were determined by inductively coupled plasma atomic-emission spectroscopy (ICP-AES) from three independent CAC1682 and CAC0951 batches. BDL, below detection limit of the method.

3.1.3 Functional *in vivo* characterization of CAC1682

In order to establish experimentally the role of CAC1682 as a genuine iron-sensing regulator *in vivo*, the ability of this protein to act as a repressor and to specifically respond to iron levels were explored within the cellular milieu of Fur deficient *E. coli* and *B. subtilis* hosts. In addition, the CAC0951 protein was used as a control in all complementation assays.

3.1.3.1 Construction of pTCatP recombinant plasmids

For the complementation studies in *E. coli* and *B. subtilis*, a modified pT vector system, designated in this work as pTCatP (Fig. 7.4 B, Appendix), was employed (Girbal *et al.*, 2005, mod.). This system was selected since the pT vector has been well established for high-level expression of target proteins in *E. coli* (Riebe, 2009) as a Gram-negative host and stable growth-phase-independent expression in *C. acetobutylicum* (Riebe, 2009; Schulz, 2013) as a Gram-positive host. Moreover, the *Strep*-tag II provides a convenient means for monitoring. The coding regions of *cac1682* and *cac0951* without their stop codons were PCR amplified from *C. acetobutylicum* ATCC 824 genomic DNA (2.6.2) using *cac1682_XmaI_fw/*

cac1682_BamHI_rev and cac0951_BamHI_fw/ cac0951_XmaI_rev primer pairs (Table 7.4), respectively. The resulting PCR products, after purification by gel extraction (2.7.1.1) were digested with *Bam*HI and *Cfr*9I (*Xma*I) and ligated into the corresponding sites of a phosphatase treated pTCatP vector (2.8.3.2 and 2.8.3.3). The ligation mixtures were then transferred into CaCl₂-competent *E. coli* DH5 α cells (2.9.1.1 and 2.9.1.2) and transformants were selected on LB agar plates supplemented with either Cam (25 μ g/ml) or Amp (100 μ g/ml). Presence of the correct inserts was verified by test restriction (2.8.3.1), as well as sequencing with primers pT_seq_fw and pT_seq_rev (Table 7.4).

3.1.3.2 Complementation of the *fur* defective *E. coli* H1780 strain

E. coli H1780 is a *fur*-null strain that carries a chromosomal *lacZ* reporter transcriptional fusion with the promoter region of the Fur repressed gene *fiu* (*fiu* λ ::placMu53), which codes for a siderophore receptor (Hantke, 1987; 1990). Moreover, lack of a functional iron-sensing repressor in this strain results in derepression of the *ent* gene cluster, responsible for biosynthesis of the catechol siderophore enterobactin (Hantke, 2001). Thus, H1780 is characterized by two easily detectable phenotypical traits, namely constitutive expression of the *lacZ* reporter gene and excretion of enterobactin. Those features create background for functional analysis of candidate iron-responsive Fur proteins from other bacterial species and were used in this study to determine the metal status of CAC1682 in the context of *E. coli* cellular environment. Introduction of an active Fur ortholog into H1780 in the presence of its co-effector Fe(II) would lead to significant inhibition of the β -galactosidase activity as well as reduction in enterobactin biosynthesis.

The constructed recombinant plasmids pTCatP::*cac1682* and pTCatP::*cac0951* (3.1.3.1), as well as a control vector without insert (pTCatP), were transformed into CaCl₂-competent *E. coli* H1780 cells giving strains H1781 (pTCatP control vector), H1782 (pTCatP::*cac1682*) and H1783 (pTCatP::*cac0951*). To confirm the expression of both proteins, *E. coli* H1780, H1781, H1782 and H1783 were grown in 50 ml LB medium supplemented with the appropriate antibiotics for selection (Table 7.1 and Table 2.1) at 37 °C with rigorous aeration (180 rpm). When the cultures reached an OD₆₀₀ of 2-2.5, samples were collected and prepared for Western blot analysis (2.15.7). Here Fig. 3.7 confirms the successful expression of CAC1682 and CAC0951 in *E. coli* H1782 and H1783, respectively, while no signal was detected in the negative control strains H1780 and H1781. Both proteins migrated on the SDS-PAGE gel as doublet forms, as has been previously reported for other members of the Fur family of proteins (Bsat *et al.*, 1998; Lee and Helmann, 2006b). *E. coli* H1717, a strain that harbours a chromosomal *lacZ* reporter construct, under control of the Fur-regulated *fhuF* promoter, but is not mutated in *fur*, was used as a positive control in all complementation assays (Hantke, 1987; Stojiljkovic *et al.*, 1994). This strain was

considered as a suitable reference since previous studies reported *fiu::lacZ* and *fhuF::lacZ* transcriptional fusions to be regulated in a similar fashion by *E. coli* Fur (Quatrini *et al.*, 2005).

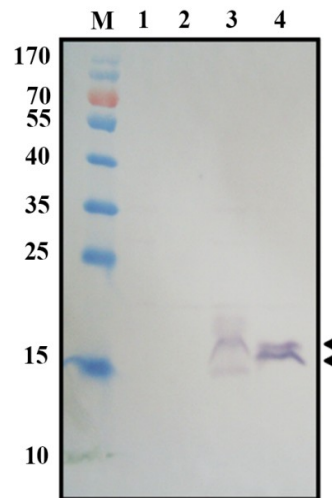


Fig. 3.7 Expression of CAC1682 and CAC0951 in *E. coli* H1780 verified by Western blot analysis. M, PageRuler Prestained Protein Ladder (Thermo Scientific); 20 μ g of total cellular protein were loaded in each slot of a 12 % [w/v] SDS-PAGE gel, which was afterwards blotted on a nitrocellulose membrane. Lane 1, *E. coli* H1780; lane 2, H1781 (pTCatP control); lane 3, H1782 (pTCatP::*cac1682*) and lane 4, H1783 (pTCatP::*cac0951*). Protein doublets are indicated by two arrows.

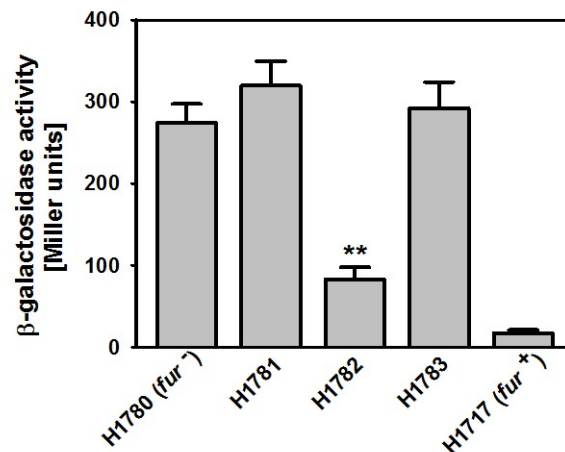
3.1.3.2.1 Quantification of β -galactosidase reporter activities

Iron-replete conditions for the assay that ensured repression of the *lacZ* reporter by Fur were determined empirically using *E. coli* H1717. The strain was grown on MacConkey-lactose agar plates (2.3.1) supplemented with different concentrations of FeSO_4 . A ferrous iron concentration of 100 μ M was found to be sufficient for repression of the transcriptional fusion as discerned by formation of white (Lac^-) instead of red or pink (Lac^+) colonies and has been therefore further used for quantification of β -galactosidase reporter activities. To achieve the latter, cultures of H1780, H1781, H1782 and H1783 strains, as well as the positive control H1717 strain, were propagated in 100 ml LB medium supplemented with the appropriate antibiotics for selection (Table 7.1 and Table 2.1) to mid-log phase. Cells were then lysed and specific β -galactosidase activities were assayed as described in Materials and Methods (2.15.5.1). The results from at least three independent experiments are illustrated on Fig. 3.8 A. As expected, in *fur* mutant background, H1780, as well as the control vector harbouring strain H1781, produced constitutively high levels of β -galactosidase. The CAC0951 expressing H1783 developed a similar profile. Introduction of CAC1682, however, led to a significant decrease in β -galactosidase activity, providing a first line of *in vivo* evidence that this protein may function as an iron-sensing repressor in *C. acetobutylicum*.

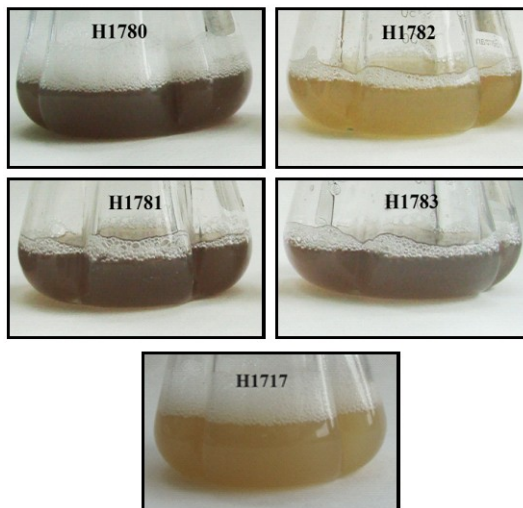
3.1.3.2.2 Detection of enterobactin production

To investigate the ability of CAC1682 to restore Fur repression activity in *E. coli* H1780 with respect to other iron-regulated cellular processes, assessment of siderophore production in the recombinant strains was performed. H1780 constitutively excretes the catechol siderophore enterobactin, which upon accumulation into the medium gives a dark purple colour (Payne, 1994).

A)



B)



C)

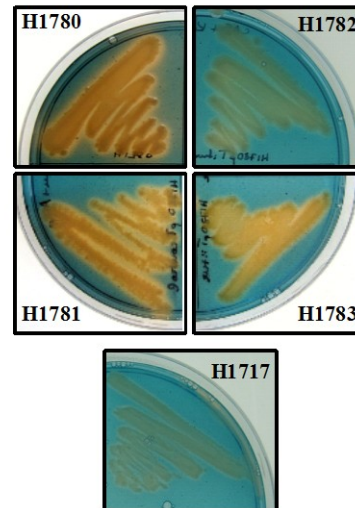


Fig. 3.8 CAC1682 from *C. acetobutylicum* restores Fur⁺ phenotype in the *fur*-null *E. coli* H1780 reporter strain. Specific β -galactosidase activities of the Fur regulated *fiu-lacZ* and *shuH-lacZ* (H1717) transcriptional fusions (A) and siderophore production (B, C) in H1780, H1781 (pTCatP), H1782 (pTCatP::*cac1682*), H1783 (pTCatP::*cac0951*) strains as well as H1717 (*fur*⁺). The presented data in (A) was obtained from at least three independent (n=3) experiments ($P < 0.005$).

To evaluate the synthesis of enterobactin, H1780, H1781, H1782 and H1783, as well as the positive control H1717, were grown overnight in 100 ml LB medium supplemented with 100 μ M

FeSO₄. As illustrated on Fig. 3.8 B, only CAC1682 was able to restore Fur⁺ phenotype in *E. coli* H1782, in concert with the results obtained from the β-galactosidase activity experiments (3.1.3.2.1). Furthermore, the identity of the secreted compound as a siderophore was confirmed *in vivo* by a Chrome Azurol-S (CAS) plate assay (2.3.1 and 2.5.10.3) (Fig. 3.8 C).

3.1.3.3 Complementation of the Fur⁻*B. subtilis* HB6543

To test if CAC1682 responds to varying levels of iron in the medium, complementation experiments in the *fur* defective *B. subtilis* H6543 (Bsat *et al.*, 1998) were carried out under iron-replete and iron-deplete conditions. For the complementation studies, pTCatP::*cac0951*, pTCatP::*cac1682* (3.1.3.1), and the pTCatP control vector without insert were introduced into *E. coli* RR1 for plasmid amplification (2.9.2.2) and afterwards transformed into HB6543 competent cells (2.9.2.1 and 2.9.2.3) giving strains: HB6544 (pTCatP control), HB6545 (pTCatP::*cac1682*) and HB6546 (pTCatP::*cac0951*). *B. subtilis* HB1000 (wild-type) served as a control in this assay (Chen *et al.*, 1993). In HB6543 the Fur regulated *dhb* operon is derepressed leading to constitutive synthesis of precursors of the catechol siderophore bacilibactin (2,3-dihydroxybenzoate (DHB) and 2,3-dihydroxybenzoylglycine (DHBG)) (Bsat *et al.*, 1998, Baichoo *et al.*, 2002). Those compounds are easily detectable in culture supernatants (Bsat *et al.*, 1998). Cells of *B. subtilis* HB1000, HB6543, HB6544, HB6545, HB6546 were grown overnight in 200 ml low-phosphate content minimal medium (2.3.2) with or without Fe(III). When iron is not available, a Fur protein (apo-Fur) is no longer active for repression of its target genes. DHB(G) quantification in culture supernatants was conducted using the Arnow assay as described in Materials and Methods (2.5.10.1) and values were normalized to the cultures' OD₆₀₀ (Fig. 3.9). HB6543, HB6544 and HB6546 strains produced constitutively high levels of DHB(G) irrespective of the iron concentration in the medium, while CAC1682 was able to partially complement Fur deficiency. Moreover, similarly to the WT, under iron-deplete conditions HB6545 exhibited significant derepression ($P < 0.005$) of the DHB(G) biosynthesis pathway compared to the iron-replete medium. These results indicate that CAC1682, but not CAC0951, is selective for iron under the conditions of the assay.

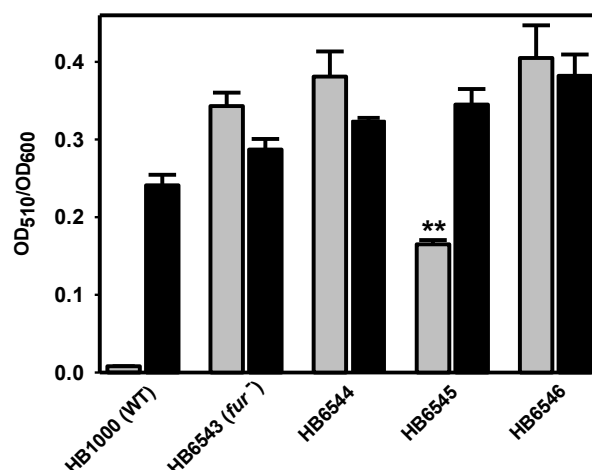


Fig. 3.9 Iron-dependent repression of the Fur-regulated siderophore biosynthesis pathway in *B. subtilis* HB6543 by CAC1682. Siderophore yields, represented as OD_{510}/OD_{600} (\pm SEM), were quantified for WT (wild-type, HB1000), HB6543 (*fur* mutant), HB6544 (HB6543 pTCatP control), HB6545 (HB6543 pTCatP::*fur*_{Cac}) and HB6546 (HB6543 pTCatP::*cac0951*) strains grown overnight in minimal medium without (black bars) or supplemented with 5 μ M Fe (III) (grey bars). The presented data was obtained from at least three independent experiments ($n=3$). Asterisks indicated significant difference between iron-replete and iron-deplete conditions ($P < 0.005$).

3.2 Generation and verification of a *fur* mutant in *C. acetobutylicum*

In silico and trans-complementation studies indicated the role of CAC1682 as a ferric uptake repressor. Therefore, the ORF *CAC1682* has been further referred as *fur*. To evaluate the biological significance of the Fur protein in *C. acetobutylicum*, *cac1682* was disrupted via directed insertional mutagenesis using the Clostron[®] system (Heap *et al.* 2007; 2010). In order to construct a *fur*-null strain, a modified pMTL007C-E2 vector was employed following an established procedure described in Materials and Methods (2.10). In order to introduce the nucleotide changes within the intron sequence, the 350 bp re-targeting region was assembled and amplified from pMTL007 by SOE PCR (2.8.2.3) using primers *fur*_IBS_271a, *fur*_EBS1d_271a, *fur*_EBS2_271a and EBS Universal (Table 7.4) (Fig. 3.10 A). The amplified re-targeting region was then ligated into the intron-encoding pMTL007C-E2 plasmid. Identification of positive clones was performed by blue-white screening on agar plates supplemented with X-Gal, followed by recombinant plasmid test restriction with *Hind*III and *Bsp*1407I (*Bsr*GI) (Fig. 3.10 B). pMTL007C-E2 harbouring group II intron modified for insertion into the *fur* gene sequence was afterwards subjected to *in vivo* methylation and electroporated into *C. acetobutylicum* ATCC 824 (2.10.2). Initial screening for presence of the desired insertion was performed through PCR at the gene-intron junction using the gene-specific *fur*_verif_rev primer and the intron-specific EBS

Universal primer (2.8.2.1) (Fig. 3.11 B). Integration of group II intron (~ 1.8 kb) into the *fur* coding sequence (456 bp) was demonstrated by whole gene PCR amplification (Fig. 3.11 C) with *fur_verif_fw* and *fur_verif_rev* primers (Table 7.4) using genomic DNA extracted from the wild-type and two representative mutant clones (2.8.2.2). Southern hybridization analysis (2.11.2) employing a *fur* gene specific probe and an intron specific ErmRAM probe further corroborated the correct insertion and ruled out multiple incorporation of the intron sequence into the genome (Fig. 3.12 A and B).

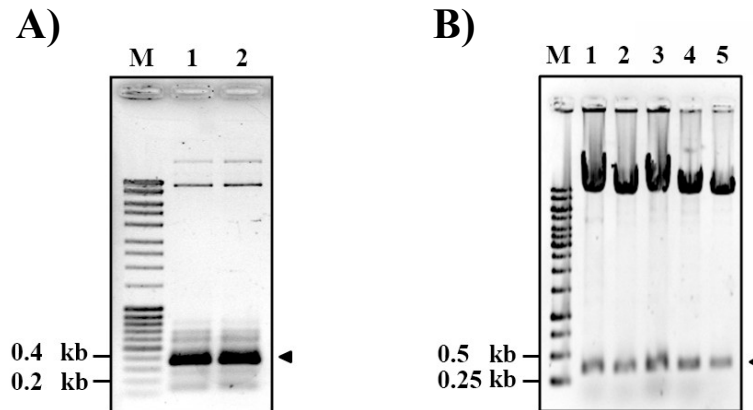
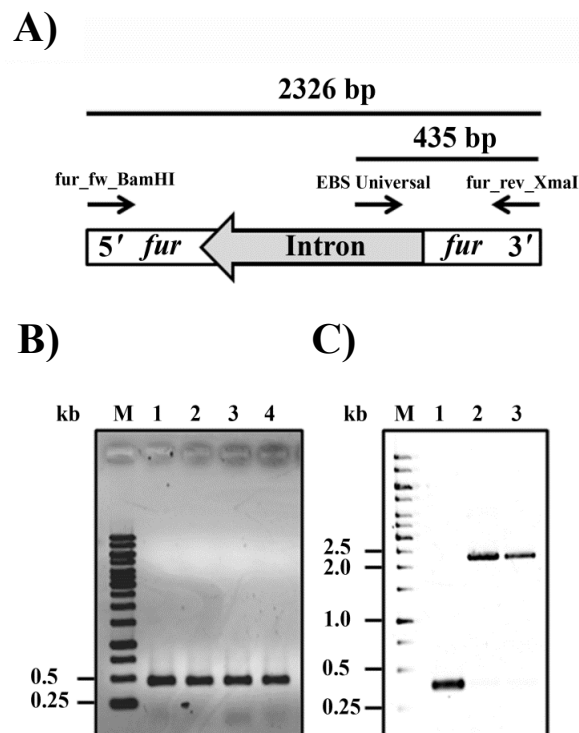


Fig. 3.10 Intron re-targeting and assembly of recombinant pMTL007C-E2, modified for disruption of the *C. acetobutylicum fur* gene. (A) Analytical gel electrophoresis (0.8 % gel) illustrating amplification of the 350 bp intron re-targeting region (lane 1-2) through SOE PCR. M, Massruler DNA Ladder Mix (Thermo Scientific). (B) Successful cloning of the intron re-targeting region into pMTL007C-E2 (lane 1-5), confirmed by test restriction using *Hind*III and *Bsp*1407I (*Bsr*GI). M, GeneRuler 1 kb DNA Ladder (Thermo Scientific).



Continued on next page

Fig. 3.11 Insertion of group II intron into the *fur* locus of *C. acetobutylicum* ATCC 824 verified by PCR. (A) Schematic representation of the PCR screening strategy employed for identification of positive integrant clones. (B) Colony PCR was performed with primers flanking the site of insertion (271 bp from the start codon) (lane 1-4). M, GeneRuler 1 kb Ladder (Thermo Scientific). (C) Whole *fur* gene PCR amplification with genomic DNA isolated from *C. acetobutylicum* WT and two representative *fur* insertional mutant clones (*fur::int(271a)*) using *fur_fw_Bam*HI and *fur_rev_Xma*I primers. M, GeneRuler 1 kb Ladder (Thermo Scientific); lane 1, WT *fur* gene PCR product; lane 2-3, *fur* gene PCR product incorporating the group II intron sequence (~ 1.8 kb).

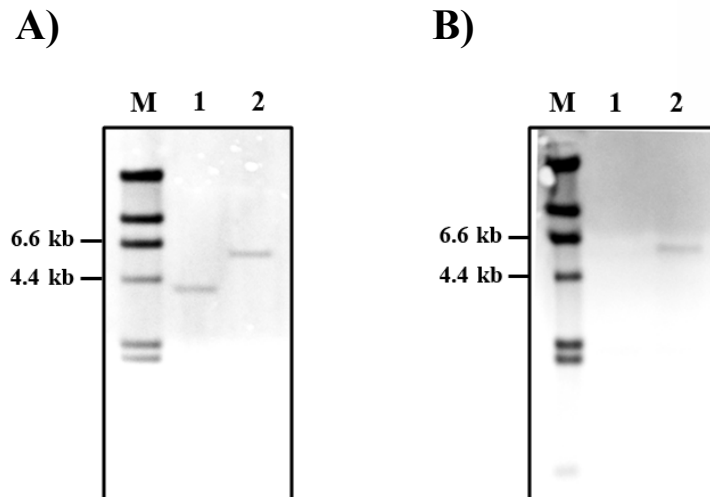


Fig. 3.12 Verification of *C. acetobutylicum fur* gene mutation by Southern blot hybridization. Genomic DNA was extracted from *C. acetobutylicum* WT and *fur::int(271a)* strains, digested with *Eco*RV and separated on a 1 % agarose gel. Next, the DNA was transferred to a nylon membrane, hybridized using DIG labeled *fur* gene specific (A) and ErmRAM cassette specific (B) probes. The signal was detected with NBT/BCIP. M, DIG labeled molecular weight marker II (Roche Applied Sciences); lane 1, WT; lane 2, *fur::int(271a)*.

3.3 Functional *in trans* complementation of the *fur* defective strain

In order to confirm that the phenotypical features of the mutant strain are due to Fur deficiency and to rule out potential polar effects or point mutations resulting from the Clostron[®] system, genetic complementation was performed. Two approaches for *in trans* complementation were implemented in this study. In the first approach, the wild-type copy of the *fur* gene along with its promoter region (positions - 500 to + 456 relative to the translational start site) were amplified from *C. acetobutylicum* ATCC 824 genomic DNA by PCR using *fur_prom_Xma*I_fw and *fur_prom_Nco*I_rev primers (Table 7.4). The amplicon was subsequently ligated into the *Xma*I and *Nco*I sites of the shuttle vector pMTL85141 (Heap *et al.*, 2009) and the resulting construct was transformed into *E. coli* DH5 α for *in vivo* amplification. Transformants were selected on LB medium supplemented with chloramphenicol (25 μ g/ml), followed by test restriction and sequencing (LGC Genomics, Berlin) to verify the presence of the correct insert. pMTL85141

carrying the *fur* gene and its cognate promoter region was then subjected to *in vivo* methylation in *E. coli* ER2275 and introduced into the *C. acetobutylicum fur* mutant strain through electroporation (2.10.2). Transformants were selected with erythromycin (30 µg/ml) and thiamphenicol (15 µg/ml). In the second complementation approach the pTCatP::*fur* (*cac1682*) construct (see 3.1.3.1), carrying the *C. acetobutylicum* wild-type *fur* gene under control of clostridial thiolase promoter (Girbal *et al.*, 2005) was electroporated in the *fur* mutant strain as described above. Transformants, selected with erythromycin (30 µg/ml) and thiamphenicol (15 µg/ml), were confirmed by colony PCR using pT_seq_fw and pT_seq_rev primers (Table 7.4). Furthermore, to evaluate any possible effects caused solely by the vector systems, negative control strains were constructed by introduction of the pMTL85141 and pTCatP vectors without inserts into the *C. acetobutylicum fur* mutant strain. Since complementation experiments demonstrated that both strategies were comparable, the results achieved with *C. acetobutylicum fur* mutant pTCatP::*fur* and *C. acetobutylicum fur* mutant pTCatP strains (Table 7.1) are presented in this work.

3.4 Physiological characterization of the *C. acetobutylicum fur* mutant

In addition to genes involved in iron supply, Fur regulators control directly and indirectly genes related to a great variety of cellular processes, including among others, energy metabolism and oxidative stress responses (Lee and Helmann, 2007; Carpenter *et al.*, 2009). The degree of functional diversity of the Fur protein differs even in closely related bacteria, thus creating a species specific unique set of physiological processes under control of this pleiotropic regulator. The capacity of Fur in *C. acetobutylicum* has been evaluated in the present work by examination of the physiology of the generated *fur* mutant strain.

3.4.1 Growth characteristics, morphology and product formation

Absence of the ferric uptake regulator (Fur) affected significantly the growth pattern of *C. acetobutylicum*, suggesting a major physiological importance of this protein. When grown anaerobically for 48 h at 37 °C on complex RCA agar medium (2.3.3), the mutant formed smaller colonies than the parental strain (Fig. 3.13 A and B). A similar profile has been observed in the *fur* defective strain carrying the empty control pTCatP vector. Introduction of a functional copy of the *fur* gene restored the size of the colonies, indicating that the growth defect is due to loss of Fur. Similarly, the *fur* defective strain produced smaller colonies than the parental strain, when grown on minimal MS-CaCO₃ agar medium (2.3.3) for 96 h (data not shown). Small colony

morphology could be a result of reduced cell size. Therefore, the length of *fur* mutant and wild-type cells was examined using light microscopy (2.5.4). Since no distinguishable difference has been observed in either cell shape or length between both strains (Fig. 3.13 C), it could be concluded that the marked decrease in colony size of the mutant strain is a result of reduction in cell number.

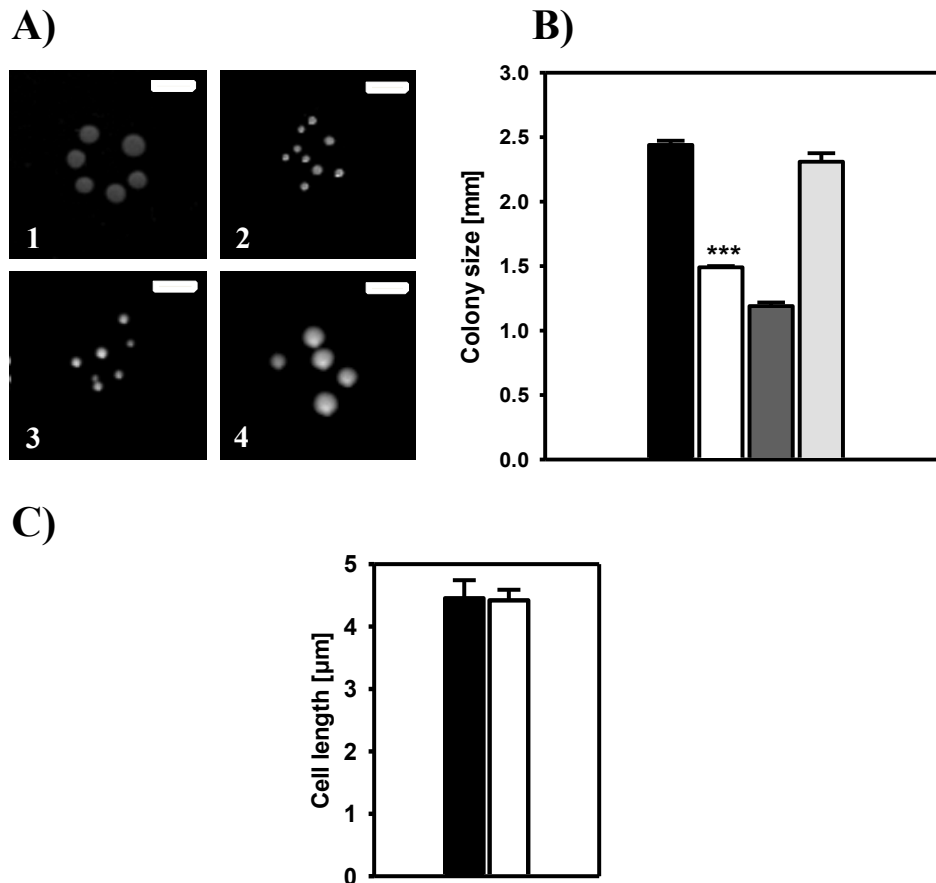


Fig. 3.13 Small colony morphology of *C. acetobutylicum fur* mutant. Cells of WT (1; black bar), *fur* mutant (2; white bar), control vector (3; dark grey bar) and complemented strains (4; light bar) were grown anaerobically for 48 h at 37 °C on complex RCA agar plates. The results presented in (B) were obtained from at least ten independent measurements ($P < 0.001$). (C) Length of wild-type (black bar) and *fur* mutant (white bar) cells as determined by light microscopy. White bars in (A) represent 5 mm.

To further investigate the behaviour of the *fur* mutant relative to the wild-type, growth of the four strains was evaluated in 200 ml liquid complex CGM medium (2.3.3) (Fig. 3.14). The *fur* mutant displayed longer lag phase, slower exponential growth rate (μ) and lower cell density at stationary phase in comparison to the wild-type. This phenotype was complemented by introduction of a functional copy of the *fur* gene.

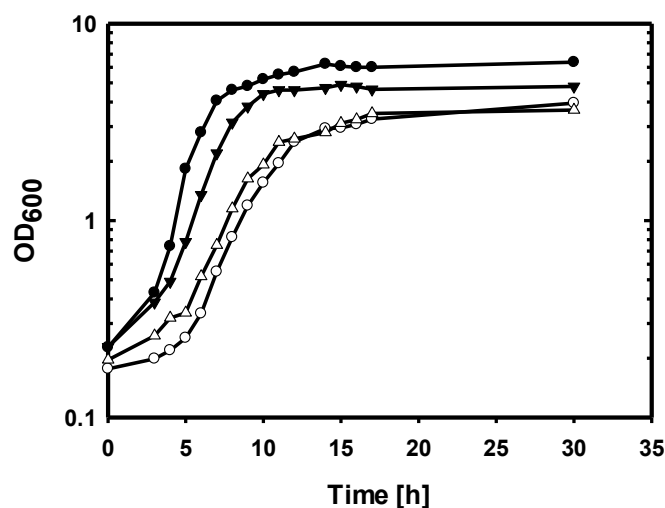


Fig. 3.14 Comparative growth profiling of *C. acetobutylicum fur* mutant relative to the WT in liquid rich medium. Cultures of *C. acetobutylicum* WT (closed circles), *fur* mutant (open circles), control vector (open triangles) and complemented (closed circles) strains were propagated in 200 ml CGM medium supplemented with 5 % glucose. The following growth rates (μ) were calculated for each strain: WT ($0.580 \pm 0.08 \text{ h}^{-1}$); *fur* mutant ($0.239 \pm 0.02 \text{ h}^{-1}$); pTCatP vector control strain ($0.222 \pm 0.03 \text{ h}^{-1}$); complemented strain ($0.543 \pm 0.07 \text{ h}^{-1}$). The presented data was obtained from four independent experiments ($n=4$), $P < 0.001$.

Upon cultivation in 200 ml minimal MS-MES medium (2.3.3), supplemented with 60 g/l glucose, the *fur* defective strain exhibited similar growth characteristics (Fig. 3.15 A). The slower growth of the mutant resulted in a delay of the metabolic switch reflected by a delay in the pH shift as illustrated on Fig. 3.15 B. The lower final yield corresponded to a significant decrease in glucose utilization (Fig 3.15 C). Another facet of special interest for the physiological characterization of *C. acetobutylicum* is quantification of the accumulated fermentation products. Previous studies reported prevalent lactate synthesis during the acidogenic growth phase ($\text{pH} > 5$) and a significantly increased butanol:acetone ratio during the solventogenic phase ($\text{pH} < 4.4$) in iron-deficient cells of *C. acetobutylicum* (Bahl *et al.*, 1986). In order to investigate a potential shift in the metabolic profile, solvents (butanol, acetone and ethanol) were measured in cell-free culture supernatants of the wild-type, *fur* mutant, negative control and complemented strain after 135 h of incubation in 200 ml MS-MES medium using gas chromatography (2.5.7). The obtained quantities were normalized to the maximal reached OD_{600} of the corresponding cultures (OD_{max}). As illustrated on Fig. 3.15 D, the *fur* mutant exhibited no statistically significant difference in product spectrum with respect to the wild-type. In addition, lactate production has been monitored (2.5.6) during the whole growth of all four strains (data not shown). Elevated lactate concentrations in the *fur* mutant strain relative to the wild-type have not been detected in this study.

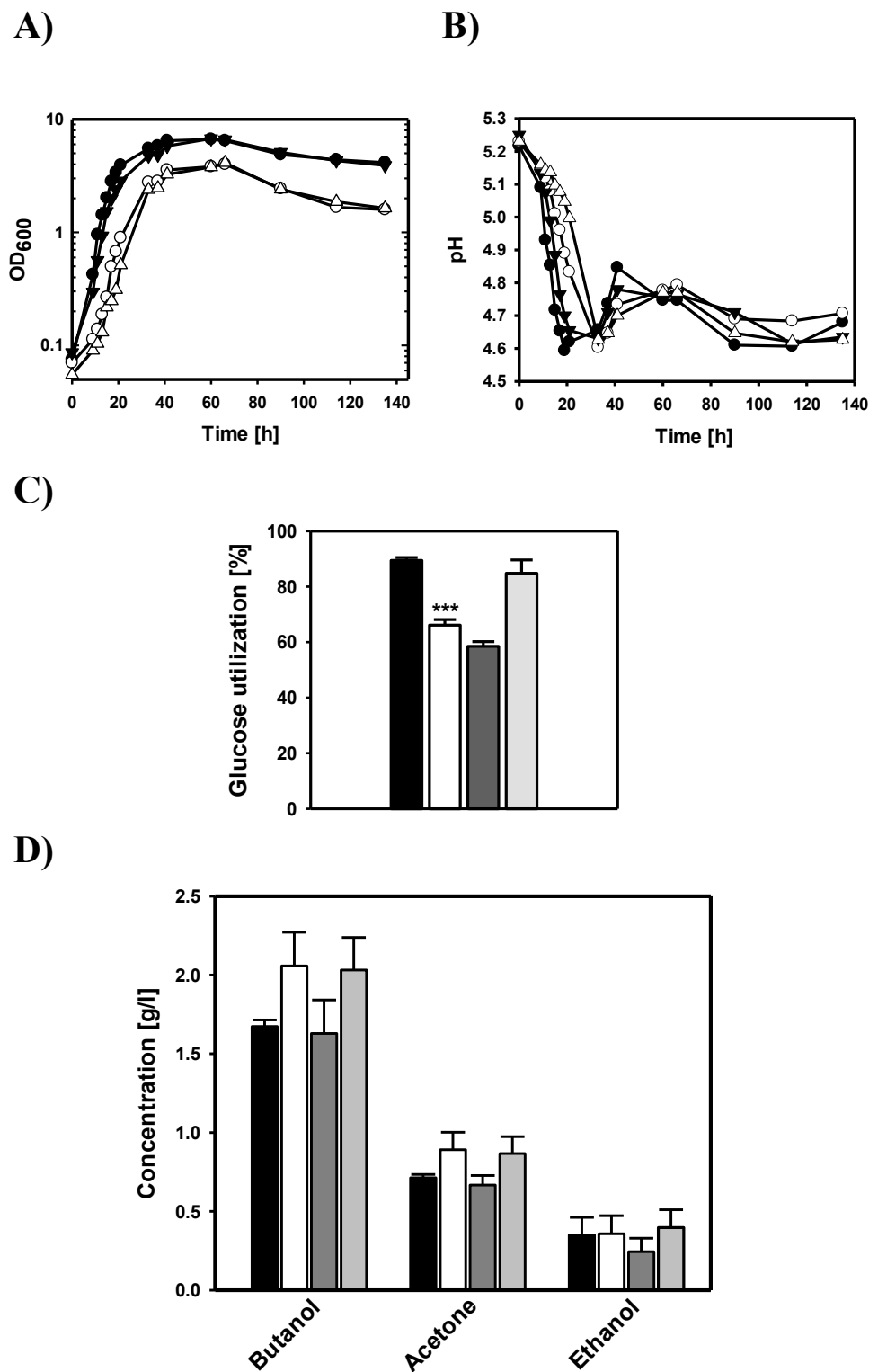


Fig. 3.15 Growth and fermentation profile of *C. acetobutylicum fur* mutant strain in minimal medium. Cultures of *C. acetobutylicum* WT (closed circles; black bars), *fur* mutant (open circles; white bars), control vector (open triangles; dark grey bars) and complemented (closed circles; light grey bars) strains were grown in 200 ml MS-MES medium. (A) OD₆₀₀ and (B) pH values were measured periodically during the whole growth (C) Glucose utilization after 135 h presented as percentage. 100 % corresponds to the initial concentration of 60 g/l. (D) Solvent concentrations, represented as g/l/OD_{max} measured after 135 h of incubation in cell-free culture supernatants. The presented data was obtained from three independent experiments (n=3), $P < 0.001$ (A) and (C). The following specific growth rates (μ) were calculated for each strain: WT ($0.170 \pm 0.04 \text{ h}^{-1}$); *fur* mutant ($0.100 \pm 0.02 \text{ h}^{-1}$); pTCatP vector control strain ($0.110 \pm 0.01 \text{ h}^{-1}$); complemented strain ($0.146 \pm 0.03 \text{ h}^{-1}$).

Activity of the H₂-evolving hydrogenase (HydA1), a major iron-rich enzyme in the metabolism of *C. acetobutylicum*, has been reported to be significantly reduced under iron-starvation conditions (Junelles *et al.*, 1988). To test if inactivation of *fur* affects formation of H₂, total gas volume, as well as the H₂:CO₂ ratio, were measured in headspace of 50-ml MS-MES cultures of the wild-type and the *fur* mutant (2.5.8) (data not shown). No significant differences have been detected in either total gas amount or H₂:CO₂ distribution between both strains in this study.

3.4.2 Growth in the presence of an iron chelator

To further investigate the biological effect of *fur* inactivation in *C. acetobutylicum*, cells of the wild-type, *fur* mutant, control vector and complemented strains were grown under iron-starvation conditions. In order to mimic iron-limiting conditions, RCA agar plates or CGM liquid medium were supplemented with increasing concentrations of 2,2'-dipyridyl (DP), a cell-wall permeable iron chelator. Fig. 3.16 represents the results from three independent experiments. Addition of 50 μ M DP to the RCA agar medium did not affect significantly the growth in comparison to the untreated cells of the wild-type and the mutant strain (see Fig. 3.11 B). A concentration of 100 μ M DP inhibited substantially the growth of both strains, however the reduction in colony size was significantly more pronounced in the *fur* mutant (~ 70 % (*fur* mutant) vs. ~ 40 % (wild-type) relative to the untreated controls). Moreover, 150 μ M DP prohibited completely the growth of the *fur* mutant, while the wild-type and complemented strains were still able to tolerate these quantities. Similar results were obtained upon incubation in 200 ml CGM medium supplemented with 100, 150 or 200 μ M DP (Fig. 7.5, Appendix).

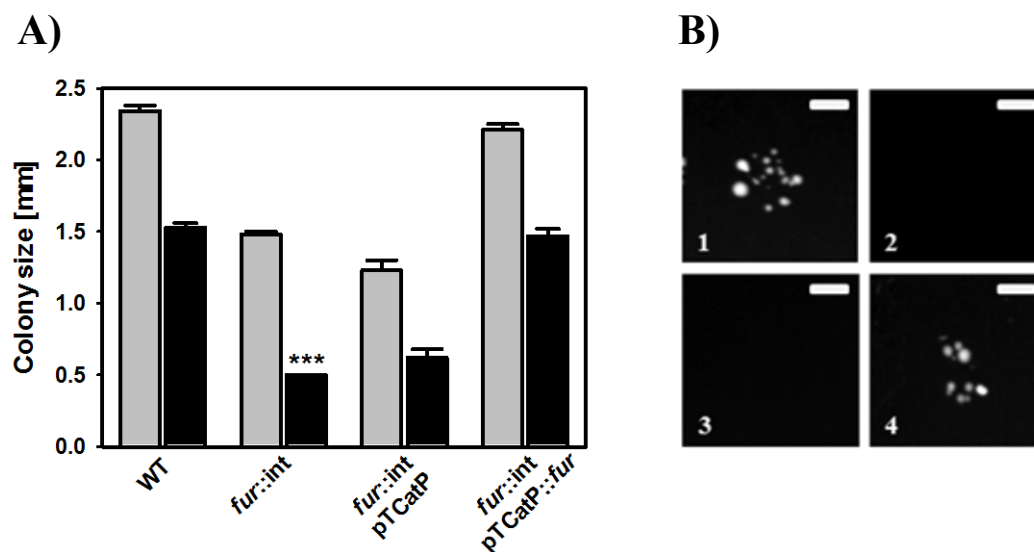


Fig. 3.16 Growth of *C. acetobutylicum fur* mutant under iron-limiting conditions. Cells of the WT, *fur* mutant, pTCatP negative control and complemented strains were grown on RCA agar plates supplemented with (A) 50 μ M (grey bars), 100 μ M (black bars) and (B) 150 μ M of the iron chelator 2,2'-dipyridyl (DP). Results presented in (A) were obtained from three independent experiments (n=3), $P < 0.001$. See text for details.

3.4.3 Quantification of intracellular iron content

Under iron sufficient conditions Fur negatively regulates an assortment of genes involved in iron uptake (Andrews *et al.*, 2003). Therefore, derepression of these transport pathways in *fur* mutant strains typically leads to accumulation of higher levels of intracellular unincorporated iron (Touati *et al.*, 1995; Fuangthong *et al.*, 2002). Results in (3.4.2), however, suggested that the *fur* mutant in *C. acetobutylicum* is iron-deficient since it showed significantly reduced growth under iron-limiting conditions relative to the wild-type. In order to examine how absence of Fur affects the cellular iron status in this microorganism, a colorimetric ferrozine assay was employed (2.5.11). Total iron concentrations were determined in cells of the wild-type, *fur* mutant, negative control vector and complemented strains, grown to stationary phase in 50 ml CGM medium (Fig. 3.17). Data derived from three independent cultures showed that the *fur* mutant accumulated higher levels of chelatable iron. These results suggest a more complex regulation, rather than a mechanistic effect of the intracellular iron concentration in the *fur* mutant strain.

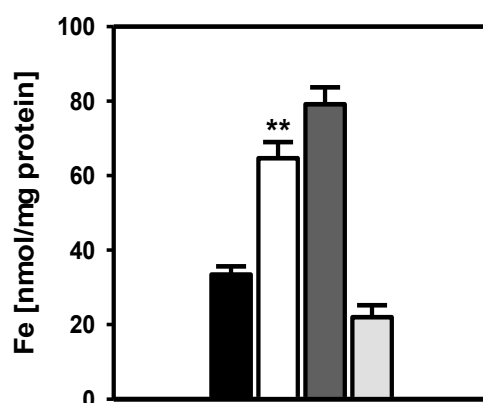


Fig. 3.17 Effect of *fur* inactivation on *C. acetobutylicum* total intracellular iron level. Total iron concentration was measured in cells of the WT (black bar), *fur* mutant (white bar), negative pTCatP vector control (dark grey bar) and complemented strain (light grey bar) using the colorimetric ferrozine assay. Quantities, represented as nmol Fe/mg soluble protein (\pm SEM) were obtained from three independent experiments ($P < 0.01$)

3.4.4 Sensitivity to oxidative stress

Limited aerobic resistance has been well documented for *C. acetobutylicum* (O'Brien and Morris, 1971; Kawasaki *et al.*, 2004; Hillmann *et al.*, 2008, 2009b). In the context of its natural habitats, this microorganism might periodically experience varying degrees of aeration. Lack of proper regulation of the intracellular iron levels (3.4.3) could lead to uncontrolled formation of deleterious ROS via the Fenton reaction under these conditions (Imlay, 1988). Therefore, the effect of *fur* inactivation on sensitivity of *C. acetobutylicum* to ambient air was tested in this study

(2.16.1). Cells of the wild-type and the mutant strain, grown to mid-exponential phase (OD_{600} 0.7-0.8) under anaerobic conditions, were transferred to sterile flasks and incubated for 2 h with rigorous aeration on a rotary shaker (180 rpm). Samples were taken periodically, diluted appropriately, plated on RCA agar plates and grown in an anaerobic chamber for 48 h. The *fur* mutant exhibited significantly reduced viability in comparison to the wild-type during the whole course of the experiment (Fig. 3.18 A). Furthermore, the wild-type and the *fur* defective strain were tested for their sensitivity to the oxidative stress agent H_2O_2 (2.16.1). The results from three independent experiments demonstrated that absence of Fur in *C. acetobutylicum* renders the cells hypersensitive to H_2O_2 (Fig. 3.18 B). Quite unexpectedly, introduction of the pTCatP vector into *C. acetobutylicum fur* mutant led to a complete lack of growth upon exposure to oxidative stress. Therefore, results performed with the complemented strain are not shown in this work.

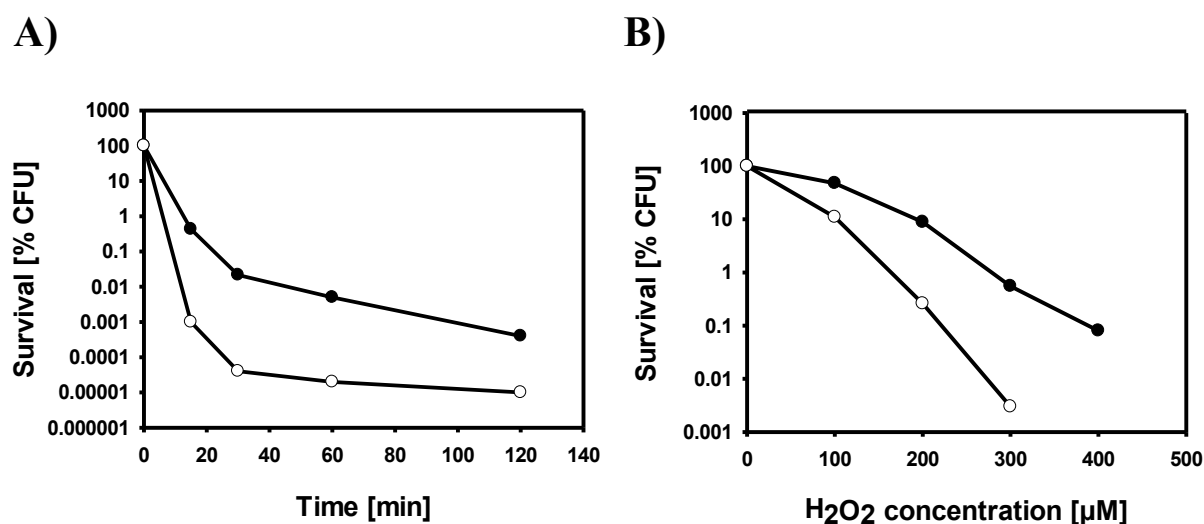


Fig. 3.18 Effect of *fur* inactivation on *C. acetobutylicum* sensitivity to oxidative stress. (A) After incubation of cells from *C. acetobutylicum* WT (closed circles) and *fur* mutant (open circles) in 10 ml CGM medium until mid-exponential phase has been reached, both strains were exposed to ambient air on a rotary shaker (180 rpm) and survival was evaluated as $cfu\ ml^{-1}$. (B) Cell aliquotes from both strains were incubated with increasing concentrations of the oxidative agent H_2O_2 for 30 min at 37 °C. Results were obtained from three independent experiments ($n=3$).

3.5 An intersection between response to *fur* mutation and iron limitation

3.5.1 Assessment of potential siderophore production

One of the most striking features of the bacterial Fur regulated iron-dependent response is the production of siderophores, small-molecule chelators that capture limiting iron from the environment (Wandersman and Delepelaire, 2004). According to the structure of their iron-

coordinating moieties siderophores could be grouped into three major classes: (i) catecholates; (ii) hydroxamates and (iii) carboxylates (Miethke and Marahiel, 2007). The first member in the group of clostridia to be shown to synthesize at least one siderophore under iron-deficient conditions is *Clostridium klyuveri* (Seedorf *et al.*, 2008). Therefore, a potential production of this class of compounds came under focus in *C. acetobutylicum*. In order to achieve iron-limiting conditions for the assay, minimal MS-MES medium was treated with the iron-chelating resin Chelex (Sigma Aldrich) to eliminate any trace amounts of iron. The medium was afterwards supplemented with 6 μM FeSO_4 , an amount chosen in concert with previous studies, which demonstrated concentrations of iron up to 10 μM to be limiting for the growth of clostridia (Schönheit *et al.*, 1979; Bahl *et al.*, 1986). Cells of the wild-type and the *fur* mutant strain were grown in 500 ml of iron-deplete and -replete MS-MES medium, respectively. Culture supernatants were then assayed for presence of hydroxamate and catecholate-type siderophores using the ferric perchlorate (2.5.10.2) and the Arnow assays (2.5.10.1) (Fig. 3.19 A and B). In addition, the cell-free supernatants from both strains were tested for siderophore compounds, which do not belong to those two major classes using the CAS liquid assay (2.5.10.3) (Fig. 3.19 C). Results from the three assays showed that *C. acetobutylicum* does not produce detectable siderophores regardless of iron availability or *fur* mutation.

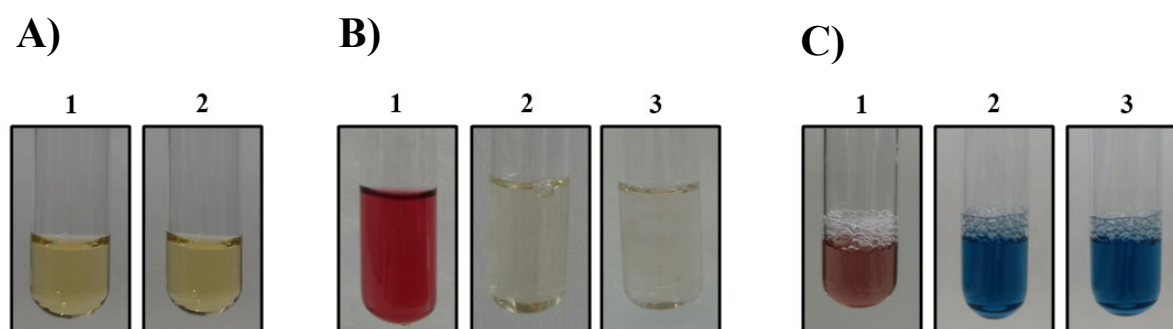


Fig. 3.19 *C. acetobutylicum* does not secrete detectable siderophores into culture supernatants. (A) Ferric perchlorate assay was performed for detection of hydroxamate-type siderophores in cell-free culture supernatants from the iron-deficient wild-type (1) and the *fur* mutant (2). When present hydroxamate siderophores produce bright orange to purple colour. (B) Arnow and (C) CAS assays for identification of catechol or other classes of siderophores. (1), positive control; cell-free supernatants from *C. acetobutylicum* iron-deficient WT (2) and *fur* mutant (3).

3.5.2 Riboflavin biosynthesis

Although no siderophore synthesis has been detected, interestingly, the culture supernatants from the *C. acetobutylicum fur* mutant strain appeared bright yellow in colour (Fig. 3.20). This unique feature was caused specifically by *fur* inactivation since introduction of a functional copy of the *fur* gene restored the parental phenotype. Furthermore, the wild-type, grown under iron-limiting conditions, exhibited a similar profile (Fig. 3.20). Several studies in bacteria have indicated a relationship between iron regulation and flavin production (Worst *et al.*, 1998; Ernst *et al.*, 2005;

Crossley *et al.*, 2007; Pich *et al.*, 2012). Therefore, cell-free supernatant from the *fur* mutant was subjected to analysis (2.5.9.1) and it displayed visible and fluorescence emission spectra characteristic for those of flavins (Fig. 3.21 A and B). Since riboflavin, flavin mononucleotide (FMN) and flavin adenine dinucleotide (FAD) share identical spectra, thin-layer chromatography (TLC) was performed to determine the nature of the secreted compound (2.5.9.2). As depicted on Fig. 3.21 C, TLC revealed riboflavin as the sole constituent of the *fur* mutant supernatant. Considering the biotechnological potential of *C. acetobutylicum*, riboflavin concentrations were determined spectrophotometrically in cell-free supernatants of the wild-type, *fur* mutant, negative control and complemented strains as well as the iron-deficient wild-type (2.5.9.3). The obtained quantities were then normalized to the OD_{max} of the corresponding cultures (Fig. 3.22).

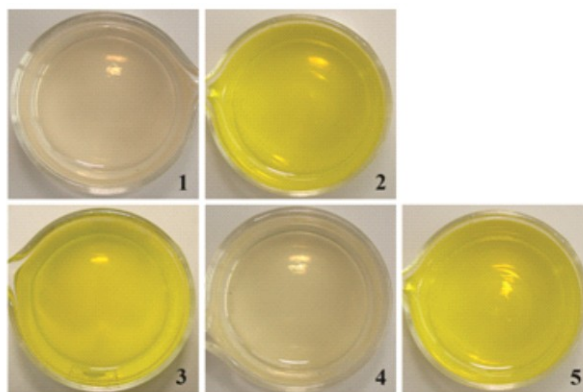
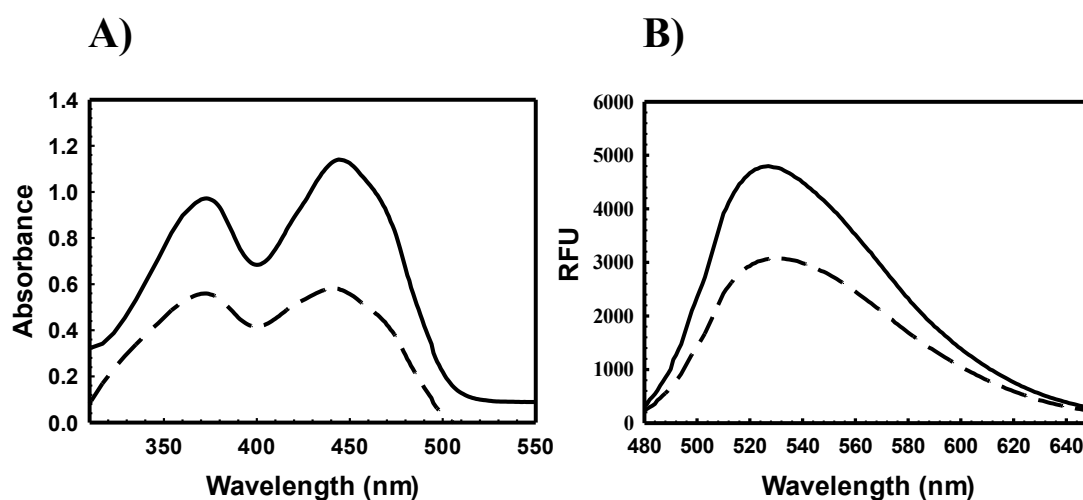


Fig. 3.20 Flavin biosynthesis in response to *fur* mutation and iron deficiency in *C. acetobutylicum*. Cell-free supernatants from WT (1), *fur* mutant (2), pTCatP negative control (3), complemented strain (4) and iron-deficient WT (5) after 60 h of incubation in 200 ml MS-MES medium.



Continued on next page

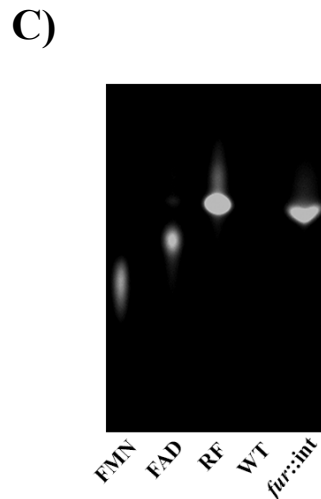


Fig. 3.21 Identification of riboflavin in culture supernatants from *C. acetobutylicum fur* mutant strain. Absorption (A) and fluorescence (B) emission spectra of a RF standard solution (solid line) and cell-free supernatant from the *fur* mutant (dashed line). (C) Flavin standards (FMN, FAD and RF) and lyophilized cell-free supernatants from the wild-type and the *fur* mutant (*fur::int*) were dissolved in 96 % ethanol and loaded on a TLC plate. The plate was afterwards developed with *n*-butanol: acetic acid: water (4: 1: 5) and visualized using a UV Illuminator.

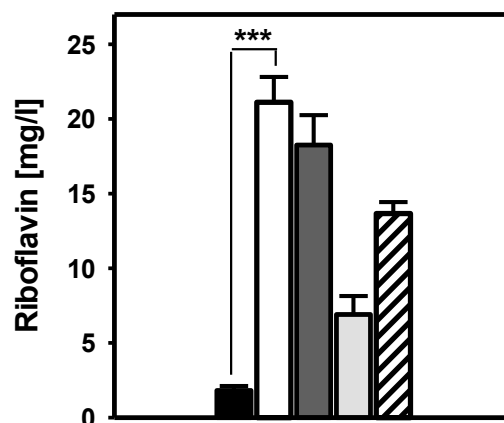


Fig. 3.22 Riboflavin yields in cultures of *C. acetobutylicum fur* mutant and iron-deficient WT. Riboflavin concentrations in supernatants of the WT (black bar), *fur* mutant (white bar), pTCatP negative control vector (dark grey bar), complemented strain (light grey bar) and the iron-deprived WT (striped bar) were determined spectrophotometrically after 135 h of growth in MS-MES medium and the values were normalized to the OD_{max} of the cultures.

The genes encoding the enzymes that compose the riboflavin biosynthesis pathway in *C. acetobutylicum* are organized in a single operon (*ribDBAH*) (Nölling *et al.*, 2001; Cai and Bennett, 2011). In order to investigate the transcriptional pattern of the *ribDBAH* gene cluster, upon iron limitation and lack of Fur, Northern blot hybridization analysis (2.11.3) was performed (Fig. 3.23). Total RNA was harvested from cells of the wild-type, grown under iron-replete and -deplete conditions, the *fur* mutant and the complemented strain (2.6.3). Both iron deficiency and *fur* gene inactivation resulted in a strong hybridization signal, which corresponded well with the

concentrations of riboflavin detected in the medium (Fig. 3.20), while introduction of a functional copy of the *fur* gene resulted in a partial complementation.

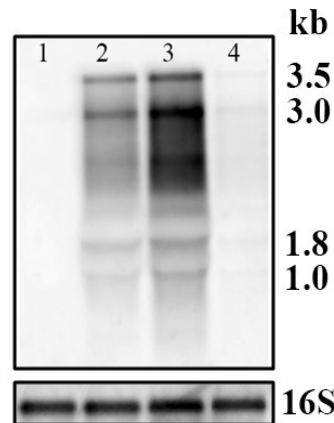


Fig. 3.23 Inactivation of *fur* and iron limitation in *C. acetobutylicum* lead to induction of the *ribDBAH* operon, responsible for riboflavin biosynthesis. Northern hybridization analysis was conducted with 20 μ g RNA extracted from mid-exponential cultures of *C. acetobutylicum* WT grown under iron-replete (lane 1) and iron-limiting (lane 2) conditions; *fur* mutant (lane 3) and complemented strain (lane 4). Hybridization with a probe specific for 16S rRNA was used as a control for equal loading. Transcript sizes are indicated on the right side.

3.6 Global expression analyses and 2D-PAGE

In order to gain further insight into the mechanisms for establishment of iron balance in *C. acetobutylicum* and the role of Fur in this process, the global transcriptional profile of the *fur* mutant and the iron-limitation stimulon of the parental strain were determined using microarray analysis (2.12). To define the iron-starvation stimulon, transcript levels from wild-type cells grown to mid-exponential phase under iron-deplete and iron-replete conditions were compared (WT(-Fe)/WT(+Fe)). Evaluation of differential gene expression resulting from Fur deficiency was performed by comparing transcript populations from cells of the mutant strain and the wild-type, propagated under iron-replete conditions (WT(+Fe)/*fur* mutant(+Fe)). To this end the extracted RNA (2.6.3) was treated with DNase I, reverse transcribed into cDNA, labeled with Cy3 and Cy5 and purified as previously described (Hillmann *et al.*, 2009b; Janssen *et al.*, 2010). Microarray data was obtained from at least three independent experiments (n=3). To rule out potential dye-specific effects each sample was labeled both with Cy3 and Cy5, resulting in at least 12 dataset scores for a single gene. In addition analytical 2D-PAGE electrophoresis (2.15.4) was conducted in order to compare the protein expression profiles of the *fur* mutant and the parental strain.

Conditions of iron starvation affected significantly the transcription of 156 genes. Among these 79 were upregulated and 77 downregulated. Inactivation of *fur*, on the other hand, resulted in a marked effect on the level of transcription of 157 genes with 73 being induced and 84

downregulated. In an attempt to visualize data structures that would reveal distinct patterns of regulation, the expression scores from both microarray datasets, represented as log values, were plotted using a two-dimensional graphical display (Fig. 3.24). Of special interest was a cluster of genes regulated in a similar manner both upon iron limitation and *fur* gene inactivation. This group defines the so-called iron-regulated Fur modulon (direct and indirect targets of Fur-Fe²⁺). Upon analysis of the generated two dimensional plot, an overlapping collection of 32 upregulated (shaded in red on Fig. 3.24) and 7 downregulated genes (coloured in green) was detected. In addition to this apparent mode of regulation, many other genes were differentially transcribed in response to iron limitation or *fur* gene inactivation.

Previous studies have reported differential Fur-dependent regulation as a function of the growth phase (Merrell *et al.*, 2003). These differences have been attributed to changes in Fur protein level, alternative sigma factors or co-regulation (Danielli *et al.*, 2006; Baichoo *et al.*, 2002; McHugh *et al.*, 2003). In order to reveal potential growth-phase-dependent variability in the spectrum of Fur-mediated regulation in *C. acetobutylicum*, transcript levels were compared between the wild-type and the *fur* mutant strain using RNA extracted from stationary phase cultures. However, significant differences in comparison to the exponentially growing cells were not detected under the conditions employed in this study (data not shown).

In addition to its classical role as an iron-sensing repressor, Fur has been reported to exhibit alternative modes of regulation (Lee and Helmann, 2007; Carpenter *et al.*, 2009). These include direct and indirect activation, as well as regulation in the absence of its cofactor Fe(II), namely apo-Fur repression and apo-Fur activation (Delany *et al.*, 2004; Yu and Genco, 2012). In order to investigate the possibility of apo-Fur mediated transcriptional control in *C. acetobutylicum*, RNA transcript levels were compared between wild-type and *fur* mutant cells, both grown under iron-limiting conditions (WT(-Fe)/*fur* mutant (-Fe)), and between *fur* mutant cultures grown under iron-replete and -deplete conditions (*fur* mutant (+Fe)/*fur* mutant (-Fe)), respectively. Results from two independent experiments (data not shown) did not reveal obvious candidate gene targets of Fur regulation in the absence of iron as a co-effector.

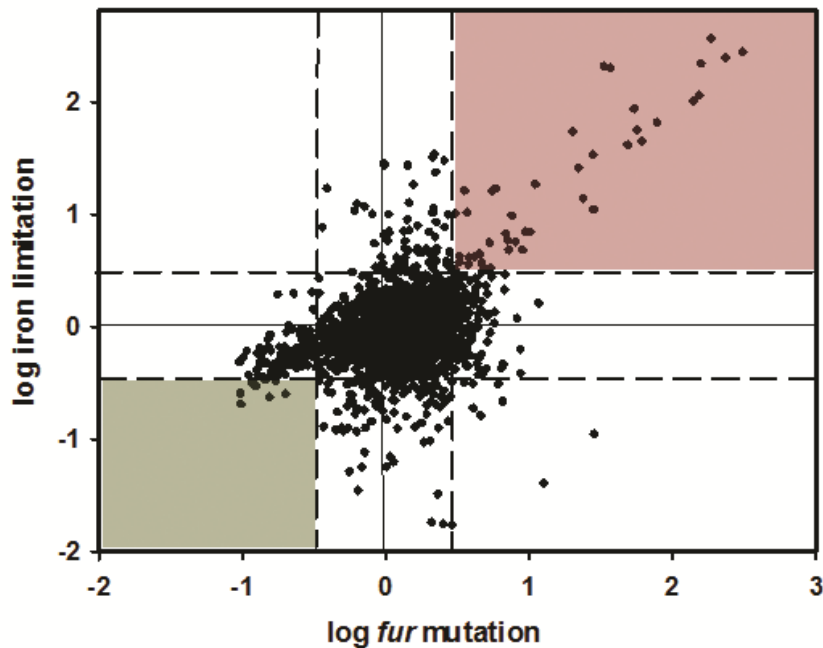


Fig. 3.24 Visualization of the Fur modulon in *C. acetobutylicum*. The iron-limitation stimulon of *C. acetobutylicum* was plotted versus the response to *fur* inactivation using a two dimensional graphical display. Genes derepressed in the *fur* mutant and upregulated in response to low-iron conditions are denoted in red and those downregulated under both conditions in green. All genes which elicited change in expression more than 3 fold were considered as differentially regulated (dashed lines).

3.6.1 Fur modulon

All genes, comprising the Fur modulon in *C. acetobutylicum* as determined by the microarray analysis are listed in Table 3.4. Consistent with the predicted role of Fur in coordinating the intracellular iron status, among the most strongly induced in both microarray datasets was a repertoire of genes associated with transport of iron. Highly upregulated were two clusters, *cac1029-1031* and *cac0788-0791*, encoding, respectively, a predicted Feo-type transport system, responsible for uptake of ferrous iron (Fe^{2+}) and a putative ferrichrome system involved in transport of ferri-siderophore complexes. Most dramatically induced (above 200-fold) was a flavodoxin encoding gene (*cac0587*), which presumably forms a bicistronic operon with another notably upregulated gene (*cac0588*) coding for a hypothetical protein. Accordingly, analytical 2D-PAGE analysis of the *fur* mutant using IPG-Strips (pI 4-7) revealed CAC0587 as a novel protein spot (Fig. 3.25). In agreement with the results presented in (3.5.2), the genes composing the *ribDBAH* cluster, were strongly upregulated. Moreover, RibH (6,7-dimethyl-8-ribityllumazine synthase) was significantly induced in the *fur* mutant relative to the WT upon 2D PAGE analysis (Fig. 3.25). The other proteins of the riboflavin biosynthesis pathway could not be identified in this study since their pI values are out of range. In concert with previous studies that reported lactate to be the predominant fermentation product during the acidogenic phase in iron-deficient

cells of *C. acetobutylicum* (Bahl *et al.*, 1986), the expression of a gene encoding a putative L-lactate dehydrogenase (*cac0267*) was significantly increased under these conditions. It is interesting to note that although no elevated concentration of lactate was detected in culture supernatants from the *fur* mutant strain, inactivation of *fur* led to approximately 18 fold increase in expression of *cac0267*. These results suggest that *cac0267* is regulated by iron and this regulation requires Fur. Among other upregulated genes with no apparent role in iron metabolism were *cac1602-cac1603*, encoding a CheY-diverged domain-containing protein and a hypothetical protein, respectively; a putative methyltransferase-encoding gene (*cac0567*); a B₁₂ biosynthesis gene cluster (*cac0582-cac0585*) and, surprisingly, a gene (*cac1478*) encoding a 30S ribosomal protein.

Table 3.4 Iron-regulated Fur modulon in *C. acetobutylicum*.

ORF#*	Gene name	Annotated function	Expression ratio*	
			-Fe/+Fe	<i>fur::int</i> /WT
CAP0141		periplasmic hydrogenase small subunit	0.6	0.1
CAP0142		periplasmic hydrogenase large subunit	0.5	0.1
CAP0143		hydrogenase maturation protease delta subunit, HyaD-like	0.3	0.1
CAP0144		steroid-binding protein	0.3	0.1
CAP0145		hypothetical protein	0.3	0.1
CAP0146		hypothetical protein	0.2	0.1
CAC0267	<i>ldh</i>	L-lactate dehydrogenase	18.5	18.5
CAC0546		uncharacterized membrane protein	0.3	0.2
CAC0567		putative methyltransferase	5.7	6.9
CAC0570		PTS enzyme II, ABC system	0.3	0.3
CAC0582		cobalamin biosynthesis protein	3.0	5.0
CAC0583		CbiK protein (chain A, anaerobic cobalt chelatase)	2.8	5.5
CAC0584		precorrin-6B methylase 1 CobL1/CbiE	2.5	3.9
CAC0587		flavodoxin	275.7	366.7
CAC0588		hypothetical protein	365.9	300.5
CAC0590	<i>ribD</i>	pyrimidine deaminase and pyrimidine reductase	65.4	61.5
CAC0591	<i>ribB</i>	riboflavin synthase subunit alpha	55.3	44.1
CAC0592	<i>ribA</i>	gtpcyclohydrolase/3,4-dihydroxy-2-butanone 4-phosphate synthase	44.2	47.3
CAC0593	<i>ribH</i>	6,7-dimethyl-8-ribityllumazine synthase	41.0	41.3
CAC0594		pyridoxal biosynthesis lyase PdxS	4.8	11.4
CAC0595		glutamine amidotransferase subunit PdxT	7.0	12.5
CAC0787		uncharacterized conserved protein	53.9	28.7
CAC0788		ferrichrome transport permease	207.1	64.3
CAC0789	<i>fhuB</i>	permease	200	58.0
CAC0790	<i>fhuD</i>	ferrichrome-binding periplasmic protein, fhuD	86.7	81.2

CAC0791	<i>fhuC</i>	ferrichrome ABC transporter ATP-binding protein	122.2	94.9
CAC0843		ribonuclease precursor (barnase), secreted	4.2	3.3
CAC0844		barstar-like protein ribonuclease (barnase) inhibitor	3.8	3.3
CAC1029	<i>feoA</i>	FeoA-like protein, involved in iron transport	100.5	151.0
CAC1030	<i>feoA</i>	FeoA-like protein, involved in iron transport	113.8	163.4
CAC1031	<i>feoB</i>	FeoB-like GTPase, responsible for iron uptake	246.7	318.5
CAC1032		transcriptional regulator	218.1	130
CAC1033		hypothetical protein, CF-31 family	3.3	6.0
CAC1478		30S ribosomal protein S4	9.6	8.5
CAC1602		diverged CheY-domain-containing protein	29.9	28.6
CAC1603		hypothetical protein	32.0	28.8
CAC2905		uncharacterized protein	0.3	0.1
CAC3314		nitroreductase family protein	3.6	3.8
CAC3622		benzoyl-CoA reductase/2-hydroxyglutaryl-CoA dehydratase	11.0	28.5
CAC3623		2-hydroxyglutaryl-CoA dehydratase activator	ND	16.7
CAC3624		6-pyruvoyl tetrahydrobiopterin synthase	ND	ND
CAC3625		MoaA family Fe-S oxidoreductase	13.8	24.1
CAC3626		GTP cyclohydrolase I	6.9	10.1
CAC3627		PP-loop superfamily ATPase	4.8	7.3
CAC3650		HD-GYP domain containing protein	6.7	6.9

* Genes whose expression ratio is below the threshold for significance, but which belong to the same operon as differentially expressed genes are indicated in bold. ND, No data available

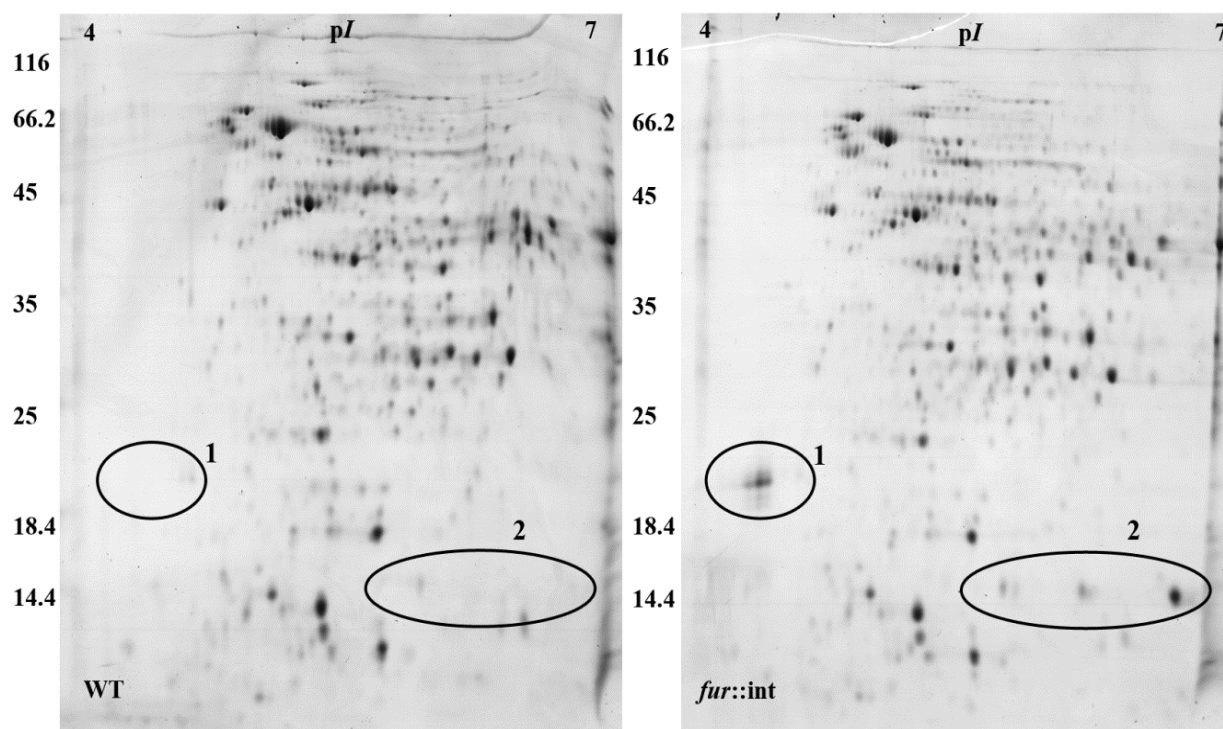


Fig. 3.25 2D-PAGE protein expression analysis of *C. acetobutylicum* *fur* mutant strain in comparison to the WT. 1, Flavodoxin (CAC0587); 2, 6,7-dimethyl-8-ribityllumazine synthase (CAC0593; RibH).

3.6.1.1 Validation of the microarray data through sqRT-PCR

Validation of the microarray data was carried out by conventional sqRT-PCR analysis (2.13) on genes selected according to their expression values. These included two genes upregulated in both microarray datasets (*cac1029* and *cac0791*), a gene putatively involved in iron uptake (*cac2877*), but appeared to be unresponsive to iron levels and *fur* mutation according to the microarray analyses, and 16S rRNA as a control for equal amount of cDNA. sqRT-PCR performed on the *cac0587* gene served as a positive control, since its expression has been confirmed by 2D-PAGE analysis (Fig. 3.25). All oligonucleotides, used for sqRT-PCR are listed in Table 7.4. As illustrated on Fig. 3.26, *cac0587*, *cac1029* and *cac0791* responded as predicted by the microarray experiments. Similarly to the global transcriptional analysis, *cac2877* did not show an altered expression pattern under the conditions of the assay. Collectively, these results indicate that the microarray data represents an accurate reflection of the transcriptional response of *C. acetobutylicum* to iron limitation and *fur* gene inactivation.

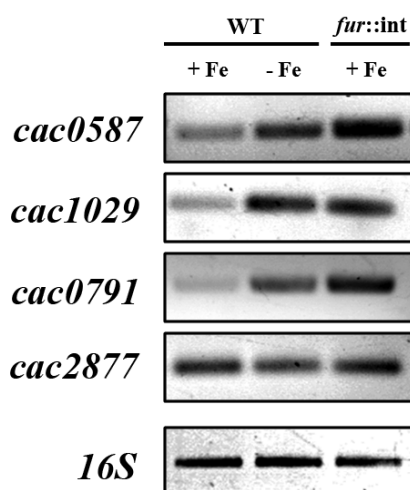


Fig. 3.26 Validation of both microarray datasets by semi-quantitative RT-PCR. Isolation of total RNA from cells of the WT, grown under iron-deplete (-Fe) and replete conditions (+Fe) as well as the *fur* mutant was performed as described in Materials and Methods. PCR from total cDNA was performed using gene specific primers for *cac1029* (*cac1029_fw-rt* and *cac1029_rev-rt*) coding for a FeoA-like protein, involved in iron transport (20 cycles; 210 bp); *cac0791* (*cac0791_fw-rt* and *cac0791_rev-rt*), coding for ferrichrome ABC transporter ATP-binding protein (30 cycles; 79 bp); *cac0587* (*cac0587_fw-rt* and *cac0587_rev-rt*) coding for a flavodoxin (30 cycles; 429 bp) and *cac2877* (*cac2877_fw-rt* and *cac2877_rev-rt*), coding for an ATPase component of a ABC-type iron (III) transport system, (30 cycles; 502 bp). To ensure that equal amounts of cDNA are used as a template, PCR was performed with primers specific for 16S rRNA (30 cycles; 1500 bp).

3.6.1.2 Bioinformatic prediction of potential Fur binding sites

Fur regulators classically recognize a 19-bp consensus sequence (5'-GATAATGATnATCATT ATC-3') composed of two 9-bp inverted repeats, separated by one unmatched nucleotide in the promoter regions of their target genes (de Lorenzo *et al.*, 1987). In an effort to identify a set of

potential direct regulatory targets of Fur, the promoter regions within 350 bp of their start codons and the coding regions of all genes listed in Table 3.4 were examined for presence of a putative Fur binding motif using the 'Virtual footprint' platform integrated into the ProDoric database (Münch *et al.*, 2003). A positional weight matrix, derived from *P. aeruginosa* (Münch *et al.*, 2003) and a cut-off score of 7.5 were implemented in this study. High-score putative Fur-binding sites have been detected upstream of several genes and gene clusters (*cac0587-88*, *cac1029-31*, *cac0788-91*, *cac1602-03*, *cac0267*, *cac0567*, *cac0582* and *cac1478*) significantly upregulated under iron-limiting conditions and in the *fur* mutant (see Table 3.4). In addition, a low-score (7.5) putative Fur binding sequence was identified in the promoter region of the *cac0842-43* operon, which is moderately upregulated in both microarray datasets. Interestingly, a Fur binding sequence was not identified in the promoter region of the *ribDBAH* operon. Although a low-score predicted Fur box was detected in the coding sequence of the first gene of the operon, we suggest here an indirect regulation (3.6.1.4). Seven genes have been found to be downregulated under iron limitation and *fur* gene inactivation (Table 3.4). However, no Fur boxes were identified in their promoter regions, implying an indirect regulation. DNA sequence logo representing the most conserved bases within the Fur-binding site was generated using a multiple alignment of all candidate Fur-binding sites (Fig. 3.27).

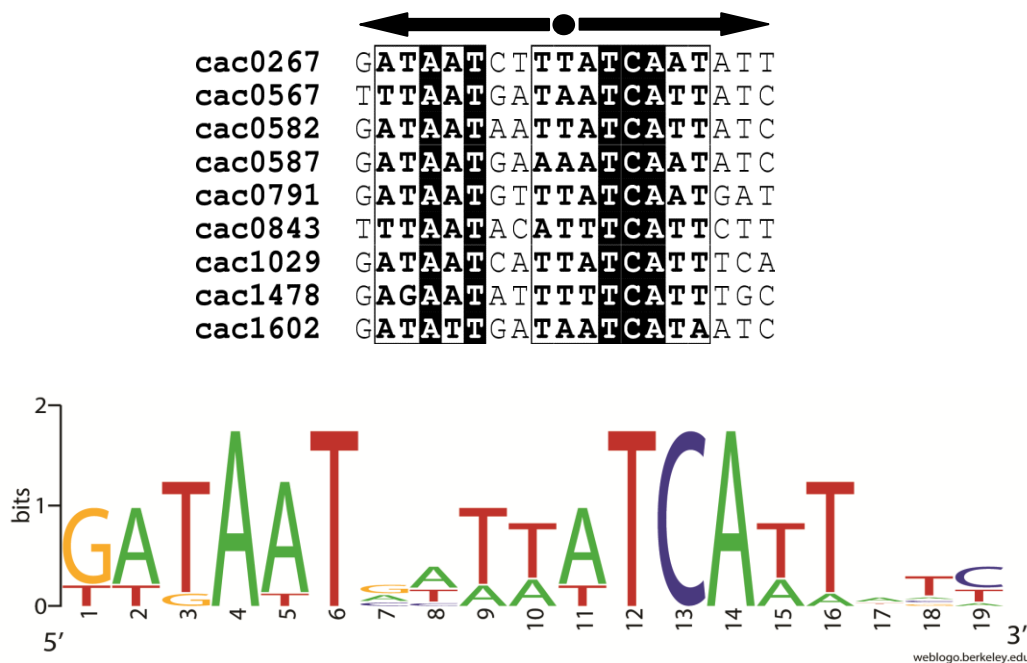
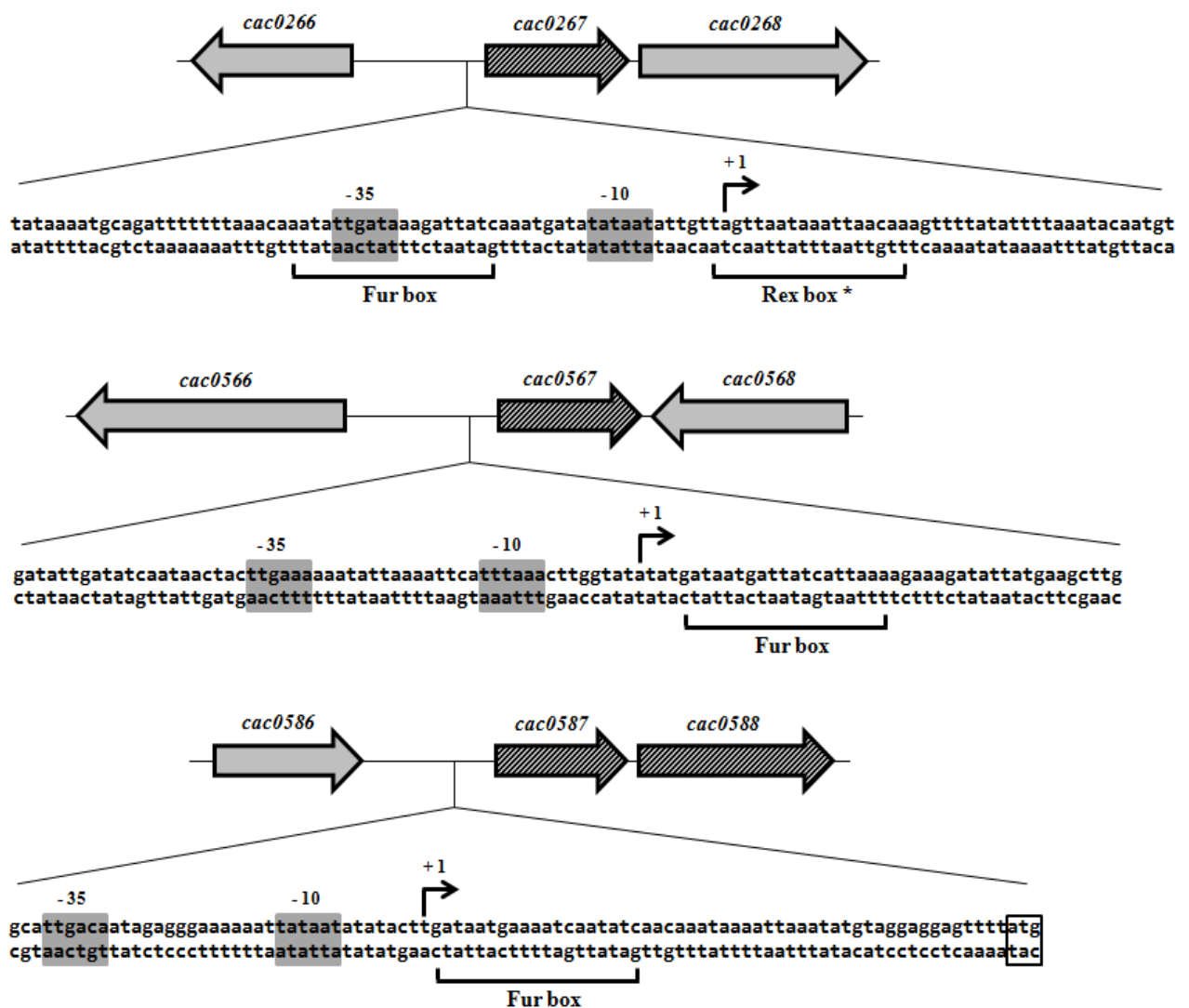


Fig. 3.27 Alignment of predicted Fur-binding motifs in *C. acetobutylicum*. (A) Putative Fur binding sequences were aligned using Clustal Omega (Goujon *et al.*, 2010; Sievers *et al.*, 2011) and the alignment was visualized with ESPript 2.2 (<http://esprict.ibcp.fr/ESPript/ESPript/>). Conserved positions are highlighted. (B) Sequence logo displaying the most highly conserved bases in the *C. acetobutylicum* predicted Fur box element.

3.6.1.3 Determination of transcriptional start sites by 5' RACE

Transcriptional start sites of a set of putative direct targets of Fur were determined (2.14), in order to analyse the position of the predicted Fur-binding sites in the context of their promoter regions (Fig. 3.28). RNA was harvested from cells of the *fur* mutant strain, followed by DNase I treatment. The 5'-end sequences were then obtained using a commercial 5'/3'RACE Kit (Roche Applied Science) and gene specific primers, listed in Table 7.4, according to the manufacturer's instructions. PCR amplification of the resultant 5'-UTR regions yielded single bands (data not shown) for all tested genes, suggesting the presence of single transcriptional start sites. The putative Fur binding motifs, denoted on Fig. 3.28, are positioned overlapping or in close proximity of the RNA polymerase binding sites, implying repression of transcription by steric hindrance.



Continued on next page

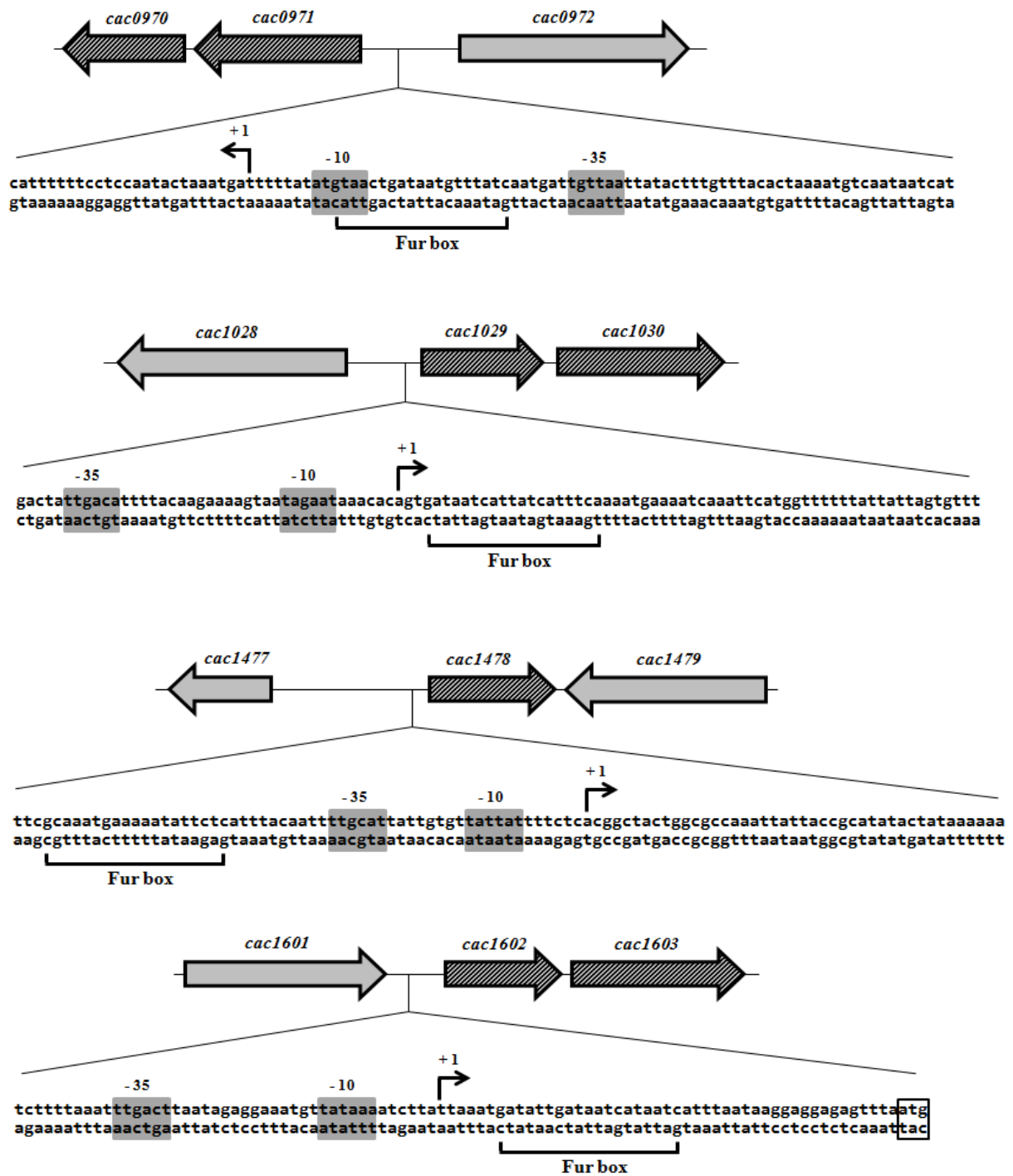


Fig. 3.28 Promoter regions of selected candidate Fur-regulated genes in *C. acetobutylicum*. The open reading frames of the putative targets of Fur regulation are indicated in striped arrows. Black arrows show the experimentally determined transcription start sites. Boxes shaded in grey highlight conserved -35 and -10 promoter elements. Annotated start codons are also indicated by boxes. A Rex (redox-sensing global regulator) binding sequence determined in a previous study (Wietzke and Bahl, 2012) is indicated in the promoter region of *cac0267*.

3.6.1.4 Relationship between flavodoxin (CAC0587) expression and riboflavin biosynthesis in *C. acetobutylicum*

In *H. pylori* the *ribBA* operon, involved in riboflavin biosynthesis, has been reported to be directly regulated by Fur in an iron-responsive manner (Ernst *et al.*, 2005; Pich *et al.*, 2012). The overflowing riboflavin production exhibited by the *fur* mutant and the iron-deficient wild-type suggested that transcription of the *ribDBAH* gene cluster is regulated in a similar manner in *C. acetobutylicum*. However, analysis of the promoter region revealed no conserved Fur-binding sequence. Although a putative Fur box was identified in the coding sequence of the first gene of the operon, we proposed that the *ribDBAH* gene cluster is not regulated directly by Fur. In Gram-positive bacteria riboflavin synthesis is regulated at transcriptional or translational level by a FMN-sensing RFN element (riboswitch) (Mironov *et al.*, 2002; Vitreschak *et al.*, 2004). FMN is the cognate cofactor of CAC0587 (Demuez *et al.*, 2007). Overproduction of flavodoxin (CAC0587) upon iron limitation and *fur* gene inactivation in *C. acetobutylicum* presumably leads to imbalance in the cellular pools of FMN and therefore to enhanced synthesis of riboflavin. In order to test this hypothesis, the *cac0587* gene was insertionally inactivated using the Clostron[®] system giving a strain *C. acetobutylicum cac0587::int(150s)* and the mutation was verified as described in 3.2 (data not shown). The *cac0587* mutant was grown in 200 ml iron-deplete MS-MES medium (6 μ M FeSO₄) for 135 h. In consistence with the proposed hypothesis for indirect regulation, no riboflavin accumulated into the medium in contrast to the wild-type cultures (Fig. 3.29).

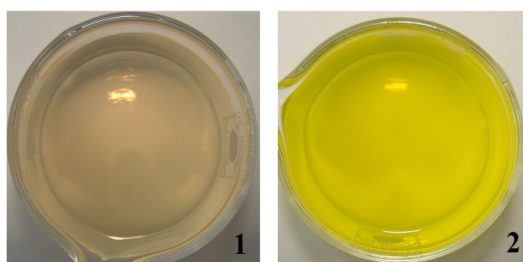


Fig. 3.29 Overproduction of flavodoxin (CAC0587) under iron-limiting conditions leads to enhanced riboflavin biosynthesis in *C. acetobutylicum*. Cell-free supernatants from *C. acetobutylicum cac0587* mutant (1) and wild-type (2) strains grown in 200 ml low-iron MS-MES medium for 135 h (see text for details).

3.6.2 Additional transcriptional reshaping in response to iron limitation and *fur* gene mutation

A total of 117 genes listed in Table 7.5 (Appendix) displayed iron-responsive differential regulation, but their transcription was not significantly altered in the *fur* mutant strain. Among

these 45 genes showed an iron-repressed (upregulated in the iron-deficient wild-type) and 72 iron-induced (downregulated in the iron-deficient wild-type) mode of regulation. This fraction was largely composed of ORF encoding hypothetical or uncharacterized proteins. The group of genes that could be assigned a function was predominantly represented by those associated with amino acid metabolism and transport. For instance, the category of iron-repressed genes included a cluster responsible for biosynthesis of arginine. Interestingly also a bicistronic operon encoding a second putative Feo-type iron-uptake system (*cac0447-cac0448*) was upregulated about 3-fold. On the other hand, the group of the iron-induced genes included a large operon encoding the components of a putative nitrogenase (*cac0253-cac0262*).

Finally, 116 genes (38 upregulated and 78 downregulated) were differentially regulated in the *fur* mutant, but their expression was not affected in the wild-type grown under iron-limiting conditions (Table 7.6, Appendix). Interestingly, a number of genes involved in sporulation were affected in the *fur* mutant. However, its ability to form heat resistant spores relative to the wild-type was not significantly altered (data not shown). Since conditions of iron limitation used in this study might not have been sufficient to alter the transcription level of these genes above the threshold for significance, their promoter regions were searched for the presence of Fur boxes in an attempt to identify putative direct targets of Fur-mediated repression and activation, respectively. However, low-score putative binding sites were identified upstream of just four downregulated genes (*cac1363*, *cac2135*, *cac2354* and *cac3081*).

4 Discussion

Transition metals are of major importance for the biological systems since they represent essential structural elements and catalytic determinants in proteins. On the other hand, when in excess, metal ions could be toxic for the cell. Therefore, the biological entities have developed a number of tools to effectively cope with the constantly changing landscape of metal availability in their natural habitats, thereby maintaining an intracellular metal balance (Giedroc and Akunkumar, 2007). Bacteria have dedicated a great variety of metal-sensing regulatory systems responsible for managing the intracellular metal ion concentrations. According to their structure metal-responsive regulators could be classified into seven families: MerR, ArsR (SmtB), CsoR, CopY, DtxR, Fur and NikR (Giedroc and Arunkumar, 2007). The metal-dependent fine-tuned control by these regulators specifies the so-called metallome, a fundamental feature of the cell, which is defined as the cellular free and protein-bound metal content (Williams, 2001; Frausto da Silva and Williams, 2001). Key transition metals, which constitute the metallome in bacteria are zinc, iron, cobalt, nickel and copper (Frausto da Silva and Williams, 2001; Pennella and Giedroc, 2005). Among these iron is unquestionably of critical value for the strictly anaerobic bacterium *C. acetobutylicum*, given the pivotal role of several iron-containing proteins for its main metabolic pathways (Fig. 1.5). Apart from the bulk biological metals (Mg, Ca and K), the metallome of *C. acetobutylicum*, as judged by ICP-AES analysis, is predominantly represented by iron (Hillmann *et al.*, 2008). Study of the mechanisms for maintenance of iron homeostasis would thus be of interest for establishing fundamental characteristics of the molecular biology in *C. acetobutylicum* and potentially could be of value for the biotechnological application of this microorganism. Moreover, delineating of the mechanisms for maintenance of an adequate iron status in *C. acetobutylicum* could provide background for future studies in notorious medically important members of the group of clostridia including *Clostridium difficile*, *Clostridium tetani* and *Clostridium botulinum*.

The milestone of the bacterial iron-dependent response is the ferric uptake repressor (Fur). Beyond its role in coordination of iron transport systems, Fur is implicated in regulation of a broad spectrum of cellular processes and the full potential of this pleiotropic regulator in microorganisms is yet to be elucidated (Andrews *et al.*, 2003). The main focus of this study was to identify a functional Fur regulator in *C. acetobutylicum* and to determine its physiological significance and regulatory capacity. For the purposes of discussion, the order presented in the Results section is not followed.

4.1 Identification and characterization of a functional Fur regulator in *C. acetobutylicum*

Apart from CAC2634, which has been characterized as an H₂O₂-responsive regulator (PerR), the genome of *C. acetobutylicum* encodes two more Fur homologues: CAC0951 (~ 16 kDa) and CAC1682 (~ 17 kDa) (Nölling *et al.*, 2001; Hillmann *et al.*, 2008; 2009b). Similarly, other members of the group of clostridia, as well as the closely related *B. subtilis*, possess multiple Fur homologues (Fuangthong and Helmann, 2003; Hillmann *et al.*, 2009b). In *B. subtilis* the three Fur paralogs function as an iron-responsive Fur, a zinc-sensing Zur and an H₂O₂-sensing PerR regulator (Moore and Helmann, 2005). Interestingly, the genome of *Clostridium difficile* revealed only two Fur homologues. In *Pasteurella multocida* the iron-responsive Fur protein regulates a high-affinity *znuACB* zinc-uptake system (Garrido *et al.*, 2003). Therefore, it could be speculated that iron- and zinc homeostasis are regulated by a single Fur-like protein in *C. difficile*.

Based on homology and phylogenetic analysis Hillmann *et al.* (2008) suggested that CAC1682 and CAC0951 function as Fur and Zur regulators, respectively. Because of the structural similarity and functional diversity within the Fur family of proteins, assignment of metal specificity based on homology might be incorrect. In *Rhizobium leguminosarum* initially considered as responsive to iron, the Fur homologue was demonstrated to exert instead control on manganese homeostasis (Mur) (de Luca *et al.*, 1998; Wexler *et al.*, 2003; Diaz-Mirelez *et al.*, 2004). Therefore, both CAC1682 and CAC0951 were subjected to a functional analysis in this study.

4.1.1 Power of the trans-complementation studies for establishing the role of CAC1682 as an iron-responsive regulator (Fur)

In contrast to CAC0951, CAC1682 was able to restore Fur⁺ phenotype in the *fur*-null reporter *E. coli* H1780 strain, suggesting that CAC1682 is the iron-sensing regulator in *C. acetobutylicum* (3.1.3.2). Trans-complementation studies in the cellular milieu of suitable mutant host strains represent a common approach to examine the functionality of putative regulatory proteins. Reversion of the wild-type phenotype would be generally sufficient to establish the function of the candidate transcriptional regulators. However, when it comes to metalloregulatory proteins from the Fur family, the picture is more complex, because of the following reasons: (i) Fur-like proteins are structurally very similar, (ii) they recognize similar DNA-binding motifs and (iii) optimal response to metal levels in the cell is a function of three factors, namely affinity, allostery and access (Lee and Helmann, 2007; Waldron and Robinson, 2009; Ma *et al.*, 2009; 2012). In terms of

affinity, metalloproteins generally tend to exhibit preference for binding of transition metals following the universal Irving-Williams series (often called the natural order of stability for divalent transition metals) with Mg^{2+} and Ca^{2+} exhibiting the weakest binding $< Mn^{2+} < Fe^{2+} < Co^{2+} < Ni^{2+} < Cu^{2+} > Zn^{2+}$ (Irving and Williams, 1948; Frausto da Silva and Williams, 2001; Waldron and Robinson, 2009). Moreover, numerous *in vitro* studies have shown that binding of non-cognate transition metals, normally not recognized *in vivo*, trigger the necessary allosteric changes for DNA binding (Xiong *et al.*, 2000; Ma *et al.*, 2012). The most emblematic example is the common usage of Mn^{2+} as a surrogate of Fe^{2+} in Fur-DNA electromobility shift assays (de Lorenzo *et al.*, 1988). Therefore, for metal sensors to acquire their cognate cofactor *in vivo*, competitive transition metals must be buffered at appropriate concentrations in the cell. This is achieved by a fine-tuned control on transport, storage and export (Waldron and Robinson, 2009). However, breakdown of these controls in *fur* mutant strains used for trans-complementation studies typically results in intracellular metal imbalance. Thus metals recognized by a candidate metal-sensing regulator can change when tested in these strains. For instance, the Mur (manganese uptake regulator) from *R. leguminosarum* was able to restore Fur deficiency in the *E. coli* 1780 reporter strain (Wexler *et al.*, 2003). Therefore, it is essential to verify experimentally the metal cofactor of a candidate metal-sensing protein from the Fur family. In order to establish iron as a cue for CAC1682, trans-complementation studies in *B. subtilis* were performed under iron-replete and -deplete conditions (3.1.3.3). These experiments demonstrated that the CAC1682 protein responds specifically to iron levels, while CAC0951 was unresponsive to iron under the conditions of the assay, supporting the tentative conclusion that *cac1682* from *C. acetobutylicum* encodes a genuine iron-sensing regulator (CacFur).

In terms of molecular biology, *C. acetobutylicum* stays far beyond the model organisms *B. subtilis* and *E. coli*. After almost 30 years since the discovery of the Fur protein in *E. coli* (Hantke, 1981), some aspects of Fur-dependent regulation are still unclear. A few perspectives discussed in the following section could contribute equally to the general understanding of the Fur-like proteins and possibly should be approached in future studies.

4.1.2 Comparative *in silico* and biochemical analysis

In order to provide an insight into the basic features of CacFur, a comparative *in silico* and biochemical analysis was performed (3.1.1 and 3.1.2). Although not the main focus of this work, CAC0951 has been examined in parallel. In general, CAC0951 served as a control, but the amino acid sequence of this protein revealed some unexpected characteristics that might be of interest for future studies. To date, crystal structure is available for four full-length iron-responsive Fur

proteins (*H. pylori* Fur (HpFur), *Campylobacter jejuni* (CjFur), *Vibrio cholerae* Fur (VcFur) and *P. aeruginosa* Fur (PaFur)); PerR from *B. subtilis* (BsuPerR); Zur from *Mycobacterium tuberculosis* (MtZur) and *S. coelicolor* (ScZur); and Nur from *S. coelicolor* (ScNur) (Pohl *et al.*, 2003; Traore *et al.*, 2006; Lucarelli *et al.*, 2007; Sheikh and Taylor, 2009; An *et al.*, 2009; Dian *et al.*, 2011; Shin *et al.*, 2011; Butcher *et al.*, 2012). Homology modelling using *H. pylori* Fur (HpFur) (pdb: 2xig; Dian *et al.*, 2011) and *S. coelicolor* Zur (ScZur) (pdb: 2mwm; Shin *et al.*, 2011) as references demonstrated extensive structural conservation of both CacFur and CAC0951 (Fig. 4.1). It should be noted that the unstructured N-terminal extension in CAC0951 stems from imperfection of the model. The generated 3D models suggested that CacFur and CAC0951 adopt a basic fold, which exhibits a bipartite structural organization consisting of a DBD (90 residues in CacFur and 79 residues in CAC0951) and DD (51 residues/56 residues), bridged by a short loop (8 residues/6 residues) (see Fig. 3.1 A and Fig. 3.2 A).

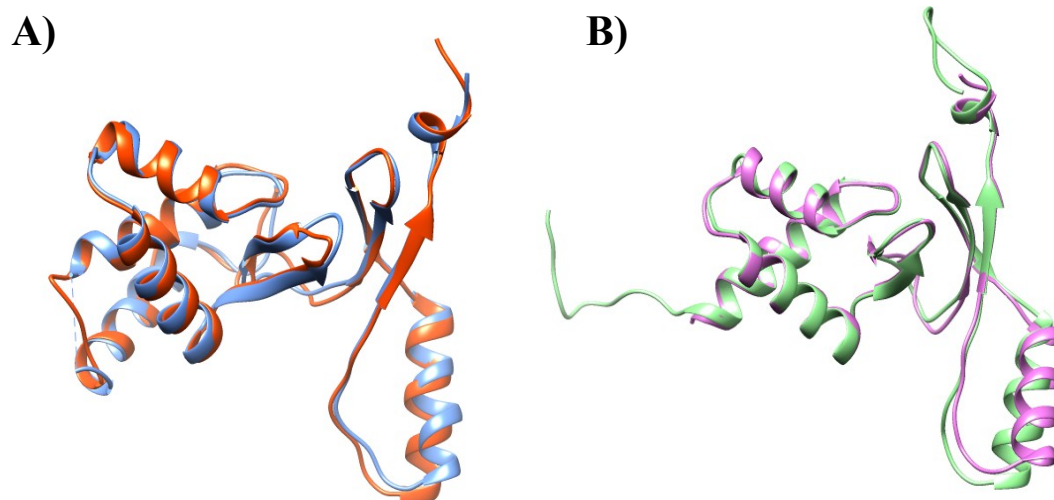


Fig. 4.1 *C. acetobutylicum* Fur and CAC0951 proteins exhibit extensive structural conservation. Superposition of (A) CacFur (orange) and (B) CAC0951 (green) monomer models with the ribbon structures of HpFur (pdb:2xig; blue) and ScZur (pdb:2mwm; violet), respectively. The 3D model structures of CacFur and CAC0951 have been generated by the Modeller (Sali and Blundell, 1993) and visualized by the graphical display Chimera (Pettersen *et al.*, 2004).

Comparative analysis of the CacFur homology model with other characterized Fur and Fur-like proteins, revealed three conserved putative metal binding sites (Fig. 4.2). Site S1 is composed of two C-XX-C motifs at the C-terminus (shaded in blue on Fig. 4.2) and presumably creates a tetrahedral environment for a structural zinc ion. In *B. subtilis* all four Cys residues have been reported to be essential for the functionality and stability of the BsuFur protein (Bsat *et al.*, 1999). Later studies demonstrated that the presence of a structural Zn(II) S1 site in HpFur, CjFur, BsuPerR and ScZur (Traore *et al.*, 2006; Dian *et al.*, 2011; Shin *et al.*, 2011; Butcher *et al.*, 2012) is associated with an α helix at the C-terminus, while, PaFur and VcFur, which do not possess a

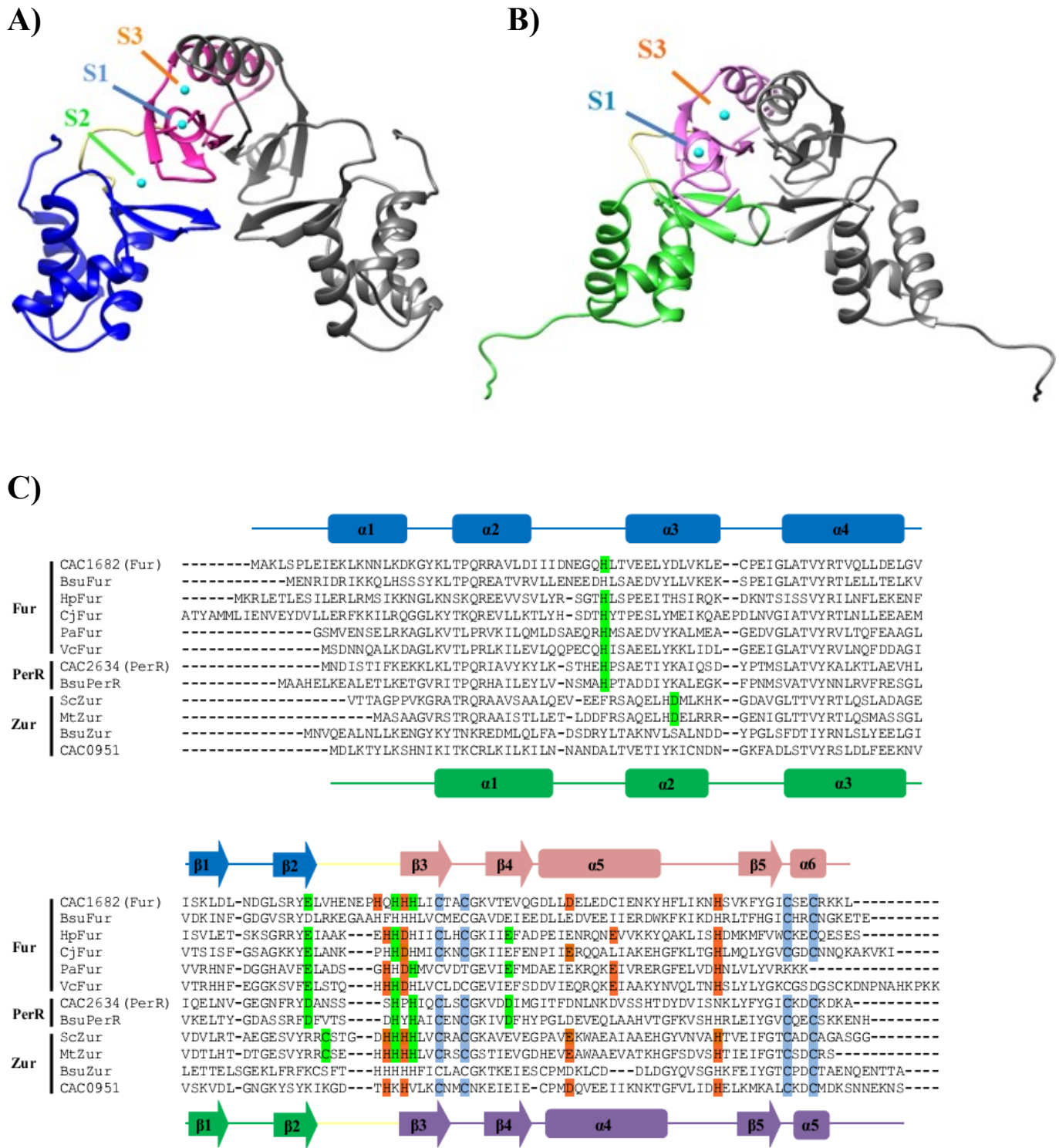


Fig. 4.2 Comparative analysis of the putative metal-binding sites from *C. acetobutylicum* Fur and CAC0951. Homology models of CacFur (A) and CAC0951 (B) indicating the position of the predicted metal-binding sites. (C) Multiple sequence alignment of the deduced protein sequences of CacFur and CAC0951 with other Fur and Fur-like proteins with resolved structure and the Fur homologues from the closely related *B. subtilis*. Secondary-structure elements of CacFur and CAC0951 as determined by the Modeller are indicated above and beneath the alignment, respectively. Residues composing S1 are shaded in blue, S2 residues are coloured in green and S3 residues are highlighted in orange. The multiple sequence alignment was performed using Clustal Omega (Goujon *et al.*, 2010; Sievers *et al.*, 2011). The second putative metal-binding site in CAC0951 is indicated as S3 to match the corresponding site in CacFur.

S1 site have not shown an additional helical structural element (Pohl *et al.*, 2003; Sheikh and Taylor, 2009). In concert with these data, the model of CacFur showed a C-terminal $\alpha 6$ helix (Fig. 4.1 and Fig. 4.2). Site S2 is located in the region between the DBD and the DD with three histidines and one glutamate as ligands (shaded in green on Fig. 4.2). S2 appears to be conserved in all Fur and Fur-like proteins characterized so far with some variability in the co-ordination environment, which mainly depends on the metal that is bound (Dian *et al.*, 2011). For instance, a cysteine residue in the S2 coordination sphere of MtZur and ScZur confers the specificity for zinc ion binding and the four histidine residues in ScNur are considered to determine the preference for nickel (Lucarelli *et al.*, 2007; An *et al.*, 2009; Dian *et al.*, 2011; Shin *et al.*, 2011). These findings coupled with functional analysis of mutant variants of several Fur and Fur-like proteins led to a model in which S2 acts as a regulatory site (Lee and Helmann, 2007). A common feature for all Fur S2 sites is the presence of a conserved histidine ligand in the loop between helices $\alpha 2$ and $\alpha 3$ (Dian *et al.*, 2011). Similarly, this residue is present in the amino-acid sequence of CacFur and presumably takes part in the coordination of the regulatory Fe^{2+} (Fig. 4.2). Several Fur and Fur-like proteins showed also a third, considered as a structural Zn(II)-binding site S3, positioned within the DD (shaded in orange on Fig. 4.2) (Pohl *et al.*, 2003; Dian *et al.*, 2011). In CacFur the putative S3 site is composed of three histidine and one aspartate residue. Collectively, the *in silico* analysis of the CacFur amino acid sequence showed features characteristic for other Fur proteins with resolved structure.

Although extensively analysed in the presented above model microorganisms, the role of the individual metal binding sites is still not completely understood and the obtained data is partially controversial. Therefore, *in silico* coupled with controlled biochemical, mutational and functional analyses in other bacterial species could provide valuable information and refinement of the existing model. In this context, quite interestingly, the protein sequence of CAC0951 revealed only two conserved metal-binding sites corresponding respectively to S1 and S3 (Fig. 4.2). Putative coordination ligands for the considered as regulatory S2 site could not be identified by *in silico* analysis. Nevertheless, the protein was functional and able to bind specifically to the promoter region of an operon involved in zinc uptake (*cac2877-cac2878*) as judged by electromobility shift assays (Vasileva, unpublished data). Future studies with CAC0951, as well as CacFur, would be therefore of interest for the general understanding of the functionality of Fur-like proteins.

Two critical functional aspects of the Fur family of proteins are the ability to assemble into dimers and to acquire the correct metallation state. In order to examine those two properties, recombinant CacFur and CAC0951 were overproduced and purified from cells of *E. coli* (3.2.1). Both proteins displayed routinely two isomers with different mobility when analysed on SDS-PAGE gels (Fig.

3.5). A similar profile has been reported for the PerR transcriptional regulator from *C. acetobutylicum*, PerR and Fur from *B. subtilis*, Fur from *Bacillus cereus* and *Streptomyces reticuli* FurS (Bsat *et al.*, 1998; Ortiz de Orue Lucana and Schrempf, 2000; Harvie and Ellar, 2005; Hillmann *et al.*, 2009b; Lee and Helmann, 2006b). In *B. subtilis*, the appearance of a PerR doublet form during SDS-PAGE analysis has been demonstrated to arise as a result of two oxidation states of the protein, which reflect the presence or absence of a bound structural S1 Zn(II) (Lee and Helmann, 2006b). These results are in agreement with the SDS-PAGE migration pattern (Fig. 3.5) and the presence of predicted C-terminal structural S1 Zn(II)-binding sites in the deduced amino acid sequences of CacFur and CAC0951 (Fig. 4.2).

The ability of CacFur and CAC0951 to form oligomers was evaluated using the cross-linking agent EGS (Fig. 3.6). Both CacFur and CAC0951 exhibited an oligomerization pattern characteristic of the Fur family of proteins (Fig. 3.6 A, B and Fig. 3.6 C). Although the most striking features of Fig. 3.6 A and B are the predominant monomeric and dimeric forms of CacFur, SDS-PAGE analysis revealed also bands of higher molecular mass corresponding to higher-order oligomeric structures. Multimerization has been previously reported for other Fur proteins (Hernandez *et al.*, 2002; Delany *et al.*, 2002; Carpenter *et al.*, 2010; Gilbreath *et al.*, 2013). A tendency of Fur to form structured helical multimers on its DNA binding sites has also been observed by electron microscopy (Le Cam *et al.*, 1994). HpFur protein mutant variants deficient in DNA binding have shown reduced ability to form higher-order structures (Carpenter *et al.*, 2010). However, the significance of Fur oligomerization *in vivo* has not been elucidated so far.

Next, the metal status of the recombinant CacFur was investigated in comparison to CAC0951. After extensive dialysis against EDTA both proteins were subjected to ICP analysis (3.1.2.3). Consistent with the predicted metal-binding sites, the His-tagged CacFur co-purified with zinc (~ 0.5 equivalents per monomer) and iron (~ 0.03 equivalents per monomer), while upon purification the recombinant CAC0951 protein retained only zinc (~ 0.8 equivalents per monomer). Similarly to CacFur, Fur from *E. coli* (EcFur) contained less than 0.05 Fe/mol protein (Althaus *et al.*, 1999). Furthermore, an EDTA treated EcFur, which harbours a C-terminal structural Zn(II)-binding site, co-purified with ~ 0.9 Zn per monomer (Althaus *et al.*, 1999). The lower amount of zinc detected in CacFur could be attributed to a few factors. Treatment of the CacFur protein with EDTA could have led to further loss of the tightly associated structural zinc as reported for the EDTA-treated Zur protein from *B. subtilis* (0.5 Zn per monomer) (Ma *et al.*, 2011). Moreover, the Bradford assay, used in this study, has been reported to overestimate Fur protein concentrations by a factor of 1.2-1.5, when BSA has been used for preparation of the standard curve (Friedman and O'Brien, 2004; Mills and Marletta, 2005). Collectively, these

results suggest that CacFur contains a tightly bound structural zinc ion, which most probably corresponds to S1 as predicted by the *in silico* analysis. CAC0951 also retained one structural zinc ion per monomer as reported for Zur from *B. subtilis* (Ma *et al.*, 2011).

4.2 Physiological importance of Fur in *C. acetobutylicum*

The physiological significance of the Fur transcriptional regulator and its functional analogues (DtxR and IdeR) has been extensively studied in aerobic and facultative anaerobic microorganisms. In *P. aeruginosa* and *Anabaena* sp. PCC 7120, Fur has been demonstrated to be an essential protein (Pohl *et al.*, 2003; Hernandez *et al.*, 2006). Upon loss of their iron-responsive regulators, other microorganisms exhibit a wide spectrum of physiological phenotypes, related to growth, energy metabolism and sensitivity to oxidative stress, among others (Bsat *et al.*, 1998; Touati *et al.*, 2000; Yang *et al.*, 2008; da Silva Neto *et al.*, 2009). In contrast, the role of the iron-sensing regulator proteins has been investigated in few strictly anaerobic bacteria. Knock-out of *fur* in the obligate anaerobes *Dichelobacter nodosus* and *Desulfovibrio vulgaris*, as well as inactivation of *dtxR* in *Pyrococcus furiosus*, have shown no overall impact on the fitness of these microorganisms (Bender *et al.*, 2007; Parker *et al.*, 2005; Zhu *et al.*, 2013). Moreover, a Fur-like protein has been reported to be cryptic in the strictly anaerobic archaeon *Thermococcus kodakarensis* (Louvel *et al.*, 2009). *D. nodosus*, *P. furiosus* and *T. kodakarensis* also exhibited less stringent iron- and/or Fur (DtxR) dependent transcriptional regulation (Louvel *et al.*, 2009; Parker *et al.*, 2005; Zhu *et al.*, 2013). Taken together these data suggest a rather limited role of the iron-responsive regulators in the lifestyle of strict anaerobes and indicate clearly the expanding significance of Fur over the course of evolution. Previous studies, however, indicated a strong physiological response of *C. acetobutylicum* and *C. pasteurianum* to iron-limiting conditions (Schönheit *et al.*, 1979; Bahl *et al.*, 1986; Junelles *et al.*, 1988; Dabrock *et al.*, 1992; Peguin and Soucaille, 1995). To address a potential role of Fur in this iron-dependent response, the *fur* gene in *C. acetobutylicum* was insertionally inactivated using the Clostron[®] system (Heap *et al.*, 2007; 2010) and the mutation was confirmed by PCR screening and Southern hybridization (3.2). Furthermore, the phenotypical changes could be reversed by functional *in trans* complementation, thus excluding any secondary effects originating from the mutagenesis system (3.3).

4.2.1 Growth profiling and product formation

The *C. acetobutylicum fur* mutant displayed a small-colony phenotype, when grown on complex and minimal agar medium (3.4.1). Formation of small colonies could be a consequence of a modified cell shape or size. Microscopy analysis of cells from the *fur* defective strain revealed no

appreciable differences with respect to the wild-type, indicating that the reduced colony size is due to slower growth. Similarly, when propagated in liquid complex and minimal medium, the mutant exhibited diminished growth rate and lower final yield (3.4.1). Derepression of iron transport systems in *fur* mutants typically causes elevated levels of free intracellular iron (Touati *et al.*, 1995; Fuangthong *et al.*, 2002). In agreement with these reports, the *fur* mutant in *C. acetobutylicum* showed an increased total intracellular iron concentration as judged by the colorimetric ferrozine assay (Fig. 3.17). Loss of cellular metal balance could theoretically lead to incorrect metallation of some important proteins considering the Irving-Williams series (Irving and Williams, 1948; Frausto da Silva and Williams, 2001). However, incubation of the *fur* mutant under iron-limiting conditions did not alleviate, but further exacerbated the slow-growth phenotype in comparison to the wild-type (3.4.2), suggesting that overload with iron is not the reason for the observed growth defect.

The central metabolism of *C. acetobutylicum* is strongly dependent on iron (Fig. 1.5). Consistently, iron-limiting conditions have been reported to pose a bottleneck for the carbon and electron flow in this microorganism (Bahl *et al.*, 1986; Junelles *et al.*, 1988). Iron-deficient cultures of *C. acetobutylicum* are characterized by predominant formation of lactate during the acidogenic growth phase, significantly increased butanol:acetone ratio during the solventogenic growth phase and decreased overall hydrogenase activity (Bahl *et al.*, 1986; Junelles *et al.*, 1988; Peguin and Soucaille, 1995). Although test of the composition of cell-free culture supernatants from the *fur* defective strain has shown no elevated lactate production, a gene encoding a L-lactate dehydrogenase was significantly upregulated in the mutant (Table 4.1). This aspect is further discussed in the following sections. In order to determine whether solvent formation is influenced by Fur, the product profile of the *fur* mutant was determined in comparison to the wild-type strain (3.4.1). As illustrated on Fig. 3.15 D, the *fur* mutant exhibited no dramatic change in fermentation pattern, suggesting that the observed effects under conditions of iron starvation are not mediated directly by Fur. Of great interest for the "Clostridium Society" is also the regulatory nature of the H₂-evolving hydrogenase. Quantification of the total gas volume and composition (H₂ and CO₂) in cultures of the *fur* mutant did not show any appreciable differences with respect to the wild-type (3.4.1), clearly demonstrating that the hydrogenase remains intact upon loss of Fur. Collectively, these results indicate that the decrease in hydrogenase activity under iron-limiting conditions occurs at enzymatic level and that the shift in solvent formation under these conditions is due to redirection of the electron flow, which arises as a result of the inhibition of the hydrogenase. Although there exist no theoretical reason why the hydrogenase would be an essential protein in *C. acetobutylicum*, numerous attempts to construct a hydrogenase defective strain using the Clostron[®] system failed (Cooksley *et al.*, 2012; Lehmann, personal communication). Therefore,

optimization of the selection procedure could be the key for successful generation of a mutant strain and application of iron-limiting conditions in this process might be considered.

Interestingly, the *fur* mutant strain accumulated approximately 78 mg/l riboflavin in MS-MES medium culture supernatants (3.5.2). Plasmid-based overexpression of the *ribDBAH* operon in *C. acetobutylicum* has resulted in comparable amounts of riboflavin released into the medium (70 mg/l) (Cai and Bennett, 2011). The study of Cai and Bennett reported that riboflavin overproduction at such levels does not affect the solvent production in *C. acetobutylicum*, which is in agreement with the results in this study. Furthermore, the same report showed that the overflowing synthesis of riboflavin did not influence the growth profile of *C. acetobutylicum*. Therefore, it could also be assumed that the slow-growing phenotype of the *fur* mutant strain is not a result of derepression of the riboflavin biosynthesis pathway.

4.2.2 Relationship between the intracellular iron levels and sensitivity to oxidative stress

As a consequence of the increased intracellular iron levels, *fur* mutants in bacteria typically exhibit increased susceptibility to oxidative stress, due to formation of deleterious ROS via the Fenton reaction (Touati *et al.*, 1995; Bsat *et al.*, 1998; da Silva Neto *et al.*, 2009). In the anoxic environments strict anaerobes seem to have escaped this iron toxicity effect. However, although an obligate anaerobe, previous studies have demonstrated that *C. acetobutylicum* is far from defenceless and can tolerate low doses of ambient air by recruiting a repertoire of inducible detoxification, protection and repair systems (O'Brien and Morris, 1971; May *et al.*, 2004; Kawasaki *et al.*, 2004; Riebe *et al.*, 2007; 2009; Hillmann *et al.*, 2008; 2009a, b). Therefore, it could be speculated that in its natural habitats this microorganism might be occasionally challenged with varying degrees of aeration upon migration from one niche to another. The study of Hillmann *et al.* (2008) has demonstrated that decrease in the viability of cells from *C. acetobutylicum* upon exposure to oxygen arises mainly as a result of the Fenton chemistry. On the other hand, iron is the cofactor for the oxidative stress enzymes, including the superoxide-reducing desulfoferrodoxin (Dfx), the oxygen-scavenging flavo-diiron proteins (FprA1 and FprA2), the peroxide-scavenging reverse rubrerythrin (revRbr) and the electron mediator rubredoxin (Rd) (May *et al.*, 2004; Riebe *et al.*, 2007; 2009; Hillmann *et al.*, 2009a, b). Therefore, exposure to aeration necessitates a dynamic, fine-tuned control on the intracellular iron levels, in order to satisfy the high demands for iron and at the same time to prevent formation of detrimental ROS in *C. acetobutylicum*. The paramount role of CacFur in this process was demonstrated in this

study by a significant reduction in the viability of cells of the *fur* mutant strain upon exposure to ambient air and treatment with the oxidative stress agent H₂O₂ (3.4.4).

4.3 Overview of the transcriptional response to iron limitation and *fur* inactivation

The unique phenotype of the *C. acetobutylicum fur* mutant strain motivated a global microarray analysis in order to identify genes whose expression is affected by conditions of iron limitation, *fur* gene inactivation or both (3.6). A conventional sqRT-PCR performed on several genes demonstrated the accuracy of the microarray data (3.6.1.1). Furthermore, 2D-PAGE analytical analysis was conducted to determine the protein expression profile of the *fur* mutant strain (3.6). Both iron deficiency and *fur* mutation resulted in an extensive transcriptional reshaping. In order to gain an initial functional overview, all genes with significant changes in level of expression under both conditions were categorized according to their predicted biological roles using the COG (cluster of orthologous groups) classification method (Fig. 4.3) (Tatusov *et al.*, 2000). As common for microarray studies, a large fraction of the differentially regulated genes (up- and downregulated) code for hypothetical proteins or proteins with uncharacterized function (Groups

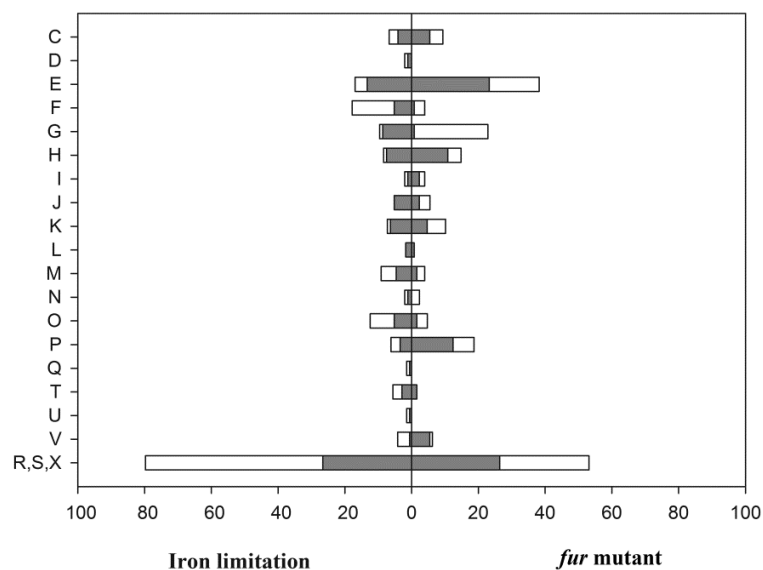


Fig 4.3 Overview of the transcriptional response of *C. acetobutylicum* WT, challenged with conditions of iron starvation and the *fur* mutant strain. The protein products of all differentially expressed genes (> 3 fold) were functionally categorized using the COG classification method (Tatusov *et al.*, 2000). Grey bars, upregulated genes and white bars, downregulated genes. C, energy; D, cell cycle control, cell division; E, amino acid metabolism and transport; F, nucleotide metabolism and transport; G, carbohydrate metabolism and transport; H, coenzyme metabolism and transport; I, lipid metabolism; J, translation; K, transcription and regulation; L, replication, recombination, and repair; M, cell wall and membrane proteins; N, cell motility; O, protein fate and chaperones; P, inorganic ion metabolism and transport; Q, secondary metabolites; T, signal transduction; U, secretion and intracellular trafficking; V, defence; X, poorly characterized or no cluster.

R, X, S). Among the genes that could be assigned a function, in both microarray datasets, predominantly present were those belonging to the following clusters: C (energy production and conversion); E (amino acid transport and metabolism); G (carbohydrate transport and metabolism); H (coenzyme transport and metabolism); K (transcription) and P (inorganic ion transport and metabolism), thus outlining the core aspects of adaptation to iron deficiency in *C. acetobutylicum*.

4.3.1 Regulatory potential of CacFur

Classically, Fur functions as an iron-bound (Fur-Fe²⁺) repressor, obstructing the transcription of target genes, whenever the concentration of iron in the medium exceeds the cellular requirements (Fig. 4.4 A) (Bagg and Neilands, 1987; de Lorenzo *et al.*, 1987; 1988). A more recently appreciated feature of Fur is the ability to act as an iron-bound activator (Fig. 4.4 B) (Carpenter *et al.*, 2009). Direct iron-dependent Fur activation of transcription (Fig. 4.4, 1) has been well characterized in *Neisseria meningitidis* and *Neisseria gonorrhoeae* (Grifantini *et al.*, 2003; Delany *et al.*, 2004; Yu and Genco, 2012). However, recent evidence suggests that this pattern of regulation is not confined to the group of *Neisseria* (da Silva Neto *et al.*, 2009; Butcher *et al.*, 2012). In order to determine putative direct targets of Fur-Fe²⁺ repression and activation, the so-called Fur-Fe²⁺ regulon in *C. acetobutylicum*, the promoter regions of all genes, which elicit changes in transcription both upon iron deficiency and *fur* inactivation (Fig. 3.24), were searched for conserved Fur-binding sequences (3.6.1.2). Although the interpretation of the Fur-binding DNA sequence has evolved over the past decade, the presence of a 19-bp inverted repeat (GATAATGATwATCATTATC; w = A or T) in the promoter regions has been associated with Fur-Fe²⁺ repressible, as well as Fur-Fe²⁺ activated gene targets, in many bacteria (Escolar *et al.*, 1999; Baichoo *et al.*, 2002; Grifantini *et al.*, 2003; Delany *et al.*, 2004; Yu and Genco, 2012). CacFur was able to complement *fur*-null *E. coli* and *B. subtilis* strains (3.1.3) providing evidence that DNA-binding specificity is conserved in *C. acetobutylicum*. Therefore, a positional weight matrix derived from *P. aeruginosa* was implemented in this study (Münch *et al.*, 2003). All genes, composing the predicted Fur regulon (4.3.2) showed an expression pattern compatible with Fur-Fe²⁺ repression mode of regulation, while no compelling evidence for direct Fur-Fe²⁺ activation was found in this study.

It is now generally appreciated that positive Fur regulation occurs more often indirectly, mediated by Fur-Fe²⁺-dependent repression of an antisense regulatory sRNA (Fig. 4.4 B, 2) (Lee and Helmann, 2007; Masse *et al.*, 2007). This sRNA controls expression of its target genes at post-translational level by repressing translation and/or affecting mRNA stability (Masse and

Gottesman, 2002). The iron-regulated sRNAs are mainly involved in control of iron usage by blocking of non-essential iron utilization pathways under iron starvation conditions (Masse and Arguin, 2005). A Fur-regulated sRNA has been also characterized in *B. subtilis* (Gaballa *et al.*, 2008; Smaldone *et al.*, 2012a, b). Genome-wide computational prediction of putative sRNAs has been performed for several members of the group of clostridia including *C. acetobutylicum* (Chen *et al.*, 2011). Scanning of the genome of *C. acetobutylicum* revealed a high-score putative Fur-binding sequence upstream of a predicted sRNA, designated by Chen *et al.* (2011) as sCAC646 (data not shown). Further discussion here would be overspeculative. Nevertheless, this aspect, as well as the role of sRNAs in the genus of *Clostridium* in general, deserves attention.

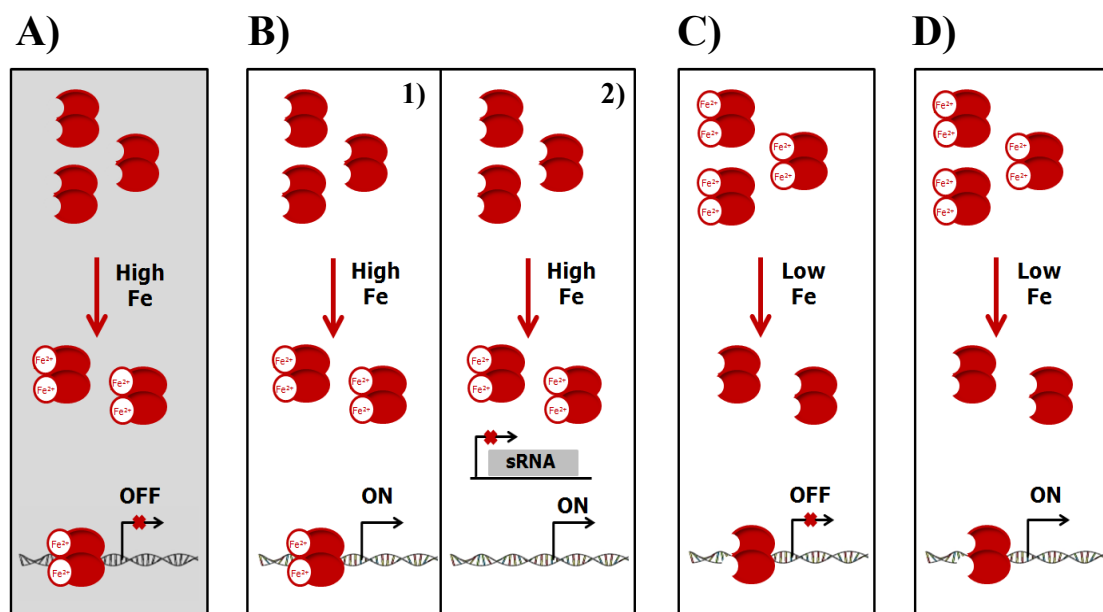


Fig 4.4 Modes of Fur regulation in bacteria (adapted from Lee and Helmann, 2007). (A) Classical Fur-Fe²⁺ mediated repression. Microarray and bioinformatic analysis have established the function of CacFur as an iron-bound repressor, while other patterns of regulation were not identified in this study. (B) Fur-Fe²⁺ dependent direct and sRNA mediated activation. (C) and (D) represent apo-Fur repression and activation, respectively.

Direct Fur mediated transcriptional activation and repression in the absence of Fe²⁺ (apo-Fur) have been characterized in *H. pylori* and *C. jejuni* (Fig. 4.4 C and D) (Delany *et al.*, 2001; Ernst *et al.*, 2005; Butcher *et al.*, 2012). In order to test if *C. acetobutylicum* exhibits similar regulation patterns, transcript levels were compared between the wild-type and the *fur* mutant, grown under iron-limiting conditions and between *fur* mutant cultures grown under iron-replete and -deplete conditions (3.6). However, no evidence for alternative modes of Fur regulation in the absence of iron as a cofactor has been identified in this study.

4.3.2 Fur-Fe²⁺ regulon

The microarray data coupled with bioinformatic analysis enabled the identification of the putative Fur regulon in *C. acetobutylicum*, which includes at least 9 operons (21 genes) (Table 4.1). When Fur functions as a repressor, the Fur-binding sequence overlaps the promoter region, while when acting as an activator, the Fur box is located upstream of the promoter (Delany *et al.*, 2004; Lee and Helmann, 2007). Consistently, all identified Fur boxes were positions in close proximity to the transcriptional start site (TSS) or overlapping the - 10 and - 35 promoter elements of the corresponding genes (Table 4.1). Table 4.1 shows the Fur boxes with the highest scores, however, the promoter regions of several genes harboured more than one putative Fur-binding site (*cac0267* (2); *cac0567* (2); *cac0791* (3); *cac1029* (3); *cac1478* (4); *cac1602* (2)). Presence of repetitive sometimes overlapping Fur-binding sequences with different scores within the promoter regions of target genes, together with the ability of the Fur protein to assemble into multimers, have been proposed as features that would allow for a gradual fine-tuned transcriptional regulation (Escolar *et al.*, 1999).

Table 4.1 Predicted Fur-Fe²⁺ regulon in *C. acetobutylicum*

Gene or gene cluster	Function	Predicted Fur-binding box			
		ATG ^a	TSS ^b	Sequence ^c	Score ^d
<i>cac0267</i>	L-lactate dehydrogenase	-118	-39	GATAATCTTTATCAATATT	8.05
<i>cac0567</i>	Putative methyltransferase	-62	+3	TTAATGATAATCATTATC	8.84
<i>cac0582-84</i>	Cobalamin biosynthesis	-208	ND	GATAATAATTATCATTATC	9.31
<i>cac0587-88</i>	Flavodoxin/ Hypothetical protein	-34	+2	GATAATGAAAATCAATATC	9.24
<i>cac0788-91</i>	Ferrichrome transport	-32	+9	GATAAACATTATCAGTTAC	8.33
<i>cac0843-44</i>	Ribonuclease precursor (barnase)/inhibitor	-94	ND	TTAATACATTTTCATTCTT	7.5
<i>cac1029-32</i>	Fe ²⁺ uptake	-56	+3	GATAATCATTATCATTTC	8.26
<i>cac1478</i>	30S Ribosomal protein S4	-94	-37	GAGAATATTTTTCATTGTC	8.46
<i>cac1602-03</i>	Hypothetical proteins	-23	+6	GATATTGATAATCATAATC	8.54

^a Distance to the annotated ATG.

^b Distance to the TSS (transcriptional start site). TSS were identified using 5' RACE (3.6.1.3).

^{c, d} Fur box sequences and scores as determined by the 'Virtual footprint' software (Münch *et al.*, 2003)

The iron-responsive transcriptional regulators Fur and DtxR govern the control of a broad array of genes in bacteria. For instance, in *E. coli*, the best studied to date model of iron homeostasis, Fur

controls the expression of over 190 genes; 59 genes are Fur regulated in *H. pylori*; 34 operons in *Yersinia pestis* and 20 operons in *B. subtilis* (Hantke, 2001; Baichoo *et al.*, 2002; Andrews *et al.*, 2003; Danielli *et al.*, 2006; Gao *et al.*, 2008). In comparison to these microorganisms, the Fur regulon in *C. acetobutylicum* encompasses a rather small set of targets (Fig. 4.1). Nevertheless, relative to other studied strict anaerobes, *C. acetobutylicum* exhibits a more dynamic Fur-dependent transcriptional response to iron deprivation suggesting that maintenance of proper cellular iron balance is an important aspect of the lifestyle of this bacterium and Fur plays an important role in this process. The data obtained in this study clearly demonstrates that CacFur exerts control not only on iron transport (4.3.2.1), but also on some basic aspects of the energy metabolism (4.3.2.2) leading to a preliminary model of Fur-dependent regulation in *C. acetobutylicum* (Fig. 4.4).

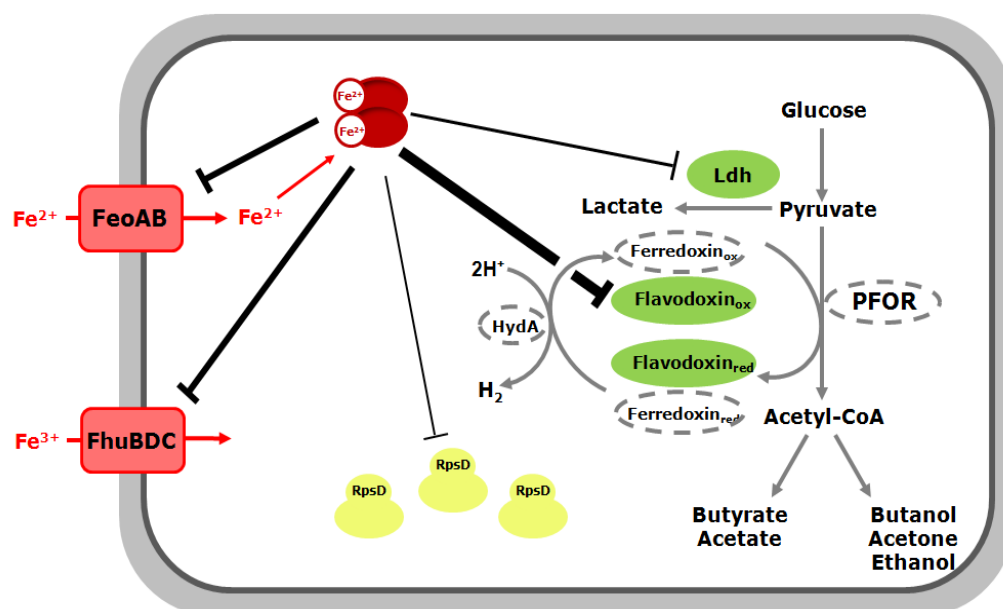


Fig 4.4 The Fur regulator in *C. acetobutylicum* mediates an iron-dependent control of iron-uptake systems as well as some basic aspects of the energy metabolism. Protein products of selected genes, predicted to be members of the Fur regulon in *C. acetobutylicum* are presented. These include two putative iron-uptake systems (coloured in red); Ldh, lactate dehydrogenase and flavodoxin (highlighted in green), which presumably compensate the function of some iron-rich enzymes (shown in dashed ellipses) from the central metabolism in the context of iron limitation. Fur-regulated is also a gene encoding a putative 30S S4 ribosomal protein (RpsD) (indicated in yellow).

Interestingly, the Fur regulon includes also several genes with no obvious role in adaptation to iron levels. The *cac1478* gene encodes a predicted 30S ribosomal protein RpsD. Screening of the genomes of other clostridial species for putative Fur-binding sites using the 'Virtual footprint software' (Münch *et al.*, 2003) suggested that Fur-dependent regulation of *rpsD* genes is conserved in this group of bacteria (data not shown). Studies in *E. coli* and *B. subtilis* have shown that RpsD functions as a regulatory protein blocking the translation of other ribosomal protein by binding to a specific sequence in the mRNA leader region (Jinks-Robertson and Nomura, 1982;

Grundy and Henkin, 1991). Therefore, it could be speculated that the putative RpsD in *C. acetobutylicum* might exhibit control at the level of translation on the expression of ribosomal proteins in response to iron limitation. Furthermore, preliminary experiments with the protein products of the Fur-regulated *cac1602-cac1603* operon and hydrophobicity plot suggested that CAC1602 is a membrane-associated protein, while CAC1603 is a soluble protein (data not shown). Further studies are necessary to determine the biological significance of the individual members of the Fur regulon in *C. acetobutylicum*.

In many bacterial species expression of Fur is subjected to auto- or cross-regulation by other metalloregulators or metabolic state sensors (de Lorenzo *et al.*, 1988; Sebastian *et al.*, 2002; Delany *et al.*, 2005; Wang *et al.*, 2008). For instance, PerR in *B. subtilis*, NikR (nickel-sensing regulator) in *H. pylori* and CAP (catabolic activator protein) in *E. coli* regulate the transcription of their Fur-encoding genes (de Lorenzo *et al.*, 1988; Fuangthong *et al.*, 2002; Delany *et al.*, 2005). The promoter of the *fur* gene in *C. acetobutylicum* did not reveal a conserved Fur-binding sequence, suggesting that its expression is not autoregulated. Similarly, PerR-dependent regulation has not been identified in previous studies (Hillmann *et al.*, 2009b). Therefore, regulation at transcriptional level of the *fur* gene in *C. acetobutylicum*, if any, is yet to be determined.

4.3.2.1 Genes involved in iron acquisition

Consistent with the predominant ferrous form of iron (Fe^{2+}) in the anaerobic environments, the Fur regulon in *C. acetobutylicum* includes a gene cluster (*cac1029-cac1032*) that codes for a putative Feo-type system associated with Fe^{2+} uptake. Feo has been originally characterized as an anaerobically induced and iron-repressible Fe^{2+} transport system in *E. coli* (Hantke, 1987; Kammler and Hantke, 1993; Andrews *et al.*, 2003). Within the Feo-system, FeoB, a transmembrane protein with GTPase activity, is well established as the main transporter for ferrous iron (Carton *et al.*, 2006; Lau *et al.*, 2013). In contrast, the role of the FeoA proteins is much less understood. The deduced amino acid sequence of CAC1031 showed 55 % similarity to the FeoB protein from *E. coli*. Furthermore, homology modelling using structural information from the cytoplasmic domain of the *E. coli* FeoB protein as template (pdb: 3i8s; Petermann *et al.*, 2009) demonstrated extensive structural conservation in CAC1031 (Fig. 7.6, Appendix). Gene clusters encoding Feo-type systems in bacteria may occasionally include a *feoC* gene (Carton *et al.*, 2006). It has been suggested that FeoC functions as a transcriptional regulator (Carton *et al.*, 2006). Although CAC1032 did not exhibit similarity in amino acid sequence to FeoC proteins, it is annotated as a putative transcriptional regulator. Thus, it could be speculated that CAC1032 is involved in a second layer of regulation of the *feo* gene cluster. Numerous attempts in this study to

generate Clostron[®]-based mutations within the Feo-system encoding operon (*cac1029*, *cac1030* and *cac1031*) were unsuccessful, suggesting that CAC1029-CAC1032 is the major iron importer in *C. acetobutylicum*. However, limitations conferred by the mutagenesis system could not be completely ruled out and further experimentation is needed to confirm this hypothesis.

CacFur also mediates the iron-dependent regulation of an operon (*cac0788-cac0791*) putatively involved in ferri-hydroxamate (ferrichrome) siderophore uptake. However, test of the composition of supernatants from the *fur* mutant and the iron-deprived wild-type demonstrated that *C. acetobutylicum* does not produce detectable siderophores (3.5.1). Moreover, analysis of the genome did not reveal genes involved in production of known siderophores, except for the *entB* gene (*cap0030*) encoding a putative isochorisamate lyase (Nölling *et al.*, 2001). Synthesis of precursors and assembly of functional siderophores is an energetically expensive process (Andrews *et al.*, 2003). Moreover, in soil, the natural habitat of *C. acetobutylicum*, fungi and streptomycetes produce plethora of hydroxamate siderophores, among which ferrichromes constitute a major class (Winkelmann, 2007). Thus, most likely *C. acetobutylicum* scavenges ferri-siderophore complexes, produced and secreted by other species (xenosiderophores), a strategy employed by many bacteria (D'Onofrio *et al.*, 2010).

Furthermore, CacFur mediates the control of an operon (*cac0582-cac0584*) involved in biosynthesis of cobalmin (vitamin B₁₂). Within this gene cluster, *cac0583* codes for a putative cobalt chelatase (CbiK). Similarly, the Fur regulon in another strict anaerobe *D. nodosus* included a CbiK encoding gene (Parker *et al.*, 2005). In *Salmonella enterica* CbiK has been shown to function as a ferrochelatase by binding Fe²⁺ (Raux *et al.*, 1997). Therefore, the CbiK ortholog in *C. acetobutylicum* might also facilitate acquisition of iron.

4.3.2.2 Genes involved in energy metabolism

The central hub of the metabolism of *C. acetobutylicum* is composed of two iron-containing proteins: pyruvate:ferredoxin oxidoreductase (PFOR) and [FeFe]-hydrogenase (HydA1) (Jones and Woods, 1986; Meinecke *et al.*, 1989; Demuez *et al.*, 2007). PFOR creates a bridge between the glycolysis and the multi-branched fermentation metabolism of *C. acetobutylicum* by catalysing the conversion of pyruvate to acetyl-CoA (Fig. 1.5 and Fig. 4.4). The hydrogenase is the major redox balancing device that provides a pathway for regeneration of NAD⁺ from NADH during the acidogenic growth phase with concomitant production of molecular H₂ (Jones and Woods, 1986). Bahl *et al.* (1986) suggested that PFOR creates a bottleneck for the carbon flow upon iron deficiency in *C. acetobutylicum*. There are no studies on the activity of this enzyme in the context of iron limitation in this microorganism. However, functionality of the PFOR in the

closely related *C. pasteurianum* has been reported not to be significantly affected under iron deprivation (Schönheit *et al.*, 1979). On the other hand, the activity of the [FeFe]-hydrogenase in *C. acetobutylicum* has been shown to be greatly reduced in low-iron medium (Junelles *et al.*, 1988). As discussed in (4.2.1) activity of the hydrogenase was not affected in the *fur* mutant strain. Furthermore, the expression of the HydA1-encoding gene *cac0028* was not affected either in the iron-deficient wild-type or in the mutant strain, corroborating the fact that inhibition of the hydrogenase occurs at enzymatic level. Under these conditions, lactate dehydrogenase would provide an alternative pathway for oxidation of NADH, in order to allow the glycolysis to proceed. Indeed, previous studies have demonstrated that the NADH-dependent L-lactate dehydrogenase activity is increased in cells of *C. acetobutylicum* under iron-limiting conditions (Freier and Gottschalk, 1987). Moreover, under conditions of iron starvation lactate rather than butyrate and acetate is the predominant metabolic product during the acidogenic growth phase in *C. acetobutylicum* and *C. pasteurianum* (Bahl *et al.*, 1986; Dabrock *et al.*, 1992). In concert with these results, a gene encoding a L-lactate dehydrogenase (*cac0267*) was significantly upregulated in the iron-deficient wild-type. Moreover, the *cac0267* was derepressed in the *C. acetobutylicum fur* mutant strain and is associated with a high-score Fur binding sequence (Table 4.1), indicating that the regulation of this gene is mediated by Fur according to the cellular iron status.

Elevated lactate production has been also reported, when the activity of the hydrogenase was inhibited by CO or by addition of the artificial electron carrier methyl viologen (Meyer *et al.*, 1986; Peguin *et al.*, 1994; Peguin und Soucaille, 1995; Peguin and Soucaille, 1996). Inactivation of this major NADH recycling enzyme during the acidogenic growth phase presumably leads to redox imbalance in the cell reflected by an increased NADH/NAD⁺ ratio (Jones and Woods, 1986). A recent study in our laboratory characterized CAC2713 as a redox-sensing transcriptional regulator (Rex) in *C. acetobutylicum* (Wietzke and Bahl, 2012). The same study demonstrated Rex-dependent derepression of the lactate-encoding *cac0267* gene in response to an elevated NADH/NAD⁺ ratio. Fig. 3.28 indicates the corresponding Rex-binding sequence positioned overlapping the transcriptional start site in the promoter region of *cac0267*. Collectively, these data indicate that the lactate production pathway in *C. acetobutylicum* is subjected to multi-layer regulation that ensures maintenance of the glycolysis whenever the activity of the hydrogenase is diminished during the acidogenic growth phase.

C. acetobutylicum fur mutant did not exhibit increased lactate production in MS-MES batch cultures relative to the wild-type strain (3.5.1). Activity of the L-lactate dehydrogenase from *C. acetobutylicum* was shown to be pH dependent with an optimum of 5.8 (Freier and Gottschalk, 1987). Consistently, lactate production has been detected in cultures of *C. acetobutylicum* only above a pH value of 5 (Bahl and Gottschalk, 1984; Bahl *et al.*, 1986). Because of the experimental

set up in this study, the pH value in MS-MES batch cultures was below 5 almost during the whole course of the growth (Fig. 3.15 B). That could explain the lack of lactate formation in the *fur* defective strain. However, when grown under conditions of continuous fermentation at pH of 5.4 (acidogenic phase), similarly the mutant did not produce lactate (data not shown). From an energetic point of view conversion of pyruvate to lactate is a much less efficient process than the synthesis of acetate and butyrate (Jones and Woods, 1986). It is thus unlikely that the fermentative metabolism is rerouted towards lactate production, when the hydrogenase is still intact, as is the case in the *fur* mutant strain.

Physiological electron donor of the hydrogenase is the iron-sulfur containing ferredoxin (Jones and Woods, 1986). Ferredoxin receives electrons mainly as a result of the oxidative decarboxylation reaction catalyzed by PFOR (Jones and Woods, 1986; Demuez *et al.*, 2007). During the acidogenic phase reduced ferredoxin is also generated via the NADH:ferredoxin oxidoreductase (Vasconcelos *et al.*, 1994; Girbal *et al.*, 1995; Demuez *et al.*, 2007). Previous studies in clostridia, cyanobacteria and algae have demonstrated that under iron-limiting conditions the intracellular levels of ferredoxin were significantly reduced, while flavodoxin has been detected in significant amounts (Knight and Hardy, 1966; Mayhew and Massey, 1969; Ragsdale and Ljungdahl, 1984; Sandmann and Malkin, 1983; Sandmann *et al.*, 1990). In iron-deficient cells of *Clostridium formicoaceticum* flavodoxin accounted for at least 2 % of the total soluble protein (Ragsdale and Ljungdahl, 1984). These results have led to a model in which flavodoxin acts as a counterpart of ferredoxin in many oxidation-reduction reactions under these conditions (Knight and Hardy, 1966). Consistently, *in vitro* enzyme assays have demonstrated that flavodoxins could successfully replace ferredoxins as electron mediators for PFOR (Mayhew, 1971; Petitdemange *et al.*, 1979; Fitzgerald *et al.*, 1980), NADH oxidoreductase (Petitdemange *et al.*, 1979) and hydrogenase (Chen and Blanchard, 1979; Fitzgerald *et al.*, 1980; Demuez *et al.*, 2007). The genome of *C. acetobutylicum* has revealed four genes (*cac0203*, *cac0587*, *cac2452* and *cac3417*) annotated as coding for putative flavodoxins (Nölling *et al.*, 2001). Previous studies have shown that *cac2452* is regulated in a PerR-dependent manner in response to oxidative stress (Kawasaki *et al.*, 2005; Hillmann *et al.* 2008; Hillmann *et al.*, 2009b), while the other three genes have not yet been assigned a function. In their study, Demuez *et al.* (2007) proposed that CAC0587 is the most likely physiological partner of the hydrogenase under iron-limiting conditions based on comparative *in silico* analysis and *in vitro* enzyme assays. In support of this hypothesis, among the most strongly upregulated in *C. acetobutylicum* upon iron limitation and *fur* gene inactivation was an operon coding for a flavodoxin (*cac0587*) and a hypothetical protein (*cac0588*) (Table 4.1). Moreover, CAC0587 was detected as a novel spot on the analytical 2D-

PAGE gels from the *fur* mutant (Fig. 3.25). The *cac0587-cac0588* gene cluster is also associated with a high-score Fur box, which corresponds to the level of derepression (Table 4.1).

The genome of *C. acetobutylicum* harbours five genes encoding putative ferredoxins (*cac0075*, *cac0105*, *cac0303*, *cac3527*, *cac3621*) (Nölling *et al.*, 2001). Demuez *et al.* (2007) reported that CAC0303 is the major ferredoxin in solventogenic cells of *C. acetobutylicum*. Apart from that study, the role of the individual ferredoxins in this microorganism is currently not known. Interestingly, the transcriptomic data from the iron-deficient wild-type and the *fur* mutant did not show differential expression of any of the ferredoxin-encoding genes. These results suggest that negative regulation of ferredoxin synthesis in iron-deficient cells of *C. acetobutylicum* is performed on a post-transcriptional level. Transcriptional analysis of ferredoxin encoding genes in several cyanobacterial species, grown under iron-starvation conditions, demonstrated similar results (Laudenbach *et al.*, 1988; Leonhardt *et al.*, 1992; Razquin *et al.*, 1994). Of interest for future studies would be the regulatory nature of the ferredoxins under iron limitation in *C. acetobutylicum* and a potential role of Fur in this process.

4.3.3 Role of the riboflavin biosynthesis

The riboflavin biosynthesis pathway in *C. acetobutylicum* was upregulated in response to iron limitation, as well as in the *fur* mutant (3.5.2). Previous studies have indicated an interrelationship between the availability of iron and the flavin status in bacteria, yeast, higher plants and mammals (Susin *et al.*, 1993; Powers, 1995; Fedorovich *et al.*, 1999; Crossley *et al.*, 2007). Studies in *C. jejuni*, *H. pylori* and *Shewanella onediensis* have led to a model in which excretion of riboflavin promotes acquisition of iron by mediating the reduction of Fe^{3+} to Fe^{2+} (Worst *et al.*, 1998; Crossley *et al.*, 2007; Marsili *et al.*, 2008). Similarly, under low-iron conditions the roots of sunflower and sugar beet excrete riboflavin-5' and riboflavin-3' sulfate, which facilitate iron uptake by reduction of Fe^{3+} (Vorwieger *et al.*, 2007). In *Pichia guilliermondii* inactivation of the riboflavin biosynthesis pathway resulted in substantially reduced growth under iron-limiting conditions (Boretsky *et al.*, 2007). Furthermore, the isoalloxazine ring of riboflavin has been shown to exhibit properties of a chelator with high specificity for iron (Albert, 1950; 1953). Transcriptional analysis in *H. pylori* has suggested that the riboflavin synthesis is regulated in a Fur-dependent manner (Ernst *et al.*, 2005). Moreover, recent studies have reported a direct interaction of the Fur protein with the promoter region of the *ribBA* gene cluster in this bacterium (Pich *et al.*, 2012). Although a putative Fur-binding sequence was identified within the first of gene of the *ribDBAH* operon in *C. acetobutylicum*, it was suggested in this study that riboflavin biosynthesis in this microorganism is not directly controlled by Fur and occurs as a consequence

of the increased flavodoxin production. This arises from the fact that a FMN-sensing riboswitch is responsible for the control of expression of *rib* operons in Gram-positive bacteria (Mironov *et al.*, 2002; Vitreschak *et al.*, 2004). In support of this hypothesis knock-out of the flavodoxin encoding gene (*cac0587*) using the Clostron[®] system gave a riboflavin-negative phenotype under conditions of iron deficiency (3.6.1.4). Nevertheless, riboflavin might also contribute to acquisition of iron in the natural environments as an accessory effect.

4.3.4 Additional transcriptional changes in response to iron-limitation and *fur* gene inactivation

Apart from the Fur mediated iron-dependent regulation, a number of genes exhibited differential expression in response *fur* gene inactivation, but were not affected in the iron-deficient wild-type (Table 7.6, Appendix). It is beyond the scope of this study to discuss all transcriptional aspects. Nevertheless, a conceivable explanation could be advanced at least for some changes in expression. Secondary effects resulting from the increased iron influx, slower growth rate and elevated riboflavin synthesis are likely to account for a fraction of the transcriptional response in the *fur* mutant. GTP is the direct precursor for biosynthesis of riboflavin (Foor and Brown, 1975). Moreover, FeoB-dependent iron transport is coupled with GTP hydrolysis (Andrews *et al.*, 2003). Thus, the overflowing production of riboflavin and the enhanced FeoB-dependent iron transport in the *fur* mutant strain could lead to imbalance in the cellular pools of GTP. CodY is a stationary phase transcriptional regulator that senses intracellular levels of GTP and controls expression of genes involved in sporulation, amino acid catabolism and transport, among others (Ratnayake-Lecamwasam *et al.*, 2001; Dineen *et al.*, 2010). Therefore, some of the transcriptional changes in the *fur* mutant might be due to derepression of members of the CodY regulon. A recent global transcriptional analysis of a *codY* (*cac1786*) mutant in *C. acetobutylicum* did not confirm this rationalization (Vasileva, unpublished data). However, significantly upregulated in the *fur* mutant was the *purECFMNHD* operon (*cac1390-cac1396*), which encodes the enzymes involved in the *de novo* synthesis of IMP, a precursor of ATP and GTP. In *B. subtilis* expression of the *pur* gene cluster is controlled by PurR, a transcriptional regulator that responds to reduced cellular purine pools (Ebbole and Zalkin, 1989; Weng *et al.*, 1995). Presumably, a similar regulation pattern mediated by the putative PurR (CAC3224) regulator functions in the *C. acetobutylicum fur* mutant to compensate for the increased consumption of GTP. In *E. coli*, transcription of the gene encoding the PurR regulator is directly regulated by Fur-Fe²⁺ (Stojiljkovic *et al.*, 1994). However, no putative Fur-binding sequence was identified in the promoter region of *cac3224*.

A broad array of genes was regulated by iron through Fur-independent pathways (Table 7.5, Appendix). Among the most dramatically up-regulated was a cluster of genes involved in arginine synthesis. Similarly, iron deficiency has resulted in induction of genes involved in arginine production in *Listeria monocytogenes* (Ledala *et al.*, 2010). In *B. subtilis* AhrC is a regulator that senses high intracellular levels of arginine and represses expression of genes involved in its biosynthesis (Czaplewski *et al.*, 1992). The genome *C. acetobutylicum* encodes an AhrC ortholog (CAC2074), which presumably exhibits control on arginine synthesis in a similar manner. The reason for the derepression of the arginine biosynthesis pathway under low-iron conditions is currently unclear, but could represent an element of a more general stress response. Slightly upregulated in the iron-deficient wild-type was also a bicistronic operon encoding a second putative Feo-type system (*cac1447-cac1448*). In the anaerobic bacterium *Porphyromonas gingivalis* a Feo-type system has been reported to mediate manganese rather than iron uptake (Dashper *et al.*, 2005). A phylogenetic tree of FeoB proteins suggested that the second FeoB from *C. acetobutylicum* might also be involved in manganese acquisition (Carton *et al.*, 2006). Manganese could substitute for iron in several cases, which could explain the induction of the second Feo-system under conditions of iron-deficiency (Martin and Imlay, 2011). On the other hand, most dramatically down-regulated was an operon putatively associated with synthesis and maturation of a nitrogenase (*cac0253-cac0261*). Since nitrogenase is an iron-containing protein, downregulation of its synthesis could be a part of an iron-sparing response.

Taken together, these results provide compelling evidence that both iron-limitation and *fur* gene inactivation have pleiotropic effects in *C. acetobutylicum*. Therefore, cross-talk between regulatory networks could likely account for a significant fraction of the observed transcriptional changes under both conditions.

4.4 Other genes with predicted role in iron transport and metabolism in *C. acetobutylicum*

In addition to *cac1029-cac1032* and *cac0788-cac0791*, only three gene clusters in the genome of *C. acetobutylicum* were annotated as encoding putative iron transport systems (*cac2441-cac2444*; *cac1988-cac1990* and *cac2877-cac2878*) (Nölling *et al.*, 2001). Recent studies in our laboratory have indicated that *cac2877-cac2878* codes for a zinc-uptake system and is directly controlled by CAC0951 (Vasileva, unpublished data). The other two predicted iron acquisition systems did not exhibit significant changes in expression either under iron limitation or in the *fur* mutant. While the promoter region of *cac2441-cac2444* revealed a low-score putative Fur-binding sequence, no Fur box was identified upstream of the *cac1988-cac1990* gene cluster. Therefore, despite their

homology to iron acquisition systems, these transporters most probably play a different role. Collectively, these data emphasize the function of Fur as the main regulator of iron transport in *C. acetobutylicum*.

Fe-S cluster containing proteins are central for the metabolism of *C. acetobutylicum*. In response to oxidative stress and iron-limitation conditions in bacteria, Suf and Nif machineries are recruited for Fe-S cluster assembly (Outten *et al.*, 2004; Zheng *et al.*, 1998). It has been demonstrated that the *suf* operon in *E. coli* is controlled by the oxidative stress sensor OxyR and by Fur (McHugh *et al.*, 2003; Zheng *et al.*, 2001). Although not directly controlled by PerR, Hillmann *et al.* (2009b) showed that the gene clusters encoding putative Suf (*cac3288-cac3292*) and Nif systems are significantly upregulated in response to oxidative stress in *C. acetobutylicum*. Interestingly, change in the level of transcription of these operons has not been observed either under iron limitation or in the *fur* mutant strain in this study. Therefore, the mechanisms for repairment of Fe-S clusters under iron limitation, if any, in this microorganism remain unclear.

Another important aspect of the bacterial iron homeostasis is the control on the synthesis of iron storage proteins (Andrews, 1998; Carrondo, 2003). When the extracellular supplies of iron are scarce, intracellular reserves are recruited in order to meet the metabolic requirements (Andrews *et al.*, 2003). On the other hand, by sequestering excess of iron, these proteins prevent formation of ROS in the cell (Cornelis *et al.*, 2011). Three types of iron storage proteins are known in bacteria: (i) non-haem ferritins, (ii) haem-containing bacterioferritins and (iii) small Dps proteins involved specifically in protection of DNA (Andrews, 1998; Andrews *et al.*, 2003). The ferritins and bacterioferritins exhibit similar structural organization composed of 24 subunits, which form a spherical protein with a central cavity that could accommodate up to 4500 iron atoms (Andrews, 1998; Nandal *et al.*, 2010). The genome of *C. acetobutylicum* has revealed a putative ferritin encoding gene (*cac0845*) (Nölling *et al.*, 2001). CAC0845 showed 49 % similarity in amino acid sequence to FtnA (Izuhara *et al.*, 1991), the major iron storage protein in *E. coli*. Fig. 7.7 (Appendix) represents a homology model of a 24meric CAC0845 protein based on the structure of *E. coli* FtnA (pdb: 1eum; Stillman *et al.*, 2001). Transcription of iron storage proteins in bacteria is typically regulated directly or indirectly by the iron-responsive regulators (Wilderman *et al.*, 2004; Ernst *et al.*, 2005; Rodriguez, 2006; Fiorini *et al.*, 2008; Nandal *et al.*, 2010). Although a putative Fur-binding sequence was identified upstream of the *cac0845* gene, its expression was not affected either in the iron-deficient wild-type or in the *fur* mutant. Therefore, methods with higher sensitivity than the microarray analysis like RT-PCR might be considered for further investigation of the *cac0845* transcriptional pattern. Of interest for future studies would be also the biological role of CAC0845 for maintenance of iron homeostasis and resistance to oxidative stress in *C. acetobutylicum*.

5 Summary

1. The Fur homologous proteins CAC0951 and CAC1682 from *C. acetobutylicum* were subjected to comparative *in silico* and biochemical characterization. The results from these experiments coupled with trans-complementation studies in *fur*-null *E. coli* and *B. subtilis* hosts emphasized the role of CAC1682 as an iron-responsive transcriptional regulator (CacFur).
2. In order to determine the role of Fur in *C. acetobutylicum*, the *fur* gene was disrupted by insertional mutagenesis using the Clostron[®] system. The resultant *fur* defective strain exhibited a slow-growing phenotype, increased intracellular iron content and enhanced sensitivity to oxidative stress, but essentially no appreciable differences in fermentation pattern relative to the wild-type. The phenotypical changes were reversed by introduction of a functional copy of the *fur* gene *in trans*. Collectively, the data from the physiological analysis of the mutant strain demonstrated the important role Fur in the lifestyle of *C. acetobutylicum*.
3. Cell-free supernatants from the *fur* mutant and the wild-type, grown under conditions of iron limitation, did not reveal detectable siderophore production in *C. acetobutylicum*. However, a unique feature of the physiology of the *fur* mutant was the excessive synthesis of riboflavin. The iron-deficient wild-type revealed a similar profile. Induction of the riboflavin biosynthesis pathway in the *fur* mutant and the iron-deprived wild-type was demonstrated also at transcriptional level using Northern blot hybridization analysis.
4. In order to get further insights into the mechanisms for maintenance of iron homeostasis in *C. acetobutylicum*, the transcriptional modifications in response to iron limitation and inactivation of *fur* were determined and compared. Both iron deficiency and loss of Fur resulted in extensive transcriptional reshaping. Bioinformatic analysis of the promotor sequences of the genes, which elicited changes in transcription under both conditions allowed the identification of the putative direct targets of CacFur (CacFur regulon). As expected, the predicted Fur regulon in *C. acetobutylicum* includes two putative iron uptake systems. In addition, the transcription of several genes involved in energy metabolism was affected. Among these most highly upregulated were two genes encoding a L-lactate dehydrogenase and a flavodoxin.
5. Taken together the results of this study indicate that *C. acetobutylicum* responds to iron using a sophisticated system and Fur plays a paramount role in this process.

6 References

- Ahn, B. E., Cha, J., Lee, E. J., Han, A. R., Thompson, C. J. & Roe, J. H. (2006).** Nur, a nickel-responsive regulator of the Fur family, regulates superoxide dismutases and nickel transport in *Streptomyces coelicolor*. *Mol Microbiol* **59**, 1848-1858.
- Albert, A. (1950).** The metal-binding properties of riboflavin. *Biochem J* **47**, 3.
- Albert, A. (1953).** Quantitative studies of the avidity of naturally occurring substances for trace metals. III. Pteridines, riboflavin and purines. *Biochem J* **54**, 646-54.
- Althaus, E. W., Outten, C. E., Olson, K. E., Cao, H. & O'Halloran, T. V. (1999).** The ferric uptake regulation (Fur) repressor is a zinc metalloprotein. *Biochemistry* **38**, 6559-6569.
- An, Y. J., Ahn, B. E., Han, A. R., Kim, H. M., Chung, K. M., Shin, J. H., Cho, Y. B., Roe, J. H. & Cha, S. S. (2009).** Structural basis for the specialization of Nur, a nickel-specific Fur homolog, in metal sensing and DNA recognition. *Nucleic Acids Res* **37**, 3442-3451.
- Andrews, S. C. (1998).** Iron storage in bacteria. *Adv Microb Physiol* **40**, 281-351.
- Andrews, S. C., Robinson, A. K. & Rodríguez-Quñones, F. (2003).** Bacterial iron homeostasis. *FEMS Microbiol Rev* **27**, 215-237.
- Arnow, L. E. (1937).** Colorimetric estimation of the components of 3,4-dihydroxy phenylalanine tyrosine mixtures. *J Biol Chem* **118**, 531-535.
- Atkin, C. L., Neilands, J. B. & Phaff, H. J. (1970).** Rhodotorulic acid from species of *Leucosporidium*, *Rhodospiridium*, *Rhodotorula*, *Sporidiobolus*, and *Sporobolomyces*, and a new alanine-containing ferrichrome from *Cryptococcus melibiosum*. *J Bacteriol* **103**, 722-733.
- Bagg, A. & Neilands, J. B. (1987).** Ferric uptake regulation protein acts as a repressor, employing iron (II) as a cofactor to bind the operator of an iron transport operon in *Escherichia coli*. *Biochemistry* **26**, 5471-5477.
- Bahl, H. & Gottschlak, G. (1984).** Parameters affecting solvent production by *Clostridium acetobutylicum* in continuous culture. *Biotechnol Bioeng Symp* **11**, 215-223.
- Bahl, H., Gottwald, M., Kuhn, A., Rale, V., Andersch, W. & Gottschalk, G. (1986).** Nutritional factors affecting the ratio of solvents produced by *Clostridium acetobutylicum*. *Appl Environ Microbiol* **52**, 169-172.
- Baichoo, N., Wang, T., Ye, R. & Helmann, J. D. (2002).** Global analysis of the *Bacillus subtilis* Fur regulon and the iron starvation stimulon. *Mol Microbiol* **45**, 1613-1629.
- Bender, K. S., Yen, H. C., Hemme, C. L. & other authors (2007).** Analysis of a ferric uptake regulator (Fur) mutant of *Desulfovibrio vulgaris* Hildenborough. *Appl Environ Microbiol* **73**, 5389-5400.

- Bijlsma, J. J., Waidner, B., Vliet, A. H. & other authors (2002).** The *Helicobacter pylori* homologue of the ferric uptake regulator is involved in acid resistance. *Infect Immun* **70**, 606-611.
- Boretsky, Y. R., Protchenko, O. V., Prokopiv, T. M., Mukalov, I. O., Fedorovych, D. V. & Sibirny, A. A. (2007).** Mutations and environmental factors affecting regulation of riboflavin synthesis and iron assimilation also cause oxidative stress in the yeast *Pichia guilliermondii*. *J Basic Microbiol* **47**, 371-377.
- Boyd, J., Oza, M. N. & Murphy, J. R. (1990).** Molecular cloning and DNA sequence analysis of a diphtheria toxin iron-dependent regulatory element (*dtxR*) from *Corynebacterium diphtheriae*. *Proc Natl Acad Sci U S A* **87**, 5968-5972.
- Bradford, M. M. (1976).** A rapid and sensitive method for the quantitation of microgram quantities of protein utilizing the principle of protein-dye binding. *Anal Biochem* **72**, 248-254.
- Braun, V. & Killmann, H. (1999).** Bacterial solutions to the iron-supply problem. *Trends Biochem Sci* **24**, 104-109.
- Breznak, J. A. & Costilow, R. N. (1994).** Physicochemical factors of growth. In *Methods of general and molecular bacteriology*. Ed. P. Gerhardt. American Society for Microbiology, Washington D.C., USA, 137-154.
- Brune, I., Werner, H., Hüser, A. T., Kalinowski, J., Pühler, A. & Tauch, A. (2006).** The DtxR protein acting as dual transcriptional regulator directs a global regulatory network involved in iron metabolism of *Corynebacterium glutamicum*. *BMC Genomics* **7**, 21.
- Bsat, N., Herbig, A., Casillas-Martinez, L., Setlow, P. & Helmann, J. D. (1998).** *Bacillus subtilis* contains multiple Fur homologues: identification of the iron uptake (Fur) and peroxide regulon (PerR) repressors. *Mol Microbiol* **29**, 189-198.
- Bsat, N. & Helmann, J. D. (1999).** Interaction of *Bacillus subtilis* Fur (ferric uptake repressor) with the *dhb* operator in vitro and in vivo. *J Bacteriol* **181**, 4299-4307.
- Butcher, J., Sarvan, S., Brunzelle, J. S., Couture, J. F. & Stintzi, A. (2012).** Structure and regulon of *Campylobacter jejuni* ferric uptake regulator Fur define apo-Fur regulation. *Proc Natl Acad Sci U S A* **109**, 10047-10052.
- Cai, X. & Bennett, G. N. (2011).** Improving the *Clostridium acetobutylicum* butanol fermentation by engineering the strain for co-production of riboflavin. *J Ind Microbiol Biotechnol* **38**, 1013-1025.
- Carpenter, B. M., Whitmire, J. M. & Merrell, D. S. (2009).** This is not your mother's repressor: the complex role of Fur in pathogenesis. *Infect Immun* **77**, 2590-2601.
- Carpenter, B. M., Gancz, H., Benoit, S. L., Evans, S., Olsen, C. H., Michel, S. L., Maier, R. J. & Merrell, D. S. (2010).** Mutagenesis of conserved amino acids of *Helicobacter pylori* Fur reveals residues important for function. *J Bacteriol* **192**, 5037-5052.
- Cartron, M. L., Maddocks, S., Gillingham, P., Craven, C. J. & Andrews, S. C. (2006).** Feo-transport of ferrous iron into bacteria. *Biometals* **19**, 143-157.

- Chen, J-S. & Blanchard, D., K. (1979).** A simple hydrogenase-linked assay for ferredoxin and flavodoxin. *Anal Biochem* **93**, 216-222.
- Chen, L., James, L. P. & Helmann, J. D. (1993).** Metalloregulation in *Bacillus subtilis*: isolation and characterization of two genes differentially repressed by metal ions. *J Bacteriol* **175**, 5428-5437.
- Chen, L., Keramati, L. & Helmann, J. D. (1995).** Coordinate regulation of *Bacillus subtilis* peroxide stress genes by hydrogen peroxide and metal ions. *Proc Natl Acad Sci USA* **92**, 8190-8194.
- Chen, Y., Indurthi, D. C., Jones, S. W. & Papoutsakis, E. T. (2011).** Small RNAs in the genus *Clostridium*. *MBio* **2**, e00340-00310.
- Cooksley, C. M., Zhang, Y., Wang, H., Redl, S., Winzer, K. & Minton, N. P. (2012).** Targeted mutagenesis of the *Clostridium acetobutylicum* acetone-butanol-ethanol fermentation pathway. *Metab Eng* **14**, 630-641.
- Carrondo, M. A. (2003).** Ferritins, iron uptake and storage from the bacterioferritin viewpoint. *EMBO J* **22**, 1959–1968.
- Cornelis, P., Wei, Q., Andrews, S. C. & Vinckx, T. (2011).** Iron homeostasis and management of oxidative stress response in bacteria. *Metallomics* **3**, 540-549.
- Coy, M. & Neilands, J. B. (1991).** Structural dynamics and functional domains of the Fur protein. *Biochemistry* **30**, 8201-8210.
- Crichton, R. (2001).** Inorganic chemistry of iron metabolism: From Molecular Mechanisms to Clinical Consequences. 2nd ed. John Wiley and Sons Ltd., Chichester, England.
- Crossley, R. A., Gaskin, D. J., Holmes, K., Mulholland, F., Wells, J. M., Kelly, D. J., van Vliet, A. H. & Walton, N. J. (2007).** Riboflavin biosynthesis is associated with assimilatory ferric reduction and iron acquisition by *Campylobacter jejuni*. *Appl Environ Microbiol* **73**, 7819-7825.
- Cutting, S. M. & Youngman, P. (1994).** Gene Transfer in Gram-Positive Bacteria. In: P. Gerhardt, R. G. E. Murray, W. A. Wood, N. R. Krieg (ed). *Methods for General and Molecular Biology*. American Society for Microbiology, Washington D. C., USA
- Czaplewski, L. G., North, A. K., Smith, M. C., Baumberg, S. & Stockley, P. G. (1992).** Purification and initial characterization of AhrC: the regulator of arginine metabolism genes in *Bacillus subtilis*. *Mol Microbiol* **6**, 267-275.
- D'Onofrio, A., Crawford, J. M., Stewart, E. J., Witt, K., Gavrish, E., Epstein, S., Clardy, J. & Lewis, K. (2010).** Siderophores from neighboring organisms promote the growth of uncultured bacteria. *Chem Biol* **17**, 254-264.
- da Silva Neto, J. F., Braz, V. S., Italiani, V. C. & Marques, M. V. (2009).** Fur controls iron homeostasis and oxidative stress defense in the oligotrophic alpha-proteobacterium *Caulobacter crescentus*. *Nucleic Acids Res* **37**, 4812-4825.

- Dabrock, B., Bahl, H. & Gottschalk, G. (1992).** Parameters affecting solvent production by *Clostridium pasteurianum*. *Appl Environ Microbiol* **58**, 1233-1239.
- Danielli, A., Roncarati, D., Delany, I., Chiarini, V., Rappuoli, R. & Scarlato, V. (2006).** In vivo dissection of the *Helicobacter pylori* Fur regulatory circuit by genome-wide location analysis. *J Bacteriol* **188**, 4654-4662.
- Dashper, S. G., Butler, C. A., Lissel, J. P. & other authors (2005).** A novel *Porphyromonas gingivalis* FeoB plays a role in manganese accumulation. *J Biol Chem* **280**, 28095-28102.
- de Lorenzo, V., Wee, S., Herrero, M. & Neilands, J. B. (1987).** Operator sequences of the aerobactin operon of plasmid ColV-K30 binding the ferric uptake regulation (Fur) repressor. *J Bacteriol* **169**, 2624-2630.
- de Lorenzo, V., Giovannini, F., Herrero, M. & Neilands, J. B. (1988).** Metal ion regulation of gene expression. Fur repressor-operator interaction at the promoter region of the aerobactin system of pColV-K30. *J Mol Biol* **203**, 875-884.
- de Luca, N. G., Wexler, M., Pereira, M. J., Yeoman, K. H. & Johnston, A. W. (1998).** Is the *fur* gene of *Rhizobium leguminosarum* essential? *FEMS Microbiol Lett* **168**, 289-295.
- Delany, I., Spohn, G., Rappuoli, R. & Scarlato, V. (2001).** The Fur repressor controls transcription of iron-activated and -repressed genes in *Helicobacter pylori*. *Mol Microbiol* **42**, 1297-1309.
- Delany, I., Spohn, G., Pacheco, A. B., Ieva, R., Alaimo, C., Rappuoli, R. & Scarlato, V. (2002).** Autoregulation of *Helicobacter pylori* Fur revealed by functional analysis of the iron-binding site. *Mol Microbiol* **46**, 1107-1122.
- Delany, I., Rappuoli, R. & Scarlato, V. (2004).** Fur functions as an activator and as a repressor of putative virulence genes in *Neisseria meningitidis*. *Mol Microbiol* **52**, 1081-1090.
- Delany, I., Ieva, R., Soragni, A., Hilleringmann, M., Rappuoli, R. & Scarlato, V. (2005).** In vitro analysis of protein-operator interactions of the NikR and Fur metal-responsive regulators of coregulated genes in *Helicobacter pylori*. *J Bacteriol* **187**, 7703-7715.
- Demuez, M., Cournac, L., Guerrini, O., Soucaille, P. & Girbal, L. (2007).** Complete activity profile of *Clostridium acetobutylicum* [FeFe]-hydrogenase and kinetic parameters for endogenous redox partners. *FEMS Microbiol Lett* **275**, 113-121.
- Dian, C., Vitale, S., Leonard, G. A. & other authors (2011).** The structure of the *Helicobacter pylori* ferric uptake regulator Fur reveals three functional metal binding sites. *Mol Microbiol* **79**, 1260-1275.
- Dineen, S. S., McBride, S. M. & Sonenshein, A. L. (2010).** Integration of metabolism and virulence by *Clostridium difficile* CodY. *J Bacteriol* **192**, 5350-5362.
- Dower, W. J., Miller, J. F. & Ragsdale, C. W. (1988).** High efficiency transformation of *E. coli* by high voltage electroporation. *Nucleic Acids Res* **16**, 6127-6145.

- Díaz-Mireles, E., Wexler, M., Sawers, G., Bellini, D., Todd, J. D. & Johnston, A. W. (2004). The Fur-like protein Mur of *Rhizobium leguminosarum* is a Mn²⁺-responsive transcriptional regulator. *Microbiology* **150**, 1447-1456.
- Dürre, P. (2007). Biobutanol: an attractive biofuel. *Biotechnol J* **2**, 1525-1534.
- Ebbole, D. J. & Zalkin, H. (1989). *Bacillus subtilis pur* operon expression and regulation. *J Bacteriol* **171**, 2136-2141.
- Ernst, F. D., Bereswill, S., Waidner, B. & other authors (2005a). Transcriptional profiling of *Helicobacter pylori* Fur- and iron-regulated gene expression. *Microbiology* **151**, 533-546.
- Escolar, L., Pérez-Martín, J. & de Lorenzo, V. (1999). Opening the iron box: transcriptional metalloregulation by the Fur protein. *J Bacteriol* **181**, 6223-6229.
- Fabiano, E., Gualtieri, G., Pritsch, C., Polla, G., & Arias, A. (1994). Extent of high-affinity iron transport systems in field isolates rhizobia. *Plant and Soil* **164**, 177-185.
- Fiedler, T. (2006). Proteomanalyse von *Clostridium acetobutylicum* unter Phosphatlimitierung und Charakterisierung des phosphatspezifischen Zwei-Komponenten-Systems PhoP/R. Dissertation. Universität Rostock.
- Fiorini, F., Stefanini, S., Valenti, P., Chiancone, E. & De Biase, D. (2008). Transcription of the *Listeria monocytogenes fri* gene is growth-phase dependent and is repressed directly by Fur, the ferric uptake regulator. *Gene* **410**, 113-121.
- Fischer, R. J., Helms, J. & Dürre, P. (1993). Cloning, sequencing, and molecular analysis of the *sol* operon of *Clostridium acetobutylicum*, a chromosomal locus involved in solventogenesis. *J Bacteriol* **175**, 6959-6969.
- Fitzgerald, M. P., Rogers, L. J., Rao, K. K. & Hall, D. O. (1980). Efficiency of ferredoxins and flavodoxins as mediators in systems for hydrogen evolution. *Biochem J* **192**, 665-672.
- Foor, F. & Brown, G. M. (1975). Purification and properties of guanosine triphosphate cyclohydrolase II from *Escherichia coli*. *J Biol Chem* **250**, 3545-51.
- Foster, J. W. & Hall, H. K. (1992). Effect of *Salmonella typhimurium* ferric uptake regulator (*fur*) mutations on iron- and pH-regulated protein synthesis. *J Bacteriol* **174**, 4317-4323.
- Frausto da Silva, J. J. R. & Williams, R. J. P. (2001). The biological chemistry of the elements. 2nd ed. Oxford University Press, NY, USA.
- Freier, D. & Gottschalk, G. (1987). L(+)-lactate dehydrogenase of *Clostridium acetobutylicum* is activated by fructose-1,6-bisphosphate. *FEMS Microbiol* **43**, 229-233.
- Friedman, Y. E. & O'Brian, M. R. (2004). The ferric uptake regulator (Fur) protein from *Bradyrhizobium japonicum* is an iron-responsive transcriptional repressor *in vitro*. *J Biol Chem* **279**, 32100-32105.
- Fuangthong, M., Herbig, A. F., Bsat, N. & Helmann, J. D. (2002). Regulation of the *Bacillus subtilis fur* and *perR* genes by PerR: not all members of the PerR regulon are peroxide inducible. *J Bacteriol* **184**, 3276-3286.

- Fuangthong, M. & Helmann, J. D. (2003).** Recognition of DNA by three ferric uptake regulator (Fur) homologs in *Bacillus subtilis*. *J Bacteriol* **185**, 6348-6357.
- Gaballa, A. & Helmann, J. D. (1998).** Identification of a zinc-specific metalloregulatory protein, Zur, controlling zinc transport operons in *Bacillus subtilis*. *J Bacteriol* **180**, 5815-5821.
- Gaballa, A., Antelmann, H., Aguilar, C., Khakh, S. K., Song, K. B., Smaldone, G. T. & Helmann, J. D. (2008).** The *Bacillus subtilis* iron-sparing response is mediated by a Fur-regulated small RNA and three small, basic proteins. *Proc Natl Acad Sci USA* **105**, 11927-11932.
- Gao, H., Zhou, D., Li, Y. & other authors (2008).** The iron-responsive Fur regulon in *Yersinia pestis*. *J Bacteriol* **190**, 3063-3075.
- Garrido, M. E., Bosch, M., Medina, R., Llagostera, M., Pérez de Rozas, A. M., Badiola, I. & Barbé, J. (2003).** The high-affinity zinc-uptake system *znuACB* is under control of the iron-uptake regulator (*fur*) gene in the animal pathogen *Pasteurella multocida*. *FEMS Microbiol Lett* **221**, 31-37.
- Giedroc, D. P. & Arunkumar, A. I. (2007).** Metal sensor proteins: nature's metalloregulated allosteric switches. *Dalton Trans*, 3107-3120.
- Gilbreath, J. J., Pich, O. Q., Benoit, S. L., Besold, A. N., Cha, J. H., Maier, R. J., Michel, S. L., Maynard, E. L. & Merrell, D. S. (2013).** Random and site-specific mutagenesis of the *Helicobacter pylori* ferric uptake regulator provides insight into Fur structure-function relationships. *Mol Microbiol* **89**, 304-323.
- Girbal, L., Croux, C., Vasconcelos, I. & Soucaille, P. (1995).** Regulation of metabolic shifts in *Clostridium acetobutylicum* ATCC 824. *FEMS Microbiol Rev* **17**, 287-297.
- Girbal, L., von Abendroth, G., Winkler, M., Benton, P. M., Meynial-Salles, I., Croux, C., Peters, J. W., Happe, T. & Soucaille, P. (2005).** Homologous and heterologous overexpression in *Clostridium acetobutylicum* and characterization of purified clostridial and algal Fe-only hydrogenases with high specific activities. *Appl Environ Microbiol* **71**, 2777-2781.
- Goujon, M., McWilliam, H., Li, W., Valentin, F., Squizzato, S., Paern, J. & Lopez, R. (2010).** A new bioinformatics analysis tools framework at EMBL-EBI. *Nucleic Acids Res* **38**, W695-699.
- Grifantini, R., Sebastian, S., Frigimelica, E., Draghi, M., Bartolini, E., Muzzi, A., Rappuoli, R., Grandi, G. & Genco, C. A. (2003).** Identification of iron-activated and -repressed Fur-dependent genes by transcriptome analysis of *Neisseria meningitidis* group B. *Proc Natl Acad Sci USA* **100**, 9542-9547.
- Grimmler, C., Janssen, H., Krausse, D., Fischer, R. J., Bahl, H., Dürre, P., Liebl, W. & Ehrenreich, A. (2011).** Genome-wide gene expression analysis of the switch between acidogenesis and solventogenesis in continuous cultures of *Clostridium acetobutylicum*. *J Mol Microbiol Biotechnol* **20**, 1-15.
- Grundy, F. J. & Henkin, T. M. (1991).** The *rpsD* gene, encoding ribosomal protein S4, is autogenously regulated in *Bacillus subtilis*. *J Bacteriol* **173**, 4595-4602.
- Hanahan, D. (1983).** Studies on transformation of *Escherichia coli* with plasmids. *J Mol Biol* **166**, 557-580.

- Hantke, K. (1981).** Regulation of ferric iron transport in *Escherichia coli* K12: isolation of a constitutive mutant. *Mol Gen Genet* **182**, 288-292.
- Hantke, K. (1987).** Selection procedure for deregulated iron transport mutants (*fur*) in *Escherichia coli* K 12: *fur* not only affects iron metabolism. *Mol Gen Genet* **210**, 135-139.
- Hantke, K. (1990).** Dihydroxybenzoylserine--a siderophore for *E. coli*. *FEMS Microbiol Lett* **55**, 5-8.
- Hantke, K. (2001).** Iron and metal regulation in bacteria. *Curr Opin Microbiol* **4**, 172-177.
- Harvie, D. R., Vilchez, S., Steggles, J. R. & Ellar, D. J. (2005).** *Bacillus cereus* Fur regulates iron metabolism and is required for full virulence. *Microbiology* **151**, 569-577.
- Heap, J. T., Pennington, O. J., Cartman, S. T., Carter, G. P. & Minton, N. P. (2007).** The ClosTron: a universal gene knock-out system for the genus *Clostridium*. *J Microbiol Methods* **70**, 452-464.
- Heap, J. T., Pennington, O. J., Cartman, S. T. & Minton, N. P. (2009).** A modular system for *Clostridium* shuttle plasmids. *J Microbiol Methods* **78**, 79-85.
- Heap, J. T., Kuehne, S. A., Ehsaan, M., Cartman, S. T., Cooksley, C. M., Scott, J. C. & Minton, N. P. (2010).** The ClosTron: Mutagenesis in *Clostridium* refined and streamlined. *J Microbiol Methods* **80**, 49-55.
- Hernández, J. A., Bes, M. T., Fillat, M. F., Neira, J. L. & Peleato, M. L. (2002).** Biochemical analysis of the recombinant Fur (ferric uptake regulator) protein from *Anabaena* PCC 7119: factors affecting its oligomerization state. *Biochem J* **366**, 315-322.
- Hernández, J. A., Muro-Pastor, A. M., Flores, E., Bes, M. T., Peleato, M. L. & Fillat, M. F. (2006).** Identification of a *furA* cis antisense RNA in the cyanobacterium *Anabaena* sp. PCC 7120. *J Mol Biol* **355**, 325-334.
- Hillmann, F., Fischer, R. J., Saint-Prix, F., Girbal, L. & Bahl, H. (2008).** PerR acts as a switch for oxygen tolerance in the strict anaerobe *Clostridium acetobutylicum*. *Mol Microbiol* **68**, 848-860.
- Hillmann, F., Riebe, O., Fischer, R. J., Mot, A., Caranto, J. D., Kurtz, D. M. & Bahl, H. (2009a).** Reductive dioxygen scavenging by flavo-diiron proteins of *Clostridium acetobutylicum*. *FEBS Lett* **583**, 241-245.
- Hillmann, F., Döring, C., Riebe, O., Ehrenreich, A., Fischer, R. J. & Bahl, H. (2009b).** The role of PerR in O₂-affected gene expression of *Clostridium acetobutylicum*. *J Bacteriol* **191**, 6082-6093.
- Ho, S. N., Hunt, H. D., Horton, R. M., Pullen, J. K. & Pease, L. R. (1989).** Site-directed mutagenesis by overlap extension using the polymerase chain reaction. *Gene* **77**, 51-59.
- Huffman, J. L. & Brennan, R. G. (2002).** Prokaryotic transcription regulators: more than just the helix-turn-helix motif. *Curr Opin Struct Biol* **12**, 98-106.

- Imlay, J. A., Chin, S. M. & Linn, S. (1988).** Toxic DNA damage by hydrogen peroxide through the Fenton reaction in vivo and in vitro. *Science* **240**, 640-642.
- Imlay, J. A. (2003).** Pathways of oxidative damage. *Annu Rev Microbiol* **57**, 395-418.
- Imlay, J. A. (2006).** Iron-sulphur clusters and the problem with oxygen. *Mol Microbiol* **59**, 1073-1082.
- Imlay, J. A. (2008).** Cellular defenses against superoxide and hydrogen peroxide. *Annu Rev Biochem* **77**, 755-776.
- Irving, H. & Williams, R. J. P. (1948).** Order of stability of metal complexes. *Nature* **162**, 746-747
- Izuhara, M., Takamune, K., & Takata, R. (1991).** Cloning and sequencing of an *Escherichia coli* K12 gene which encodes a polypeptide having similarity to the human ferritin H subunit. *Mol Gen Genet* **225**, 510-513.
- Jacquemet, L., Aberdam, D., Adrait, A., Hazemann, J. L., Latour, J. M. & Michaud-Soret, I. (1998).** X-ray absorption spectroscopy of a new zinc site in the fur protein from *Escherichia coli*. *Biochemistry* **37**, 2564-2571.
- Janssen, H., Döring, C., Ehrenreich, A., Voigt, B., Hecker, M., Bahl, H. & Fischer, R. J. (2010).** A proteomic and transcriptional view of acidogenic and solventogenic steady-state cells of *Clostridium acetobutylicum* in a chemostat culture. *Appl Microbiol Biotechnol* **87**, 2209-2226.
- Janssen, H. (2010).** Das Proteom und Transkriptom von *Clostridium acetobutylicum* bei unterschiedlichen pH-Werten im Chemostaten. Dissertation. Universität Rostock.
- Jinks-Robertson, S. & Nomura, M. (1982).** Ribosomal protein S4 acts in trans as a translational repressor to regulate expression of the alpha operon in *Escherichia coli*. *J Bacteriol* **151**, 193-202.
- Jones, D. T., van der Westhuizen, A., Long, S., Allcock, E. R., Reid, S. J. & Woods, D. R. (1982).** Solvent production and morphological changes in *Clostridium acetobutylicum*. *Appl Environ Microbiol* **43**, 1434-1439.
- Jones, D. T. & Woods, D. R. (1986).** Acetone-butanol fermentation revisited. *Microbiol Rev* **50**, 484-524.
- Junelles M. A., Idrissi-Janati, R., Petitdemange, H. & Gay, R. (1988).** Iron effect on acetone-butanol fermentation. *Current Microbiol* **17**, 299-303.
- Kammler, M., Schön, C. & Hantke, K. (1993).** Characterization of the ferrous iron uptake system of *Escherichia coli*. *J Bacteriol* **175**, 6212-6219.
- Kawasaki, S., Ishikura, J., Watamura, Y. & Niimura, Y. (2004).** Identification of O₂-induced peptides in an obligatory anaerobe, *Clostridium acetobutylicum*. *FEBS Lett* **571**, 21-25.
- Kawasaki, S., Watamura, Y., Ono, M., Watanabe, T., Takeda, K. & Niimura, Y. (2005).** Adaptive responses to oxygen stress in obligatory anaerobes *Clostridium acetobutylicum* and *Clostridium aminovalericum*. *Appl Environ Microbiol* **71**, 8442-8450.

- Knight, E., Jr & Hardy, R. W. (1966).** Isolation and characteristics of flavodoxin from nitrogen-fixing *Clostridium pasteurianum*. *J Biol Chem* **241**, 2752–2756.
- Köster, W. (2001).** ABC transporter-mediated uptake of iron, siderophores, heme and vitamin B₁₂. *Res Microbiol* **152**, 291–301.
- Lau, C. K., Ishida, H., Liu, Z. & Vogel, H. J. (2013).** Solution structure of *Escherichia coli* FeoA and its potential role in bacterial ferrous iron transport. *J Bacteriol* **195**, 46-55.
- Laudenbach, D. E., Reith, M. E. & Straus, N. A. (1988).** Isolation, sequence analysis, and transcriptional studies of the flavodoxin gene from *Anacystis nidulans* R2. *J Bacteriol* **170**, 258-265.
- Le Cam, E., Frechon, D., Barray, M., Fourcade, A. & Delain, E. (1994).** Observation of binding and polymerization of Fur repressor onto operator-containing DNA with electron and atomic force microscopes. *Proc Natl Acad Sci USA* **91**, 11816-11820.
- Ledala, N., Sengupta, M., Muthaiyan, A., Wilkinson, B. J. & Jayaswal, R. K. (2010).** Transcriptomic response of *Listeria monocytogenes* to iron limitation and Fur mutation. *Appl Environ Microbiol* **76**, 406-416.
- Lee, J. W. & Helmann, J. D. (2006a).** The PerR transcription factor senses H₂O₂ by metal-catalysed histidine oxidation. *Nature* **440**, 363-367.
- Lee, J. W. & Helmann, J. D. (2006b).** Biochemical characterization of the structural Zn²⁺ site in the *Bacillus subtilis* peroxide sensor PerR. *J Biol Chem* **281**, 23567-23578.
- Lee, J. W. & Helmann, J. D. (2007).** Functional specialization within the Fur family of metalloregulators. *Biometals* **20**, 485-499.
- Lee, S. Y., Park, J. H., Jang, S. H., Nielsen, L. K., Kim, J. & Jung, K. S. (2008).** Fermentative butanol production by Clostridia. *Biotechnol Bioeng* **101**, 209-228.
- Lehmann, D. & Lütke-Eversloh, T. (2011).** Switching *Clostridium acetobutylicum* to an ethanol producer by disruption of the butyrate/butanol fermentative pathway. *Metab Eng* **13**, 464-473.
- Lehmann, D., Hönicke, D., Ehrenreich, A., Schmidt, M., Weuster-Botz, D., Bahl, H. & Lütke-Eversloh, T. (2012a).** Modifying the product pattern of *Clostridium acetobutylicum*: physiological effects of disrupting the acetate and acetone formation pathways. *Appl Microbiol Biotechnol* **94**, 743-754.
- Lehmann, D., Radomski, N. & Lütke-Eversloh, T. (2012b).** New insights into the butyric acid metabolism of *Clostridium acetobutylicum*. *Appl Microbiol Biotechnol* **96**, 1325-1339.
- Lehmann, D. (2012).** Neue Einblicke in den Gärungsstoffwechsel von *Clostridium acetobutylicum*. Dissertation. Universität Rostock.
- Leonhardt, K. & Straus, N. A. (1992).** An iron stress operon involved in photosynthetic electron transport in the marine cyanobacterium *Synechococcus* sp. PCC 7002. *J Gen Microbiol* **138 Pt 8**, 1613-1621.

- Liu, X. & Millero, F. J. (2002). The solubility of iron in seawater. *Marine Chemistry* **77**, 43-54.
- Louvel, H., Kanai, T., Atomi, H. & Reeve, J. N. (2009). The Fur iron regulator-like protein is cryptic in the hyperthermophilic archaeon *Thermococcus kodakaraensis*. *FEMS Microbiol Lett* **295**, 117-128.
- Lucarelli, D., Russo, S., Garman, E., Milano, A., Meyer-Klaucke, W. & Pohl, E. (2007). Crystal structure and function of the zinc uptake regulator FurB from *Mycobacterium tuberculosis*. *J Biol Chem* **282**, 9914-9922.
- Lütke-Eversloh, T. & Bahl, H. (2011). Metabolic engineering of *Clostridium acetobutylicum*: recent advances to improve butanol production. *Curr Opin Biotechnol* **22**, 634-647.
- Ma, Z., Jacobsen, F. E. & Giedroc, D. P. (2009). Coordination chemistry of bacterial metal transport and sensing. *Chem Rev* **109**, 4644-4681.
- Ma, Z., Gabriel, S. E. & Helmann, J. D. (2011). Sequential binding and sensing of Zn(II) by *Bacillus subtilis* Zur. *Nucleic Acids Res* **39**, 9130-9138.
- Ma, Z., Faulkner, M. J. & Helmann, J. D. (2012). Origins of specificity and cross-talk in metal ion sensing by *Bacillus subtilis* Fur. *Mol Microbiol* **86**, 1144-1155.
- Mann, M. S. (2012). Metabolic Engineering von *Clostridium acetobutylicum*: Steigerung der Butanolbildung durch homologe Genexpression. Dissertation. Universität Rostock.
- Marsili, E., Baron, D. B., Shikhare, I. D., Coursolle, D., Gralnick, J. A. & Bond, D. R. (2008). *Shewanella* secretes flavins that mediate extracellular electron transfer. *Proc Natl Acad Sci USA* **105**, 3968-3973.
- Martin, J. E. & Imlay, J. A. (2011). The alternative aerobic ribonucleotide reductase of *Escherichia coli*, NrdEF, is a manganese-dependent enzyme that enables cell replication during periods of iron starvation. *Mol Microbiol* **80**, 319-334.
- Massé, E. & Gottesman, S. (2002). A small RNA regulates the expression of genes involved in iron metabolism in *Escherichia coli*. *Proc Natl Acad Sci USA* **99**, 4620-4625.
- Massé, E. & Arguin, M. (2005). Ironing out the problem: new mechanisms of iron homeostasis. *Trends Biochem Sci* **30**, 462-468.
- Massé, E., Salvail, H., Desnoyers, G. & Arguin, M. (2007). Small RNAs controlling iron metabolism. *Curr Opin Microbiol* **10**, 140-145.
- May, M. E. & Fish, W. W. (1978). The UV and visible spectral properties of ferritin. *Arch Biochem Biophys* **190**, 720-725.
- May, A., Hillmann, F., Riebe, O., Fischer, R. J. & Bahl, H. (2004). A rubrerythrin-like oxidative stress protein of *Clostridium acetobutylicum* is encoded by a duplicated gene and identical to the heat shock protein Hsp21. *FEMS Microbiol Lett* **238**, 249-254.
- Mayhew, S. G. & Massey, V. (1969). Purification and characterization of flavodoxin from *Peptostreptococcus elsdenii*. *J Biol Chem* **244**, 794-802.

- Mayhew S. G. (1971).** Properties of two clostridial flavodoxins. *Biochim Biophys Acta* **235**, 276-288.
- McHugh, J. P., Rodríguez-Quinoñes, F., Abdul-Tehrani, H., Svistunenko, D. A., Poole, R. K., Cooper, C. E. & Andrews, S. C. (2003).** Global iron-dependent gene regulation in *Escherichia coli*. A new mechanism for iron homeostasis. *J Biol Chem* **278**, 29478-29486.
- Meinecke, B., Bertram, J. & Gottschalk, G. (1989).** Purification and characterization of the pyruvate-ferredoxin oxidoreductase from *Clostridium acetobutylicum*. *Arch Microbiol* **152**, 244-250.
- Meng, E. C., Pettersen, E. F., Couch, G. S., Huang, C. C. & Ferrin, T. E. (2006).** Tools for integrated sequence-structure analysis with UCSF Chimera. *BMC Bioinformatics* **7**, 339.
- Mermelstein, L. D., Welker, N. E., Bennett, G. N. & Papoutsakis, E. T. (1992).** Expression of cloned homologous fermentative genes in *Clostridium acetobutylicum* ATCC 824. *Biotechnology (NY)* **10**, 190-195.
- Mermelstein, L. D. & Papoutsakis, E. T. (1993).** *In vivo* methylation in *Escherichia coli* by the *Bacillus subtilis* phage phi 3T I methyltransferase to protect plasmids from restriction upon transformation of *Clostridium acetobutylicum* ATCC 824. *Appl Environ Microbiol* **59**, 1077-1081.
- Merrell, D. S., Thompson, L. J., Kim, C. C., Mitchell, H., Tompkins, L. S., Lee, A. & Falkow, S. (2003).** Growth phase-dependent response of *Helicobacter pylori* to iron starvation. *Infect Immun* **71**, 6510-6525.
- Meyer CL, Roos JW, Papoutsakis ET. (1986).** Carbon monoxide gasing leads to alcohol production and butyrate uptake without acetone formation in continuous cultures of *Clostridium acetobutylicum*. *Appl Microbiol Biotechnol* **24**,159-167.
- Miethke, M. & Marahiel, M. A. (2007).** Siderophore-based iron acquisition and pathogen control. *Microbiol Mol Biol Rev* **71**, 413-451.
- Miller, J. H. (1972).** Assay of β -galactosidase, p. 319-353, Experiments in molecular genetics. Cold Spring Harbor Laboratory Press, Cold Spring Harbor, NY.
- Mills, S. A. & Marletta, M. A. (2005).** Metal binding characteristics and role of iron oxidation in the ferric uptake regulator from *Escherichia coli*. *Biochemistry* **44**, 13553-13559.
- Mironov, A. S., Gusarov, I., Rafikov, R., Lopez, L. E., Shatalin, K., Kreneva, R. A., Perumov, D. A. & Nudler, E. (2002).** Sensing small molecules by nascent RNA: a mechanism to control transcription in bacteria. *Cell* **111**, 747-756.
- Monot, F., Martin, J. R., Petitdemange, H. & Gay, R. (1982).** Acetone and butanol production by *Clostridium acetobutylicum* in a synthetic medium. *Appl Environ Microbiol* **44**, 1318-1324.
- Moore, C. M. & Helmann, J. D. (2005).** Metal ion homeostasis in *Bacillus subtilis*. *Curr Opin Microbiol* **8**, 188-195.
- Münch, R., Hiller, K., Barg, H., Heldt, D., Linz, S., Wingender, E. & Jahn, D. (2003).** PRODORIC: prokaryotic database of gene regulation. *Nucleic Acids Res* **31**, 266-269.

- Nandal, A., Huggins, C. C, Woodhall, M. R., McHugh, J., Rodriguez-Quinones, F., Quail, M. A., Guest, J. R. & Andrews, S. C. (2010). Induction of the ferritin gene (*ftnA*) of *Escherichia coli* by Fe²⁺-Fur is mediated by reversal of H-NS silencing and is RyhB independent. *Mol Microbiol* **75**, 637-657.
- Neilands, J. B. (1995). Siderophores: structure and function of microbial iron transport compounds. *J Biol Chem* **270**, 26723-26726.
- Ni, Y. & Sun, Z. (2009). Recent progress on industrial fermentative production of acetone-butanol-ethanol by *Clostridium acetobutylicum* in China. *Appl Microbiol Biotechnol* **83**, 415-423.
- Nölling, J., Breton, G., Omelchenko, M. V. & other authors (2001). Genome sequence and comparative analysis of the solvent-producing bacterium *Clostridium acetobutylicum*. *J Bacteriol* **183**, 4823-4838.
- O'Brien, R. W. & Morris, J. G. (1971). Oxygen and the growth and metabolism of *Clostridium acetobutylicum*. *J Gen Microbiol* **68**, 307-318.
- Oelmüller, U., Krüger N., Steinbüchel A., & Friedrich C. (1990). Isolation of prokaryotic RNA and detection of specific mRNA with biotinylated probes. *J Microbiol Meth* **11**: 73-81.
- Oglesby, A. G., Farrow, J. M., Lee, J. H., Tomaras, A. P., Greenberg, E. P., Pesci, E. C. & Vasil, M. L. (2008). The influence of iron on *Pseudomonas aeruginosa* physiology: a regulatory link between iron and quorum sensing. *J Biol Chem* **283**, 15558-15567.
- Ortiz de Orué Lucana, D. & Schrempf, H. (2000). The DNA-binding characteristics of the *Streptomyces reticuli* regulator FurS depend on the redox state of its cysteine residues. *Mol Gen Genet* **264**, 341-353.
- Outten, F. W., Djaman, O. & Storz, G. (2004). A *suf* operon requirement for Fe-S cluster assembly during iron starvation in *Escherichia coli*. *Mol Microbiol* **52**, 861-872.
- Parker, D., Kennan, R. M., Myers, G. S., Paulsen, I. T. & Rood, J. I. (2005). Identification of a *Dichelobacter nodosus* ferric uptake regulator and determination of its regulatory targets. *J Bacteriol* **187**, 366-375.
- Patzer, S. I. & Hantke, K. (1998). The ZnuABC high-affinity zinc uptake system and its regulator Zur in *Escherichia coli*. *Mol Microbiol* **28**, 1199-1210.
- Payne, S. M. (1994). Detection, isolation, and characterization of siderophores. *Methods Enzymol* **235**, 329-344.
- Peguin, S., Goma, G., Delorme, P. & Soucaille, P. (1994). Metabolic flexibility of *Clostridium acetobutylicum* in response to methyl viologen addition. *Appl Microbiol Biotechnol* **42**, 611-616
- Peguin, S. & Soucaille, P. (1995). Modulation of carbon and electron flow in *Clostridium acetobutylicum* by iron limitation and methyl viologen addition. *Appl Environ Microbiol* **61**, 403-405.
- Peguin, S. & Soucaille, P. (1996). Modulation of metabolism of *Clostridium acetobutylicum* grown in chemostat culture in a three-electrode potentiostatic system with methyl viologen as electron carrier. *Biotechnol and Bioeng* **51**, 342-348.

- Pennella, M. A. & Giedroc, D. P. (2005).** Structural determinants of metal selectivity in prokaryotic metal-responsive transcriptional regulators. *Biometals* **18**, 413-428.
- Perutka, J., Wang, W., Goerlitz, D. & Lambowitz, A. M. (2004).** Use of computer-designed group II introns to disrupt *Escherichia coli* DExH/D-box protein and DNA helicase genes. *J Mol Biol* **336**, 421-439.
- Petitdemange, H., Marczak, R. & Gay, R. (1979)** NADH-flavodoxin oxidoreductase activity in *Clostridium tyrobutyricum*. *FEMS Microbiol Lett* **5**, 291-294.
- Petterman, N., Schmidt, C. L., Wagner, A. K., Hogg, T., Hansen, G. & Hilgenfeld, R. (2009).** Structural basis for the intrinsic GTPase and GDI activities of FeoB. Poster. 17th Annual Meeting of the German Crystallographic Society, Hannover
- Pettersen, E. F., Goddard, T. D., Huang, C. C., Couch, G. S., Greenblatt, D. M., Meng, E. C. & Ferrin, T. E. (2004).** UCSF Chimera--a visualization system for exploratory research and analysis. *J Comput Chem* **25**, 1605-1612.
- Pich, O. Q., Carpenter, B. M., Gilbreath, J. J. & Merrell, D. S. (2012).** Detailed analysis of *Helicobacter pylori* Fur-regulated promoters reveals a Fur box core sequence and novel Fur-regulated genes. *Mol Microbiol* **84**, 921-941.
- Pohl, E., Haller, J. C., Mijovilovich, A., Meyer-Klaucke, W., Garman, E. & Vasil, M. L. (2003).** Architecture of a protein central to iron homeostasis: crystal structure and spectroscopic analysis of the ferric uptake regulator. *Mol Microbiol* **47**, 903-915.
- Powers, H. J. (1995).** Riboflavin-iron interactions with particular emphasis on the gastrointestinal tract. *Proc Nutr Soc* **54**, 509-517.
- Quatrini, R., Lefimil, C., Holmes, D. S. & Jedlicki, E. (2005).** The ferric iron uptake regulator (Fur) from the extreme acidophile *Acidithiobacillus ferrooxidans*. *Microbiology* **151**, 2005-2015.
- Ragsdale, S. W. & Ljungdahl, L. G. (1984).** Characterization of ferredoxin, flavodoxin, and rubredoxin from *Clostridium formicoaceticum* grown in media with high and low iron contents. *J Bacteriol* **157**, 1-6.
- Raleigh, E. A., Murray, N. E., Revel, H., Blumenthal, R. M., Westaway, D., Reith, A. D., Rigby, P. W., Elhai, J. & Hanahan, D. (1988).** McrA and McrB restriction phenotypes of some *E. coli* strains and implications for gene cloning. *Nucleic Acids Res* **16**, 1563-1575.
- Ranjan, S., Yellaboina, S. & Ranjan, A. (2006).** IdeR in mycobacteria: from target recognition to physiological function. *Crit Rev Microbiol* **32**, 69-75.
- Ratledge, C. & Dover, L. G. (2000).** Iron metabolism in pathogenic bacteria. *Annu Rev Microbiol* **54**, 881-941.
- Ratnayake-Lecamwasam, M., Serrero, P., Wong, K. W. & Sonenshein, A. L. (2001).** *Bacillus subtilis* CodY represses early-stationary-phase genes by sensing GTP levels. *Genes Dev* **15**, 1093-1103.

- Raux, E., Thermes, C., Heathcote, P., Rambach, A. & Warren, M. J. (1997).** A role for *Salmonella typhimurium* *cbiK* in cobalamin (vitamin B₁₂) and siroheme biosynthesis. *J Bacteriol* **179**, 3202-3212.
- Razquin, P., Schmitz, S., Fillat, M. F., Peleato, M. L. & Böhme, H. (1994).** Transcriptional and translational analysis of ferredoxin and flavodoxin under iron and nitrogen stress in *Anabaena* sp. strain PCC 7120. *J Bacteriol* **176**, 7409-7411.
- Riebe, O., Fischer, R. J. & Bahl, H. (2007).** Desulfoferredoxin of *Clostridium acetobutylicum* functions as a superoxide reductase. *FEBS Lett* **581**, 5605-5610.
- Riebe, O., Fischer, R. J., Wampler, D. A., Kurtz, D. M. & Bahl, H. (2009).** Pathway for H₂O₂ and O₂ detoxification in *Clostridium acetobutylicum*. *Microbiology* **155**, 16-24.
- Riebe, O. (2009).** Enzyme und Reaktionswege zur Abwehr reaktiver Sauerstoffspezies in *Clostridium acetobutylicum*. Dissertation. Universität Rostock.
- Riemer, J., Hoepken, H. H., Czerwinska, H., Robinson, S. R. & Dringen, R. (2004).** Colorimetric ferrozine-based assay for the quantitation of iron in cultured cells. *Anal Biochem* **331**, 370-375.
- Rodriguez, G. M. (2006).** Control of iron metabolism in *Mycobacterium tuberculosis*. *Trends Microbiol* **14**, 320-327.
- Sali, A. & Blundell, T. L. (1993).** Comparative protein modelling by satisfaction of spatial restraints. *J Mol Biol* **234**, 779-815.
- Sambrook, J. & Russell, D.W. (2001).** Molecular cloning: a laboratory Manual, 3rd ed. Cold Spring Harbor Laboratory Press, Cold Spring Harbor, NY, USA.
- Sandmann, G. & Malkin, R. (1983).** Iron-sulfur centers and activities of the photosynthetic electron transport chain in iron-deficient cultures of the blue-green alga *Aphanocapsa*. *Plant Physiol* **73**, 724-728.
- Sandmann, G., Luisa Peleato, M., Fillat, M. F., Carmen Lazaro, M. & Gomez-Moreno, C. (1990).** Consequences of the iron-dependent formation of ferredoxin and flavodoxin on photosynthesis and nitrogen fixation on *Anabaena* strains. *Photosynth Res* **26**, 119-125.
- Schröder, I., Johnson, E. & de Vries, S. (2003).** Microbial ferric iron reductases. *FEMS Microbiol Rev* **27**, 427-447.
- Schulz, F. (2013).** Fluoreszenzproteine in *Clostridium acetobutylicum* - Ein neues *in vivo* Reportersystem. Dissertation. Universität Rostock.
- Schwarz, K., Fiedler, T., Fischer, R. J. & Bahl, H. (2007).** A Standard Operating Procedure (SOP) for the preparation of intra- and extracellular proteins of *Clostridium acetobutylicum* for proteome analysis. *J Microbiol Methods* **68**, 396-402.
- Schwyn, B. & Neilands, J. B. (1987).** Universal chemical assay for the detection and determination of siderophores. *Anal Biochem* **160**, 47-56.

- Schönheit, P., Brandis, A. & Thauer, R. K. (1979).** Ferredoxin degradation in growing *Clostridium pasteurianum* during periods of iron deprivation. *Arch Microbiol* **120**, 73-76.
- Sebastian, S., Agarwal, S., Murphy, J. R. & Genco, C. A. (2002).** The gonococcal Fur regulon: identification of additional genes involved in major catabolic, recombination, and secretory pathways. *J Bacteriol* **184**, 3965-3974.
- Seedorf, H., Fricke, W. F., Veith, B. & other authors (2008).** The genome of *Clostridium kluyveri*, a strict anaerobe with unique metabolic features. *Proc Natl Acad Sci USA* **105**, 2128-2133.
- Sheikh, M. A. & Taylor, G. L. (2009).** Crystal structure of the *Vibrio cholerae* ferric uptake regulator (Fur) reveals insights into metal co-ordination. *Mol Microbiol* **72**, 1208-1220.
- Shin, J. H., Jung, H. J., An, Y. J., Cho, Y. B., Cha, S. S. & Roe, J. H. (2011).** Graded expression of zinc-responsive genes through two regulatory zinc-binding sites in Zur. *Proc Natl Acad Sci USA* **108**, 5045-5050.
- Sievers, F., Wilm, A., Dineen, D. & other authors (2011).** Fast, scalable generation of high-quality protein multiple sequence alignments using Clustal Omega. *Mol Syst Biol* **7**, 539.
- Smaldone, G. T., Antelmann, H., Gaballa, A. & Helmann, J. D. (2012a).** The FsrA sRNA and FbpB protein mediate the iron-dependent induction of the *Bacillus subtilis* LutABC iron-sulfur-containing oxidases. *J Bacteriol* **194**, 2586-2593.
- Smaldone, G. T., Revelles, O., Gaballa, A., Sauer, U., Antelmann, H. & Helmann, J. D. (2012b).** A global investigation of the *Bacillus subtilis* iron-sparing response identifies major changes in metabolism. *J Bacteriol* **194**, 2594-2605.
- Stillman, T. J., Hempstead, P. D., Artymiuk, P. J., Andrews, S. C., Hudson, A. J., Treffry, A., Guest, J. R., and Harrison, P. M. (2001).** The high-resolution x-ray crystallographic structure of the ferritin (EcFtnA) of *Escherichia coli*; comparison with human H ferritin (HuHF) and the structures of the Fe³⁺ and Zn²⁺ derivatives. *J Mol Biol* **307**, 587-603.
- Stojiljkovic, I., Bäumlner, A. J. & Hantke, K. (1994).** Fur regulon in gram-negative bacteria. Identification and characterization of new iron-regulated *Escherichia coli* genes by a Fur titration assay. *J Mol Biol* **236**, 531-545.
- Stojiljkovic, I. & Hantke, K. (1995).** Functional domains of the *Escherichia coli* ferric uptake regulator protein (Fur). *Mol Gen Genet* **247**, 199-205.
- Susín, S., Abián, J., Sánchez-Baeza, F., Peleato, M. L., Abadía, A., Gelpí, E. & Abadía, J. (1993).** Riboflavin 3'- and 5'-sulfate, two novel flavins accumulating in the roots of iron-deficient sugar beet (*Beta vulgaris*). *J Biol Chem* **268**, 20958-20965.
- Tatusov, R. L., Galperin, M. Y., Natale, D. A. & Koonin, E. V. (2000).** The COG database: a tool for genome-scale analysis of protein functions and evolution. *Nucleic Acids Res* **28**, 33-36.
- Touati, D., Jacques, M., Tardat, B., Bouchard, L. & Despied, S. (1995).** Lethal oxidative damage and mutagenesis are generated by iron in delta *fur* mutants of *Escherichia coli*: protective role of superoxide dismutase. *J Bacteriol* **177**, 2305-2314.

- Touati, D. (2000).** Iron and oxidative stress in bacteria. *Arch Biochem Biophys* **373**, 1-6.
- Traoré, D. A., El Ghazouani, A., Ilango, S., Dupuy, J., Jacquamet, L., Ferrer, J. L., Caux-Thang, C., Duarte, V. & Latour, J. M. (2006).** Crystal structure of the apo-PerR-Zn protein from *Bacillus subtilis*. *Mol Microbiol* **61**, 1211-1219.
- Vasconcelos, I., Girbal, L. & Soucaille, P. (1994).** Regulation of carbon and electron flow in *Clostridium acetobutylicum* grown in chemostat culture at neutral pH on mixtures of glucose and glycerol. *J Bacteriol* **176**, 1443-1450.
- Vasileva, D., Janssen, H., Hönicke, D., Ehrenreich, A. & Bahl, H. (2012).** Effect of iron limitation and *fur* gene inactivation on the transcriptional profile of the strict anaerobe *Clostridium acetobutylicum*. *Microbiology* **158**, 1918-1929.
- Vitreschak, A. G., Rodionov, D. A., Mironov, A. A. & Gelfand, M. S. (2004).** Riboswitches: the oldest mechanism for the regulation of gene expression? *Trends Genet* **20**, 44-50.
- Vorwieger, A., Gryczka, C., Czihal, A. & other authors (2007).** Iron assimilation and transcription factor controlled synthesis of riboflavin in plants. *Planta* **226**, 147-158.
- Waldron, K. J., Rutherford, J. C., Ford, D. & Robinson, N. J. (2009).** Metalloproteins and metal sensing. *Nature* **460**, 823-830.
- Wandersman, C. & Delepelaire, P. (2004).** Bacterial iron sources: from siderophores to hemophores. *Annu Rev Microbiol* **58**, 611-647.
- Wang, F., Cheng, S., Sun, K. & Sun, L. (2008).** Molecular analysis of the *fur* (ferric uptake regulator) gene of a pathogenic *Edwardsiella tarda* strain. *J Microbiol* **46**, 350-355.
- Weng, M., Nagy, P. L. & Zalkin, H. (1995).** Identification of the *Bacillus subtilis pur* operon repressor. *Proc Natl Acad Sci USA* **92**, 7455-7459.
- Wennerhold, J. & Bott, M. (2006).** The DtxR regulon of *Corynebacterium glutamicum*. *J Bacteriol* **188**, 2907-2918.
- Wexler, M., Todd, J. D., Kolade, O., Bellini, D., Hemmings, A. M., Sawers, G. & Johnston, A. W. (2003).** Fur is not the global regulator of iron uptake genes in *Rhizobium leguminosarum*. *Microbiology* **149**, 1357-1365.
- Wiesenborn, D. P., Rudolph, F. B. & Papoutsakis, E. T. (1988).** Thiolasase from *Clostridium acetobutylicum* ATCC 824 and its role in the synthesis of acids and solvents. *Appl Environ Microbiol* **54**, 2717-2722.
- Wietzke, M. & Bahl, H. (2012).** The redox-sensing protein Rex, a transcriptional regulator of solventogenesis in *Clostridium acetobutylicum*. *Appl Microbiol Biotechnol* **96**, 749-761.
- Wietzke, M. (2013).** Der Redoxsensor Rex- Ein Transkriptionsregulator der Lösungsmittelbildung in *Clostridium acetobutylicum*. Dissertation. Universität Rostock.

- Wilderman, P. J., Sowa, N. A., FitzGerald, D. J., FitzGerald, P. C., Gottesman, S., Ochsner, U. A., & Vasil, M. L. (2004).** Identification of tandem duplicate regulatory small RNAs in *Pseudomonas aeruginosa* involved in iron homeostasis. *Proc Natl Acad Sci USA* **101**, 9792-9797.
- Williams, R. J. P. (2001).** Chemical selection of elements by cells. *Coord Chem Rev* **216-217**, 583-595.
- Winkelmann, G. (2007).** Ecology of siderophores with special reference to the fungi. *Biometals* **20**, 379-392.
- Worst, D. J., Gerrits, M. M., Vandenbroucke-Grauls, C. M. & Kusters, J. G. (1998).** *Helicobacter pylori* *ribBA*-mediated riboflavin production is involved in iron acquisition. *J Bacteriol* **180**, 1473-1479.
- Xiong, A., Singh, V. K., Cabrera, G. & Jayaswal, R. K. (2000).** Molecular characterization of the ferric-uptake regulator, Fur, from *Staphylococcus aureus*. *Microbiology* **146**, 659-668.
- Yang, Y., Harris, D. P., Luo, F., Wu, L., Parsons, A. B., Palumbo, A. V. & Zhou, J. (2008).** Characterization of the *Shewanella oneidensis* *fur* gene: roles in iron and acid tolerance response. *BMC Genomics* **9 Suppl 1**, S11.
- Yu, C. & Genco, C. A. (2012).** Fur-mediated activation of gene transcription in the human pathogen *Neisseria gonorrhoeae*. *J Bacteriol* **194**, 1730-1742.
- Zheng, L., Cash, V. L., Flint, D. H. & Dean, D. R. (1998).** Assembly of iron-sulfur clusters. Identification of an *iscSUA-hscBA-fdx* gene cluster from *Azotobacter vinelandii*. *J Biol Chem* **273**, 13264-13272.
- Zheng, M., Wang, X., Templeton, L. J., Smulski, D. R., LaRossa, R. A. & Storz, G. (2001).** DNA microarray-mediated transcriptional profiling of the *Escherichia coli* response to hydrogen peroxide. *J Bacteriol* **183**, 4562-4570.
- Zhu, Y., Kumar, S., Menon, A. L., Scott, R. A. & Adams, M. W. (2013).** Regulation of iron metabolism by *Pyrococcus furiosus*. *J Bacteriol* **195**, 2400-2407.

7 Appendix

Table 7.1 Bacterial strains

Strain	Relevant characteristics	Reference or source
<i>E. coli</i> DH5 α	<i>supE44</i> , Δ <i>lacU169</i> , <i>hsdR17</i> , (ϕ 80 <i>lacZ</i> Δ M15), <i>recA1</i> , <i>endA1</i> , <i>gyrA96</i> , <i>thi-1</i> , <i>relA1</i>	Hanahan, 1983/ Strain collection Nr. 272
<i>E. coli</i> ER2275 pAN-II	<i>trp-31</i> , <i>his-1</i> , <i>tonA2</i> , <i>rpsL104</i> , <i>supE44</i> , <i>xyl-7</i> , <i>mtl-2</i> , <i>metB1</i> , <i>el4</i> , Δ (<i>lac</i>)U169, <i>endA1</i> , <i>recA1</i> , R(zbgZ10::Tn10) <i>Tc</i> ^s , Δ (<i>mcr-hsd-mrr</i>)114::1510, [F', <i>proAB</i> , <i>laqI</i> ^q Z Δ M15 <i>zsd</i> ::mini Tn10(Kan ^r)]	NEB, New England Biolabs/ Strain collection Nr. 271
<i>E. coli</i> RR1	K12 RR1, Δ M15: <i>leu</i> , <i>pro</i> , <i>thi</i> , <i>strA</i> , <i>hsd</i> , r ⁻ , m ⁻ , <i>lacZ</i> Δ M15, F', <i>lac I Q Z</i> Δ M15, <i>pro</i> ⁺	Raleigh <i>et al.</i> , 1988/ Strain collection Nr. 806
<i>E. coli</i> BL21	F', <i>ompT hsdSB</i> (rB ⁻ , mB ⁻), <i>gal dcm</i> , <i>rne131</i>	Novagen
<i>E. coli</i> BL21-DE3 (pLys)	F- <i>ompT hsdSB</i> (rB ⁻ , mB ⁻) <i>gal dcm</i> (DE3)	Novagen
<i>E. coli</i> BL21 pT:: <i>cac0951</i>	pT:: <i>cac0951</i> (Amp ^r , Erm ^r)	This study/ Strain collection Nr. 432
<i>E. coli</i> BL21-DE3 (pLys) pET-30a:: <i>cac1682</i> (<i>fur</i>)	pET-30a:: <i>cac1682</i> (<i>fur</i>) (Kan ^r , Cam ^r)	This study/ Strain collection Nr. 433
<i>E. coli</i> H1780	<i>araD139</i> , Δ ^a <i>argF-lacU169</i> , <i>rpsL150</i> , <i>relA1</i> , <i>flbB5301</i> , <i>deoC1</i> , <i>ptsF25</i> , <i>rbsR</i> , <i>fnuF</i> :: λ <i>placMu</i> , <i>fur</i> :: <i>kan</i> , Sm ^r , Kan ^r	Hantke, 1987/ Strain collection Nr. 434
<i>E. coli</i> H1780 pTCatP	pTCatP vector without an insert (Amp ^r , Cam ^r)	This study/ Strain collection Nr. 435
<i>E. coli</i> H1780 pTCatP:: <i>cac1682</i> (<i>fur</i>)	pTCatP:: <i>cac1682</i> (Amp ^r , Cam ^r)	This study/ Strain collection Nr. 436
<i>E. coli</i> H1780 pTCatP:: <i>cac0951</i>	pTCatP:: <i>cac0951</i> (Amp ^r , Cam ^r)	This study/ Strain collection Nr. 437
<i>E. coli</i> H1717	<i>araD139</i> , Δ ^a <i>argF-lacU169</i> , <i>rpsL150</i> , <i>relA1</i> , <i>flbB5301</i> , <i>deoC1</i> , <i>ptsF25</i> , <i>rbsR</i> , <i>fnuF</i> :: λ <i>placMu</i> , Sm ^r , Kan ^r	Hantke, 1987; Stojiljkovic <i>et al.</i> , 1994/ Strain collection Nr. 438
<i>B. subtilis</i> HB1000	ZB307A <i>attSPb</i>	Chen <i>et al.</i> , 1993/ Strain collection Nr. 92

<i>B. subtilis</i> HB6543	HB1000 <i>fur::kan</i>	Bsat <i>et al.</i> , 1998/ Strain collection Nr. 94
<i>B. subtilis</i> HB6543 pTCatP	pTCatP vector without an insert (Amp ^r , Cam ^r)	This study/ Strain collection Nr. 439
<i>B. subtilis</i> HB6543 pTCatP:: <i>cac1682 (fur)</i>	pTCatP:: <i>cac1682 (fur)</i> (Amp ^r , Cam ^r)	This study/ Strain collection Nr. 440
<i>B. subtilis</i> HB6543 pTCatP:: <i>cac0951</i>	pTCatP:: <i>cac0951</i> (Amp ^r , Cam ^r)	This study/ Strain collection Nr. 441
<i>C. acetobutylicum</i> ATCC 824	Wild-type	Strain collection
<i>C. acetobutylicum</i> <i>fur::int</i> (271a)	Derivative of the wild-type, <i>fur</i> insertional mutant (Erm ^r)	This study/ Strain collection Nr. 442
<i>C. acetobutylicum</i> <i>fur::int</i> (271a) pTCatP	<i>fur</i> mutant, pTCatP (Erm ^r , Tm ^r)	This study/ Strain collection Nr. 443
<i>C. acetobutylicum</i> <i>fur::int</i> (271a) pTCatP:: <i>fur</i>	<i>fur</i> mutant, pTCatP:: <i>fur</i> (Erm ^r , Tm ^r)	This study/ Strain collection Nr. 444
<i>C. acetobutylicum</i> <i>fur::int</i> (271a) pMTL85141	<i>fur</i> mutant, pMTL85141 (Erm ^r , Tm ^r)	This study/ Strain collection Nr. 445
<i>C. acetobutylicum</i> <i>fur::int</i> (271a) pMTL85141:: <i>fur</i>	<i>fur</i> mutant, pMTL85141:: <i>fur</i> (Erm ^r , Tm ^r)	This study/ Strain collection Nr. 446
<i>C. acetobutylicum</i> <i>cac0587::int</i> (150s)	Derivative of the wild-type, <i>cac0587</i> insertional mutant (Erm ^r)	This study/ Strain collection Nr. 447

Table 7.2 Vectors

Plasmid vector	Relevant characteristics	Reference or source
pMTL007	Group II intron retargeting region-encoding plasmid, Cam ^r	Heap <i>et al.</i> , 2007/ Strain collection Nr. 19
pMTL007C-E2	<i>ltrA</i> , L1. <i>ltrB</i> -Intron, ColE1 ori, Cam ^r	Heap <i>et al.</i> 2010/ Strain collection Nr. 20
pAN-II	Tc ^r , $\Phi 3tI$; p15A oriR	Heap <i>et al.</i> 2007/ Strain collection Nr. 271
pT:: <i>hydA</i>	P _{<i>thlA</i>} , <i>hydA</i> , <i>Strep</i> -Tag II, Amp ^r , Erm ^r , <i>repL</i> , ColE1 ori	Girbal <i>et al.</i> , 2005/ Strain collection Nr. 22

pTCatP:: <i>hydA</i>	Derivative of pT, (Amp ^r , Cam ^r)	Girbal <i>et al.</i> , 2005, mod./ Strain collection Nr. 397
pTCatP	Derivative of pT, without insert (Amp ^r , Cam ^r)	Girbal <i>et al.</i> , 2005, mod.
pET-30a Xa/LIC	T7 promoter, T7 terminator, N-terminal His•Tag and S•Tag, an optional C-terminal S•Tag, pBR322 ori, fl ori, <i>lacI</i> , Kan ^r , ligation-independent cloning	Novagen
pMTL85141	pIM13, <i>catP</i> , ColE1, MCS	Heap <i>et al.</i> , 2009/ Strain collection Nr. 150

Table 7.3 Recombinant plasmids

Plasmid	Relevant characteristics	Insert size	Source
pMTL007C-E2:: <i>fur</i>	pMTL007C-E2 retargeted for <i>fur</i> gene disruption, <i>HindIII</i> / <i>Bsp1407I</i> (<i>BsrGI</i>)	350 bp	This study/ Strain collection Nr. 448
pMTL007C-E2:: <i>cac0587</i>	pMTL007C-E2 retargeted for <i>cac0587</i> gene disruption, <i>HindIII</i> / <i>Bsp1407I</i> (<i>BsrGI</i>)	350 bp	This study/ Strain collection Nr. 449
pT:: <i>cac0951</i>	pT, <i>cac0951</i> gene, <i>BamHI</i> / <i>Cfr9I</i> (<i>XmaI</i>)	432 bp	This study/ Strain collection Nr. 450
pTCatP:: <i>cac0951</i>	pTCatP, <i>cac0951</i> gene, <i>BamHI</i> / <i>Cfr9I</i> (<i>XmaI</i>)	432 bp	This study/ Strain collection Nr. 451
pTCatP:: <i>cac1682 (fur)</i>	pTCatP, <i>fur</i> gene, <i>BamHI</i> / <i>Cfr9I</i> (<i>XmaI</i>)	456 bp	This study/ Strain collection Nr. 452
pET-30a:: <i>cac1682 (fur)</i>	pET-30a, <i>fur</i> gene, ligation- independent cloning	456 bp	This study/ Strain collection Nr. 453
pMTL85141:: <i>fur</i>	pMTL85141, <i>fur</i> gene and promoter region (- 500 to + 456 relative to the translational start site), <i>Cfr9I</i> (<i>XmaI</i>)/ <i>NcoI</i>	956 bp	This study/ Strain collection Nr. 454

Table 7.4 Oligonucleotides

Primer name	5' → 3' Sequence *	Restriction site	Used for
EBS Universal	CGAAATTAGAACTTGC GTTCAGTAAAC	-	Intron specific primer Clostron
IBS_ <i>fur</i> _271a	AAAAAAGCTTATAATTATCCTTACATTTCCGTG CAGTGCGCCAGATAGGGTG	<i>HindIII</i>	<i>fur</i> -specific primer Clostron
EBS1d_ <i>fur</i> _271a	CAGATTGTACA AATGTGGTGATAACAGATAAG TCCGTGCACCTAACTTACCTTCTTTGT	<i>Bsp1407I</i> (<i>BsrGI</i>)	<i>fur</i> -specific primer Clostron

EBS2_fur_271a	TGAACGCAAGTTTCTAATTCGGTTAAATGTCTG ATAGAGGAAAGTGTCT	-	<i>fur</i> -specific primer Clostron
IBS_cac0587_150s	AAAA AAGCTT TATAATTATCCTTAAAAAACGCG GATGTGCGCCAGATAGGGTG	<i>Hind</i> III	<i>cac0587</i> -specific primer Clostron
EBS1d_cac0587_150s	CAGAT TGTACA AATGTGGTGATAACAGATAAG TCGCGGATGTAACTTACCTTTCTTTGT	<i>Bsp</i> 1407I (<i>Bsr</i> GI)	<i>cac0587</i> -specific primer Clostron
EBS2_cac0587_150s	TGAACGCAAGTTTCTAATTCGGTTTTTTTCCG ATAGAGGAAAGTGTCT	-	<i>cac0587</i> -specific primer Clostron
fur_verif_fw	ATGGCAAAATTATCTCCTTTAG	-	Verification of <i>fur</i> mutation
fur_verif_rev	TTATAGTTTTTTTCTACATTCCTGC	-	Verification of <i>fur</i> mutation
ErmRAM_fw	ACGCGTTATATTGATAAAAATAATAATAGTGG G	-	Southern blot
ErmRAM_rev	ACGCGTGC GACTCATAGAATTATTCCTCCCG	-	Southern blot
fur_prom_XmaI_fw	TTTTT CCCGGG ACATAAATGTACCATAAAGAT GTGGG	<i>Cfr</i> 9I (<i>Xma</i> I)	Complementation
fur_prom_NcoI_rev	TTTTT CCATGG TTATAGTTTTTTTCTACATTCAC TGCATATTCC	<i>Nco</i> I	Complementation
cac1682_pET30a_fw	GGTATTGAGGGTCGCATGGCAAAATTATCTCCT TTAGAAATAG	-	Overexpression
cac1682_pET30a_rev	AGAGGAGAGTTAGAGCCTAGTTTTTTTCTACAT TCACTGCATATTC	-	Overexpression
cac0951_BamHI_fw	TTTTT GGATCC ATGGATTTGAAAACGTACG	<i>Bam</i> HI	Overexpression/ Complementation
cac0951_XmaI_rev	TTTTT CCCGGG AGAATTCCTTTTCATTGTTTA	<i>Cfr</i> 9I (<i>Xma</i> I)	Overexpression/ Complementation
fur_BamHI_fw	TTTTT GGATCC ATGGCAAAATTATCTCCTTTAG	<i>Bam</i> HI	Complementation
fur_XmaI_rev	TTTTT CCCGGG TAGTTTTTTTCTACATTCCTGC	<i>Cfr</i> 9I (<i>Xma</i> I)	Complementation
pT_seq_fw	GGGATAAACTATGGAACCTATGAAA	-	Sequencing
pT_seq_rev	TGCAAGAATGTGAGAGCTAGAAA	-	Sequencing
cac0590_fw_NB	AATTGCAGAAAAGGGGAGTG	-	Northern blot
cac0590_rev_NB	TCCCCTATTTAGGTATCTGACA	-	Northern blot
cac0587_fw_rt	ATGGTGAAAATAAACATAATTTATTGCTCAG	-	sqRT-PCR
cac0587_rev_rt	CTAGCTATTTATAAGAGCCTTACCAAATC	-	sqRT-PCR
cac1029_fw_rt	CAAAAGGTATAGGTCTTAATGAAGTTG	-	sqRT-PCR
cac1029_rev_rt	CCTTAGCTTCACTTTTTCTTAAACTCA	-	sqRT-PCR
cac0791_fw_rt	ATGACTAGGTTATATACTGACATGCTTAA	-	sqRT-PCR
cac0791_rev_rt	TTACTTCATCTCCTTGATTAAGTTGTATG	-	sqRT-PCR
cac2877_fw_rt	GGAACAGGAAAAAGCACCTT	-	sqRT-PCR
cac2877_rev_rt	GCAAAGAGCCACTTTCTCCA	-	sqRT-PCR

Eub1 (fw)	GAGTTTGATCCTGGCTCAG	-	16S rRNA Northern blot/sqRT-PCR control
Eub2 (rev)	AGAAAGGAGGTGATCCAGCC	-	16S rRNA Northern blot/sqRT-PCR control
cac0267_SP1	AGACTTTGGAAAACCTGAAAGTTTATG	-	5' RACE
cac0267_SP2	CTTGTCTCACCTGGTTTCTG	-	5' RACE
cac0267_SP3	CTACTATAACTATCTCAGATGCAA	-	5' RACE
cac0567_SP1	CTCACTTGCCCATCTAACACAATC	-	5' RACE
cac0567_SP2	ATTTTATCTAGTCCCCAACCTG	-	5' RACE
cac0567_SP3	CTACAACCTTCCCTTGATCTC	-	5' RACE
cac0587_SP1	CTAGCTATTTATAAGAGCCTTACCAAA	-	5' RACE
cac0587_SP2	CCGTATGAACCAATAGAGCTACTTT	-	5' RACE
cac0587_SP3	CTTCTAATACCTCATCACCCATTG	-	5' RACE
cac0791_SP1	TCGGCTACAGTTATTCCATCTG	-	5' RACE
cac0791_SP2	CCAGTTTTAGTTGGAATTATACGA	-	5' RACE
cac0791_SP3	CAATCAAATTATTGTCATAAGCGAC	-	5' RACE
cac1029_SP1	CTAAGTGCTATTGGATCACCCATA	-	5' RACE
cac1029_SP2	CAATTCCAATAACTTTAACCTTTGA	-	5' RACE
cac1478_SP1	CTAGATTGTCCAACCTTCTTTCAAGAC	-	5' RACE
cac1478_SP2	CTTTCCAACAGCTGTTCCACCATAC	-	5' RACE
cac1478_SP3	ATTAACCCCCAAATGTCTTGCTAATTT	-	5' RACE
cac1602_SP1	CCTGGAGCTGATCCTCCATA	-	5' RACE
cac1602_SP2	CCAATACTAGAACTAAATCTAAATTT	-	5' RACE
cac1602_SP3	CCTAATTTATCTCCACCTATAAGCA	-	5' RACE

* Red letters indicate the corresponding restriction sites.

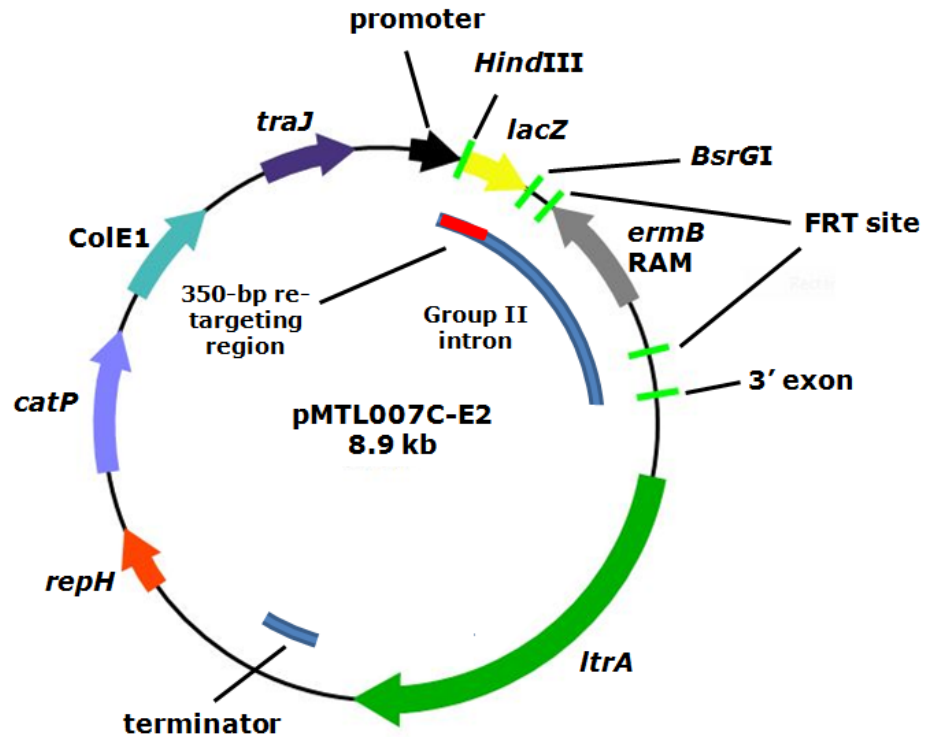
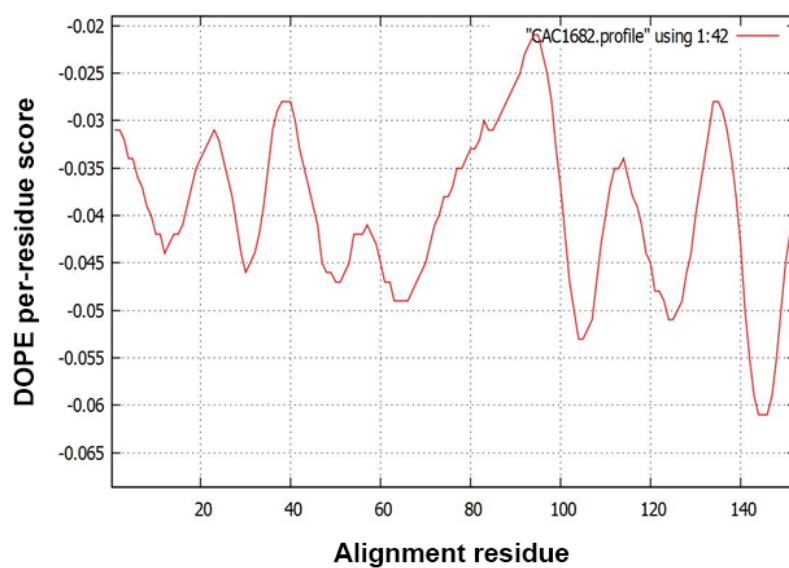


Fig. 7.1 pMTL007C-E2 vector map (Heap *et al.*, 2010). pMTL007C-E2 is a second generation Clostron[®] modular plasmid vector, which carries a derivative of the L1.LtrB intron from *Lactococcus lactis*, designed for disruption of target genes in *C. acetobutylicum*. The plasmid harbours an origin for replication for Gram-positive bacteria (*repH* from pIM13) and an origin for replication in *E. coli* (ColE1). A 350-bp intron re-targeting region is modified appropriately via a SOE PCR (2.8.2.3) and cloned into the *HindIII* and *BsrGI* sites of the vector. The presence of *lacZα* ORF facilitates the identification of positive clones through blue-white screening on medium supplemented with X-Gal. Expression of the intron in *C. acetobutylicum* is directed by a constitutive promoter from the *fdx* gene of *Clostridium sporogenes*. The FRT (flippase recognition target) sites allow for removal of the *ermB* selective marker, if necessary.

A)



B)

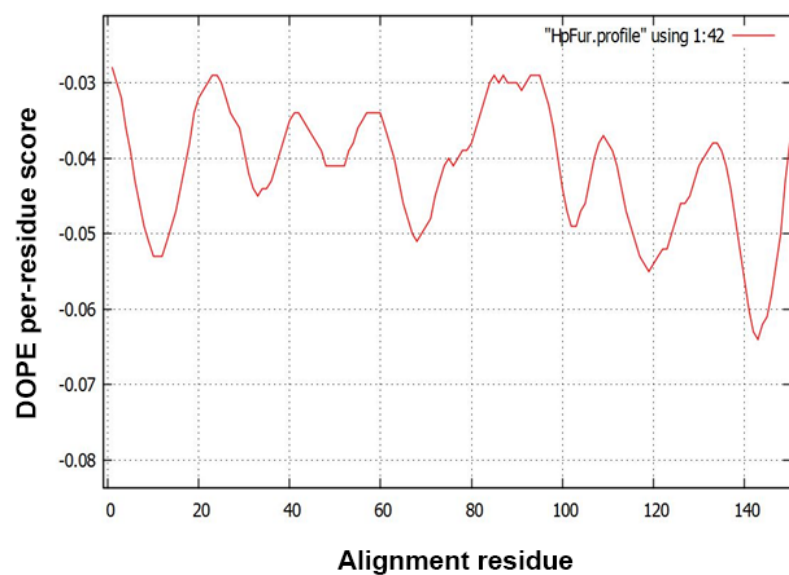


Fig. 7.2 DOPE score profiles for the predicted CAC1682 3D structure (A) and the HpFur template (B) (pdb: 2xig; Dian *et al.*, 2011). (A) and (B) represent pseudo-energy plots, which confirm that the CAC1682 homology model is reasonable. The model was generated using the Modeller program (Sali and Blundell, 1993) and the plot was visualized using the Python-based Gnuplot graphing utility (<http://www.gnuplot.info/>).

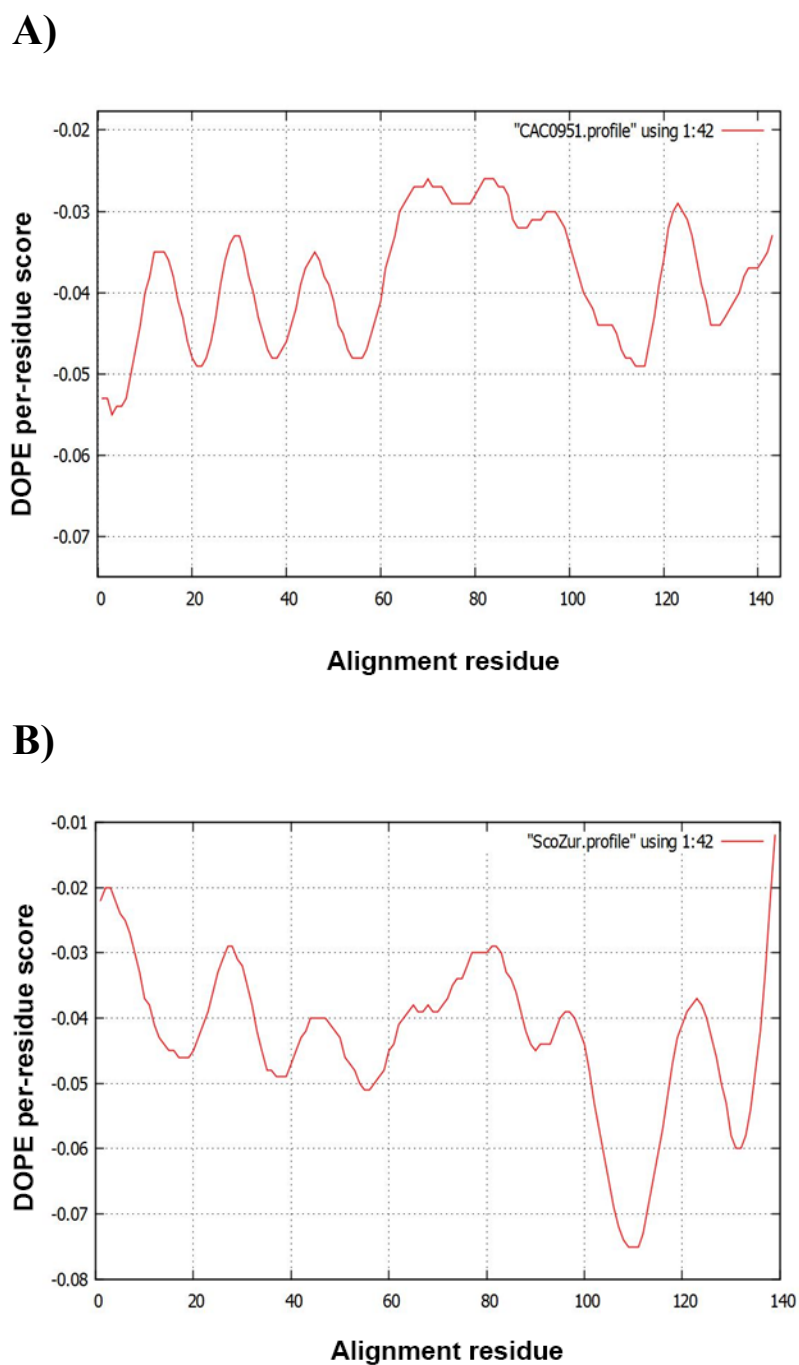


Fig. 7.3 DOPE score profiles for the CAC0951 predicted 3D structure (A) and the ScoZur template (B) (pdb: 2mwm; Shin *et al.*, 2011). (A) and (B) represent pseudo-energy plots, which confirm that the CAC0951 homology model is reasonable. The model was generated using the Modeller program (Sali and Blundell, 1993) and the plot was visualized using the Python-based Gnuplot graphing utility (<http://www.gnuplot.info/>).

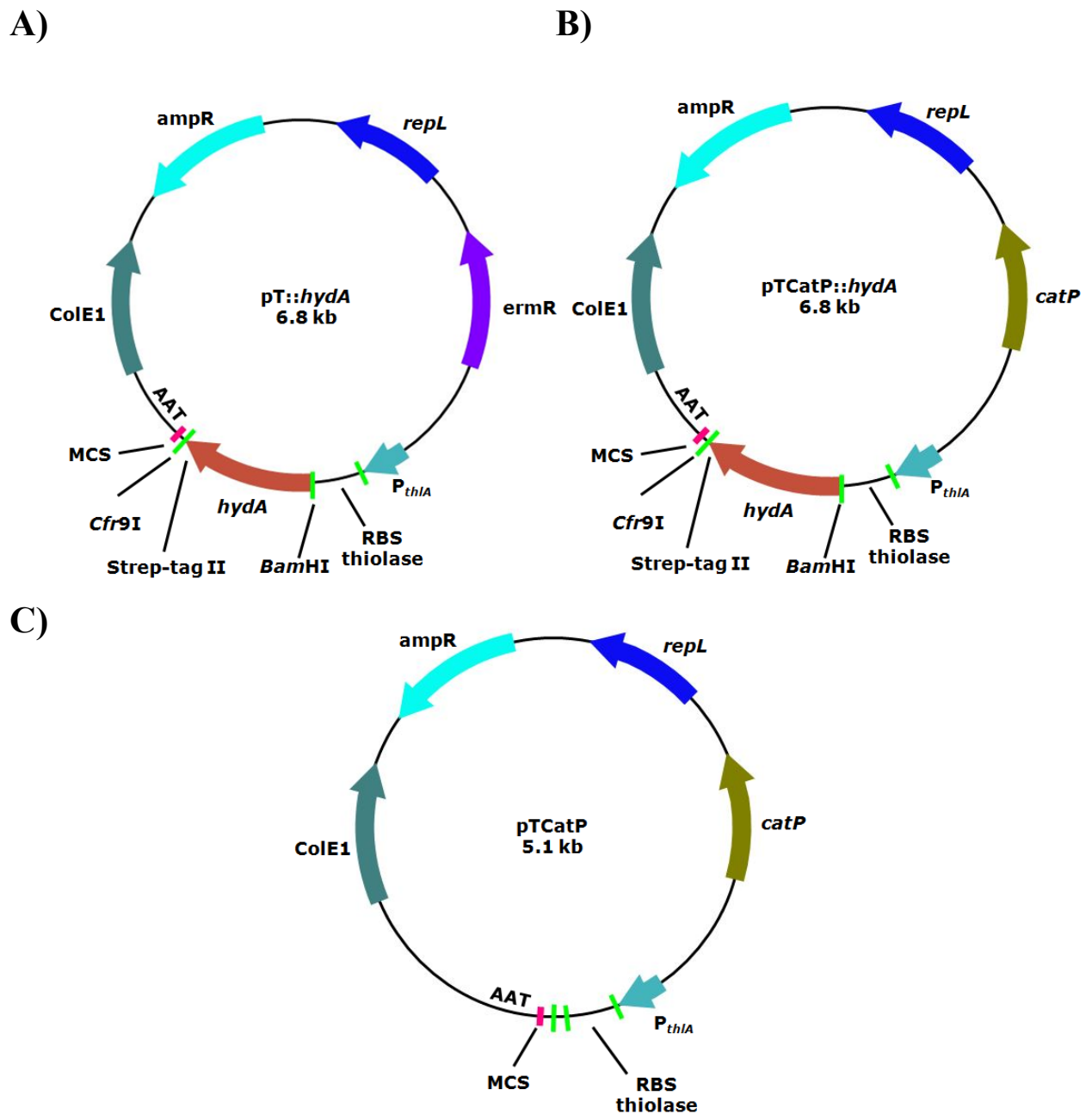


Fig. 7.4 Schematic representation of the pT vector system (Girbal *et al.*, 2005 mod.). (A) The pT vector is a plasmid designed for expression of C-terminal *Strep*-tag II fusion proteins under control of the RBS (ribosome binding site) and promoter (P_{thIA}) of the thiolase-encoding gene from *C. acetobutylicum*. The plasmid carries an origin of replication for Gram-positive bacteria (*repL* from pIM13) and an origin of replication for *E. coli* (ColE1). The pT plasmid employed in this study harbours the clostridial *hydA* gene, which has been replaced by the genes of interest. (B) Schematic representation of the modified pT vector system, designated in this work as pTCatP. The erythromycin resistance determinant was replaced by a chloramphenicol/thiamphenicol resistance gene, which makes the system suitable for complementation studies in the erythromycin resistant Clostron[®] insertional mutants. (C) pTCatP vector without insert used as a negative control.

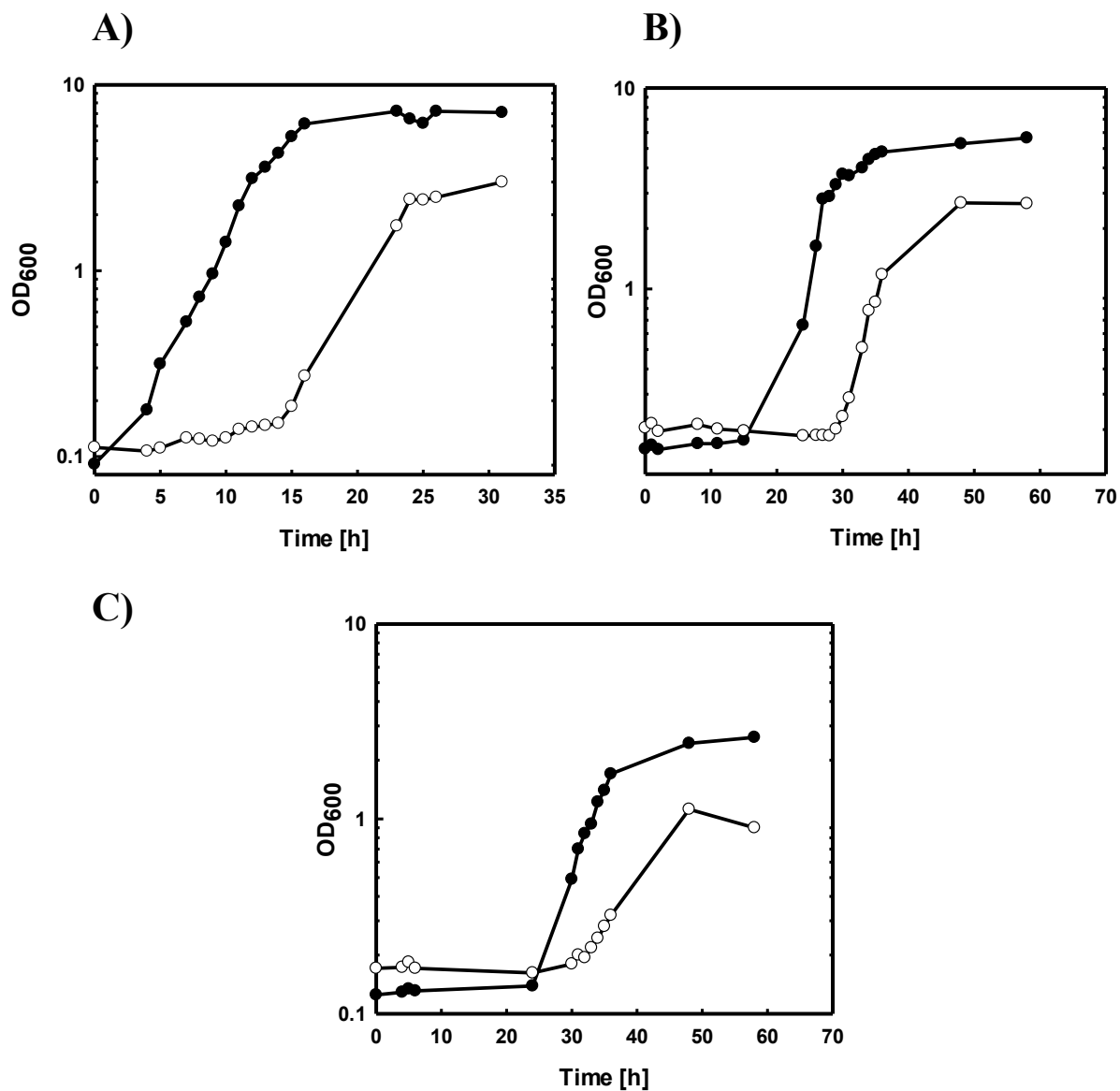


Fig. 7.5 Effect of absence of Fur on the growth profile of *C. acetobutylicum* under iron-limiting conditions. *C. acetobutylicum* wild-type and *fur* mutant were grown in 200 ml CGM medium supplemented with the cell-wall permeable iron chelator 2,2'-dipyridyl (Sigma Aldrich) at concentrations of 100 μM (A), 150 μM (B) and 200 μM (C). The results were obtained from three independent experiments (n=3).

Table 7.5 List of genes, exclusively regulated in *C. acetobutylicum* wild-type strain grown under iron limitation.

ID#	Expressionratio	SD*	COG	Protein function
CAP0155	0.31	0.05	X	hypothetical protein
CAP0160	0.19	0.06	N	cell-adhesion domain-containing protein
CAP0162	7.00	3.26	C	aldehyde/alcohol dehydrogenase
CAP0163	6.51	4.82	I	butyrate-acetoacetate CoA-transferase subunit A
CAP0164	5.71	2.99	I	butyrate-acetoacetate CoA-transferase subunit B
CAP0168	0.18	0.04	G	Alpha-amylase
CAC0056	0.23	0.07	X	hypothetical protein
CAC0057	0.20	0.08	X	hypothetical protein
CAC0058	0.24	0.09	X	hypothetical protein
CAC0059	0.23	0.02	X	hypothetical protein
CAC0060	0.28	0.07	X	predicted membrane protein
CAC0061	0.30	0.05	X	Phage-related protein, gp16
CAC0062	0.28	0.07	S	Phage-related protein
CAC0063	0.29	0.07	S	Phage-related protein
CAC0106	4.54	2.24	P	sulfate ABC transporter periplasmic-binding protein
CAC0107	6.84	3.31	P	ABC-type sulfate transporter, ATPase component
CAC0108	7.21	1.78	P	sulfate ABC transporter permease
CAC0110	6.21	5.30	P	GTPase, sulfate adenylate transferase subunit 1
CAC0149	0.12	0.05	X	Xre family DNA-binding domain-/TPR repeat-containing protein
CAC0175	0.20	0.12	R	N-acetylmuramic acid-6-phosphate etherase
CAC0176	0.17	0.07	E	oligopeptide-binding protein, periplasmic component
CAC0177	0.18	0.04	E,P	oligopeptide transport permease
CAC0231	0.08	0.05	K,G	transcriptional regulator of sugar metabolism
CAC0232	0.18	0.23	G	1-phosphofructokinase (fructoso 1-phosphate kinase)
CAC0233	0.13	0.17	G,T	PTS system, IIA component
CAC0234	0.10	0.02	G	PTS system, fructoso-specific IIBC component
CAC0252	0.17	0.09	P	molybdate-binding protein
CAC0253	0.03	0.01	P	nitrogenase iron protein (nitrogenase component II) gene nifH
CAC0254	0.02	0.01	E	nitrogen regulatory protein PII (nitrogen fixation NifHD)
CAC0255	0.02	0.01	E	nitrogen regulatory protein PII (nitrogen fixation NifHD)

CAC0256	0.02	0.00	C	nitrogenase molybdenum-iron protein, alpha chain (nitrogenase component I) gene nifD
CAC0257	0.17	0.04	C	nitrogenase molybdenum-iron protein, beta chain, gene nifK
CAC0258	0.05	0.01	C	nitrogenase molybdenum-cofactor biosynthesis protein NifE
CAC0259	0.03	0.01	C	fusion nifN/K+nifB
CAC0260	0.06	0.02	E	homocitrate syntase, omega subunit nifV (nivO)
CAC0261	0.18	0.00	E	homocitrate synthase, alpha subunit nifV(nioA)
CAC0281	0.25	0.08	P	molybdate-binding periplasmic protein
CAC0282	0.33	0.09	F,R	cytosine/guanine deaminase related protein
CAC0316	34.30	17.91	E	ornithine carbomoyltransferase
CAC0380	15.95	4.63	E,T	periplasmic amino acid-binding protein
CAC0385	0.06	0.05	G	Beta-glucosidase
CAC0386	0.14	0.07	G	PTS cellobiose-specific component IIC
CAC0447	3.23	1.00	P	feoA FeoA protein, involved in Fe ²⁺ transport
CAC0448	3.76	1.02	P	ferrous iron transport protein B (feoB2)
CAC0489	0.28	0.11	I	4'-phosphopantetheinyl transferase
CAC0490	0.24	0.13	G	sugar kinase, N-terminal region - uncharacterized protei
CAC0554	0.27	0.05	M	1,4-beta-N-acetylmuramidase
CAC0625	0.13	0.06	O	periplasmic aspartyl protease
CAC0751	3.70	1.29	E	permease
CAC0896	0.26	0.09	E	chorismate synthase
CAC0898	0.23	0.02	E	shikimate kinase
CAC0929	4.14	2.52	H	SAM-dependent methyltransferase
CAC0930	5.47	2.94	E	cystathionine gamma-synthase
CAC0973	29.86	11.74	E	argininosuccinate synthase
CAC0974	31.98	8.41	E	argininosuccinate lyase
CAC0975	12.21	5.47	X	Predicted P-loop kinase or ATPase distantly related to phosphoenolpyruvate carboxykinase
CAC0979	3.42	1.53	T	CBS domain-containing protein
CAC1041	4.08	1.32	J	arginyl-tRNA synthetase
CAC1470	11.57	8.02	X	2-Hydroxy-6-Oxo-6-Phenylhexa-2,4-Dienoate hydrolase
CAC1471	10.01	4.45	H	ketopantoate reductase
CAC1589	7.04	4.33	C	malate dehydrogenase
CAC1590	18.29	13.73	P	2-oxoglutarate/malate translocator
CAC2021	0.16	0.00	H	molybdopterin biosynthesis protein MoaA
CAC2022	0.19	0.05	H	molybdopterin biosynthesis protein MoaB
CAC2023	0.14	0.03	X	Membrane protein, related to copy number protein COP from <i>Clostridium perfringens</i> plasmid pIP404
CAC2024	0.21	0.10	I	phosphatidylglycerophosphate synthase related protein (fragment)

CAC2025	0.21	0.03	X	hypothetical protein
CAC2113	0.27	0.15	F	bifunctional pyrimidine regulatory protein PyrR uracil phosphoribosyltransferase
CAC2226	0.27	0.10	N,U,O	branched-chain amino acid aminotransferase
CAC2227	0.30	0.11	E	phosphoserine phosphatase family protein
CAC2235	3.70	0.71	E	cysteine synthase/cystathionine beta-synthase, CysK
CAC2241	27.73	8.70	P	cation transport P-type ATPase
CAC2242	16.89	16.42	K	ArsR family transcriptional regulator
CAC2293	3.21	2.47	X	hypothetical secreted protein
CAC2328	0.26	0.02	G,M	polysaccharide ABC transporter ATP-binding protein
CAC2388	28.32	9.24	E	acetylornithine aminotransferase
CAC2389	23.44	12.12	E	acetylglutamate kinase
CAC2390	26.99	3.22	E	N-acetyl-gamma-glutamyl-phosphate reductase
CAC2391	27.03	8.45	E	bifunctional ornithine acetyltransferase/N- acetylglutamate synthase protein
CAC2514	0.29	0.07	G	Beta galactosidase
CAC2556	3.32	1.70	G	endoglucanase family protein
CAC2610	0.14	0.07	G	L-fucose isomerase related protein
CAC2644	16.10	10.30	E,F	carbamoyl phosphate synthase large subunit
CAC2645	16.81	11.12	E,F	carbamoyl phosphate synthase small subunit
CAC2658	0.15	0.04	R	glutamine synthetase type III
CAC2771	0.29	0.07	E	amino acid transporter
CAC2809	0.04	0.02	H	HD superfamily hydrolase
CAC2810	0.11	0.10	G	glucoamylase family protein
CAC2828	0.30	0.11	F	MutT/NUDIX family hydrolase /pyrophosphatase
CAC2905	0.31	0.17	X	uncharacterized protein, YABG <i>B. subtilis</i> ortholog
CAC2913	6.92	3.51	X	hypothetical protein
CAC2914	7.63	4.37	H	3-methyl-2-oxobutanoate hydroxymethyltransferase
CAC2915	8.46	4.98	H	pantoate-beta-alanine ligase
CAC2916	11.20	5.39	H	aspartate alpha-decarboxylase
CAC3019	5.82	1.35	V	sensory transduction protein
CAC3020	7.85	3.68	E	bifunctional ornithine acetyltransferase/ N-acetylglutamate synthase protein
CAC3098	0.30	0.08	J	50S ribosomal protein L13
CAC3130	0.32	0.09	J	50S ribosomal protein L2
CAC3132	0.30	0.05	J	50S ribosomal protein L4
CAC3285	0.26	0.06	E	amino acid transporter
CAC3325	9.90	5.38	E,T	periplasmic amino acid binding protein
CAC3326	8.88	0.12	E	amino acid ABC transporter permease
CAC3327	10.25	1.31	E	amino acid ABC transporter ATPase

CAC3422	0.22	0.13	G	sugar:proton symporter (xylulose)
CAC3618	10.03	1.84	E	ABC-type polar amino acid transport system, ATPase component
CAC3619	12.58	4.11	E	amino acid ABC transporter permease
CAC3620	9.87	0.87	E,T	amino acid ABC transporter periplasmic-binding protein
CAC3633	0.12	0.04	X	hypothetical protein
CAC3634	0.18	0.03	E	oligopeptide ABC transporter, periplasmic substrate-binding component
CAC3635	0.12	0.03	E	oligopeptide ABC transporter, ATPase component
CAC3636	0.12	0.02	E,P	oligopeptide ABC transporter, ATPase component
CAC3637	0.12	0.02	E,P	oligopeptide ABC transporter, permease component
CAC3638	0.12	0.04	E,P	oligopeptide ABC transporter, permease component
CAC3639	0.07	0.01	X	oligopeptide ABC transporter, permease component

* SD, Standard deviation

Table 7.6 List of genes, exclusively regulated in the *C. acetobutylicum fur* mutant strain.

ID#	Expression ratio	SD*	COG	Protein function
CAP0055	0.29	0.10	X	similar to CAAX-like membrane endopeptidase
CAP0064	0.20	0.14	G	fructose-1,6-bisphosphate aldolase
CAP0100	4.20	1.81	K	TetR/AcrR family transcriptional regulator
CAP0101	3.84	1.20	X	hypothetical protein
CAP0149	5.04	3.32	K	Xre family DNA-binding domain-/TPR repeat-containing protein
CAP0177	4.19	2.00	D	SpoOJ regulator
CAC0079	11.75	10.22	X	hypothetical protein
CAC0082	5.77	4.56	V	predicted membrane protein
CAC0168	0.18	0.05	S	t-RNA-processing ribonuclease BN
CAC0187	3.01	0.50	G	glucosamine-6-phosphate deaminase
CAC0189	3.09	0.90	K	GntR family transcription regulator
CAC0327	6.86	5.20	O	bacterioferritin comigratory protein (AHPC/TSA family)
CAC0469	0.13	0.10	R	spore maturation protein A (gene spmA)
CAC0470	0.22	0.14	S	spore maturation protein B (gene spmB)
CAC0546	0.17	0.13	X	uncharacterized membrane protein, homolog of Methanobacterium (2621593)
CAC0557	0.30	0.06	O	Zn-dependent protease with chaperone function
CAC0570	0.20	0.03	G	PTS enzyme II, ABC component

CAC0579	0.14	0.07	T	serine protein kinase (prkA protein), P-loop containing
CAC0580	0.14	0.11	S	similar to yhbH <i>B.subtilis</i>
CAC0581	0.20	0.12	S	stage V sporulation protein R
CAC0614	0.30	0.07	M	spore coat protein F
CAC0623	0.21	0.11	X	hypothetical protein
CAC0658	3.23	0.86	R	Fe-S oxidoreductase
CAC0659	3.07	1.01	R	Zn-dependent peptidase
CAC0682	0.28	0.17	P	ammonium transporter
CAC0747	0.30	0.08	S	secreted protein containing uncharacterized conserved protein of ErfK family
CAC0792	3.48	1.26	E, H	D-amino acid aminotransferase
CAC0808	0.23	0.05	O	hydrogenase expression factor (hybG)
CAC0809	0.24	0.22	O	hydrogenase formation factor (hypE)
CAC0810	0.14	0.08	O	hydrogenase maturation factor (hypF)
CAC0811	0.29	0.15	O	hydrogenase expression-formation factor (hypD)
CAC0857	0.10	0.06	G	glucan phosphorylase
CAC0863	4.14	1.18	T	sensory transduction histidine kinase
CAC0935	6.80	2.64	E	ATP phosphoribosyltransferase regulatory subunit
CAC0936	5.17	2.22	E	ATP phosphoribosyltransferase catalytic subunit
CAC0937	3.18	1.60	E	histidinol dehydrogenase
CAC0938	3.91	1.14	E	imidazoleglycerol-phosphate dehydratase
CAC0939	3.04	0.86	E	imidazole glycerol phosphate synthase subunit HisH
CAC0940	3.06	1.38	E	Phosphoribosylformimino-5-aminoimidazole carboxamide ribonucleotide (ProFAR) isomerase
CAC0957	3.67	1.52	K	Xre family DNA-binding domain-/TPR repeat-containing protein
CAC0998	5.80	2.74	E	homoserine dehydrogenase
CAC0999	4.75	1.53	E	threonine synthase
CAC1000	3.09	0.72	S	Uncharacterized protein, homolog of yhfF <i>B. subtilis</i>
CAC1049	3.22	0.77	S	Uncharacterized conserved protein, ortholog of YaaR <i>B. subtilis</i>
CAC1093	0.21	0.16	X	hypothetical secreted protein
CAC1101	0.23	0.15	X	hypothetical protein, CF-34 family (identical)
CAC1230	0.28	0.08	X	hypothetical protein
CAC1231	0.28	0.07	R	predicted dehydrogenase, YulF <i>B. subtilis</i> ortholog
CAC1236	0.31	0.13	X	hypothetical protein
CAC1252	0.19	0.10	M	membrane metalloendopeptidase

CAC1253	0.16	0.12	R	sporulation protein IVFB related protein, metallopeptidase
CAC1281	3.73	1.16	O	heat shock protein GrpE
CAC1282	3.58	1.30	O	molecular chaperone DnaK
CAC1298	0.23	0.11	R	uncharacterized protein, related to <i>B. subtilis</i> spore coat protein COTS
CAC1347	0.15	0.14	G	putative transaldolase
CAC1348	0.15	0.13	G	transketolase
CAC1349	0.13	0.10	G	aldose-1-epimerase
CAC1356	0.26	0.05	H,R	thiamine biosynthesis protein ThiH
CAC1363	0.18	0.09	P	Cu/Zn family superoxide dismutase
CAC1390	6.66	0.51	F	purE phosphoribosylaminoimidazole carboxylase
CAC1391	6.66	0.50	F	purC phosphoribosylaminoimidazole-succinocarboxamide synthase
CAC1392	5.55	0.13	F	purF amidophosphoribosyltransferase
CAC1393	5.55	0.19	F	purM phosphoribosylaminoimidazole synthetase
CAC1394	4.55	0.31	F	PurN phosphoribosylglycinamide formyltransferase
CAC1402	0.13	0.09	G	uncharacterized conserved protein, similar to IcaC of <i>Staphylococcus</i> ; YHJR <i>B. subtilis</i> family
CAC1469	3.23	1.02	K	Iron-dependent transcription repressor
CAC1475	0.27	0.15	E	proline/glycine betaine ABC transport system, ATPase component
CAC1713	0.32	0.10	X	coat morphogenesis sporulation protein spoIVA
CAC1843	4.26	1.72	K	transcriptional regulator
CAC1974	0.31	0.08	X	hypothetical secreted protein
CAC1978	0.26	0.05	N,U	predicted membrane protein
CAC2050	0.32	0.01	X	predicted membrane protein
CAC2086	0.19	0.09	X	stage III sporulation protein AH, SpoIII AH
CAC2087	0.19	0.11	X	stage III sporulation protein AG, SpoIII AG
CAC2088	0.19	0.14	X	stage III sporulation protein AF, SpoIII AF
CAC2089	0.13	0.10	X	stage III sporulation protein AE, SpoIII AE
CAC2090	0.21	0.18	X	stage III sporulation protein AD, SpoIII AD
CAC2091	0.16	0.13	X	stage III sporulation protein AC, SpoIII AC
CAC2092	0.17	0.11	X	stage III sporulation protein AB, SpoIII AB
CAC2093	0.18	0.12	S	stage III sporulation protein AA, SpoIII AA
CAC2135	0.15	0.09	O	ATP-dependent serine protease
CAC2137	0.16	0.08	P	cation transport P-type ATPase
CAC2239	0.33	0.24	G	glycogen synthase
CAC2342	0.16	0.04	X	predicted membrane protein

CAC2352	0.15	0.01	X	hypothetical protein
CAC2353	0.13	0.01	X	hypothetical protein
CAC2354	0.19	0.05	E	Nifs family aminotransferase
CAC2383	0.15	0.07	G	xylanase/chitin deacetylase
CAC2418	0.27	0.05	X	uncharacterized conserved membrane protein
CAC2518	3.34	0.95	E	extracellular neutral metalloprotease NPPE
CAC2635	0.33	0.07	X	hypothetical protein
CAC2650	3.77	1.87	F	dihydroorotate dehydrogenase 1B
CAC2651	4.81	2.58	H, C	dihydroorotate dehydrogenase electron transfer subunit
CAC2654	4.15	1.26	F	aspartate carbamoyltransferase catalytic subunit (pyrB)
CAC2692	0.31	0.09	R	O-Acetyltransferase, from isoleucine patch superfamily
CAC2728	0.11	0.08	X	hypothetical protein, CF-30 family
CAC2791	0.18	0.10	R	MoaA/NirJ family Fe-S oxidoreductase
CAC2794	0.16	0.05	K	Lpr family transcriptional regulator
CAC2795	0.15	0.09	R	MoaA/NirJ family Fe-S oxidoreductase
CAC2843	0.11	0.09	R	protein containing aminopeptidase domain (iap family)
CAC2857	0.21	0.12	X	spore protease GPR related protein, YYAC <i>B. subtilis</i> ortholog
CAC2903	0.16	0.06	X	LysM domain containing membrane protein
CAC2905	0.12	0.07	X	uncharacterized protein, YABG <i>B. subtilis</i> ortholog
CAC2906	0.10	0.04	R	spore coat protein cotS related
CAC2984	0.26	0.07	X	hypothetical protein
CAC3075	3.40	0.82	C	butyrate kinase
CAC3081	0.18	0.14	M	spore-cortex-lytic enzyme, SLEB
CAC3223	5.40	3.33	M	regulatory protein SpoVG
CAC3241	0.25	0.20	S	uncharacterized conserved membrane protein, YYAD <i>B. subtilis</i> ortholog
CAC3242	0.24	0.13	R	uncharacterized Fe-S protein, PflX (pyruvate formate lyase activating protein) homolog
CAC3244	0.17	0.13	M	spore cortex-lytic protein
CAC3245	0.22	0.04	O	subtilisin like protease
CAC3278	0.15	0.11	N	ChW repeat-containing protein
CAC3295	0.21	0.09	V	cation efflux pump (multidrug resistance protein)
CAC3314	3.81	0.85	R	nitroreductase family protein
CAC3315	3.39	1.35	O	heat shock protein 90
CAC3402	0.21	0.11	E	dipeptidyl aminopeptidase/acylaminoacyl-peptidase related protein
CAC3403	0.23	0.06	V	predicted membrane protein

CAC3526	5.35	1.38	X	FMN-binding protein
CAC3558	0.27	0.06	X	probable S-layer protein
CAC3668	3.54	1.11	G	MDR-type permease
CAC3703	3.08	1.10	X	hypothetical protein

* SD, Standard deviation

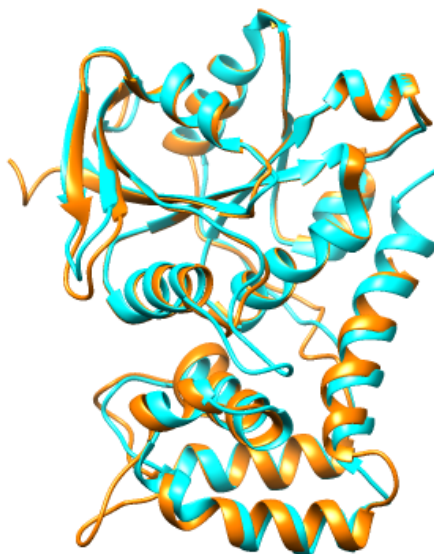


Fig 7.6 Homology model of the putative FeoB protein (CAC1031) from *C. acetobutylicum*. Superposition of the *E. coli* FeoB cytoplasmic domain ribbon structure (blue; Petterman *et al.*, 2009) and the homology model of the CAC1031 cytoplasmic domain (orange). The model was generated using *E. coli* FeoB (pdb: 3i8s) as reference and the Modeller program (Sali and Blundell, 1993). Visualization was performed using the graphical interface Chimera (Pettersen *et al.*, 2004). Scripts are not shown.

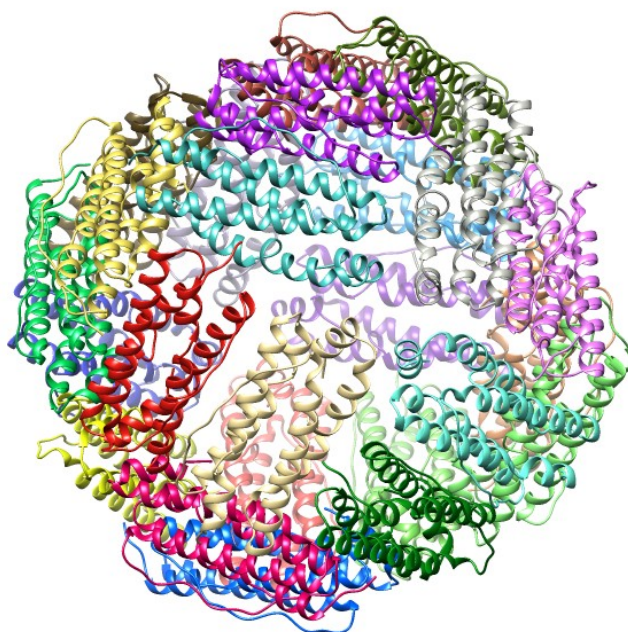


Fig 7.7 3D homology model of a 24meric CAC0845 (putative ferritin) protein from *C. acetobutylicum*. The model was generated using structural information from *E. coli* FtnA (pdb: 1eum; Stillman *et al.*, 2001) and the Phyton-based program Modeller (Sali and Blundell, 1993). The multimer structure was created employing the Matchmaker extension of Chimera (Meng *et al.*, 2006). Scripts are not shown.

Acknowledgements

First and foremost I would like to express my gratitude to **Prof. Dr. Hubert Bahl** for giving me the opportunity to pursue a doctoral degree in his laboratory and for his guidance and support.

Furthermore, I would like to gratefully acknowledge **Dr. Ralf-Jörg Fischer** and **Dr. Tina Lütke-Eversloh** for helpful discussions and useful critiques. I especially thank **Dr. Ralf-Jörg Fischer** for the support in moments of doubt.

My grateful thanks are extended to **Christine Voigt** and **Dr. Holger Janssen** who have been abundantly helpful since the very beginning. They have been a steady influence throughout my PhD career and have provided ideas, support, encouragement and care.

I have been privileged to work with **Dr. Mandy Wietzke**, **Dr. Dörte Lehmann**, **Dr. Miriam Mann**, **Dr. Antje May**, **Daniela Wetzels**, **Henrique Machado**, **Katja Zimmermann**, **Ronny Uhlig** and **Mareen Nipkow** who all have immensely contributed to my personal and professional life in Rostock.

Furthermore, I thank **Dr. Miriam Mann** for reading this thesis.

I am thankful to all the present and former members of the Division of Microbiology at the University of Rostock for providing a productive working atmosphere. Thank you to: **Dr. Oliver Riebe**, **Dr. Franziska Schulz**, **Dr. Michael Scheel**, **Markus Klipp**, **Ilona Boldt**, **Hella Goschke**, **Regina Karstädt** and **Monika Timm**. I greatly appreciate the help of **Regina Karstädt** concerning all the administrative issues.

I am particularly grateful to **Daniel Hönicke** and **Dr. Armin Ehrenreich** from TU Munchen for assistance with the microarray analyses. I thank also **Dr. Birgit Voigt** from the Institute of Microbiology and Molecular Biology at Ernst-Moritz-Arndt University, Greifswald for performing the MALDI-TOF analysis.

Furthermore, I thank **Prof. Klaus Hantke** from the University of Tübingen for kindly providing the *E. coli* H1717 and H1780 strains; **Prof. Nigel P. Minton** and **Dr. John T. Heap** from the University of Nottingham, UK, for providing the Clostron[®] plasmids; and **Prof. Philippe Soucaille**, INSA, Toulouse for providing the pT vector system.

I would like to thank **Dr. Mandy Wietzke** and **Dr. Franziska Schulz** for construction of the modified pT plasmid (pTCatP::*hydA*) and the pTCatP control vector, respectively.

The research leading to the results presented in this work has received funding from the EC's Seventh Framework Programme FP7/2007–2013 under grant agreement no. 237942 (CLOSTNET).

I am especially grateful to my family for all their love, encouragement and infinite support in all my pursuits!

Selbständigkeitserklärung

Hiermit versichere ich, dass ich die vorliegende Arbeit selbständig verfasst und keine anderen als die angegebenen Quellen und Hilfsmittel verwendet habe.

Rostock, 15.01.2014

Delyana Vasileva